




ADVERTIMENT. L'accés als continguts d'aquesta tesi queda condicionat a l'acceptació de les condicions d'ús establertes per la següent llicència Creative Commons:  <https://creativecommons.org/licenses/?lang=ca>

ADVERTENCIA. El acceso a los contenidos de esta tesis queda condicionado a la aceptación de las condiciones de uso establecidas por la siguiente licencia Creative Commons:  <https://creativecommons.org/licenses/?lang=es>

WARNING. The access to the contents of this doctoral thesis it is limited to the acceptance of the use conditions set by the following Creative Commons license:  <https://creativecommons.org/licenses/?lang=en>

DOCTORAL THESIS

**OPTIMIZATION OF THE ASSESSMENT OF BODY COMPOSITION MEASURED BY MEANS
OF IMAGING TECHNIQUES:
COMPUTED TOMOGRAPHY AND MUSCLE ULTRASOUND**

Author:
Fiorella Ximena Palmas Candia

Supervisors:
Rosa Burgos
Andreea Ciudin

Tutor:
Cristina Hernandez



Doctorate Program in Medicine
Department of Medicine
Universitat Autònoma de Barcelona
Barcelona, 2024



DOCTORAL THESIS

**OPTIMIZATION OF THE ASSESSMENT OF BODY COMPOSITION MEASURED BY MEANS
OF IMAGING TECHNIQUES:
COMPUTED TOMOGRAPHY AND MUSCLE ULTRASOUND**

Author:

Fiorella Ximena Palmas Candia

Supervisors:

Rosa Burgos

Andreea Ciudin

Tutor:

Cristina Hernandez

**Doctorate Program in Medicine
Department of Medicine
Universitat Autònoma de Barcelona
Barcelona, 2024**

ACKNOWLEDGEMENTS

Agradecer a todas aquellas personas que han estado a mi lado y me han acompañado en el proceso de la tesis y del crecimiento profesional, en especial a:

A la Dra Burgos, por hablarme del TC y la CC por primera vez y confiar en que “yo podía” y ayudarme a encontrar mi camino y mi devoción en el campo de la nutrición.

A la Dra Ciudin, por elegirme y permitirme así vivir unos de los años profesionales más importantes de mi vida, ojalá nunca me sueltes de la mano.

A la Dra Hernandez, por ser una tutora dedicada y con la puerta siempre abierta.

Al Dr Raul Guerra, con quien empezó todo y sin el que nada de esto hubiese ocurrido, o al menos no *en tres patadas*.

Al futuro Dr Melian, por ayudarnos a tomar tierra y poner cordura en este trio.

Al Dr Simó, por apostar por nuestros proyectos y ayudarnos a poder lanzarlos.

A la Dra Rosón y el Dr. Rodriguez, del servicio de Radiología, cuyo apoyo ha sido fundamental para la realización de esta tesis y cuya colaboración ha sido amable y constante, por este y muchos trabajos más.

A mis compañeros del equipo de endocrino con los que comparto una gran complicidad. Gracias por el interés que siempre han mostrado por mi trabajo, es un aliento que ayuda a continuar.

A mis compañeros de nutrición por soportarme día a día. Especialmente a los que han decidido tomar alguna aventura de recerca conmigo, espero que su inversión les haya valido la pena, y que les haya enseñado el camino como mis mentores han hecho conmigo. Para mí ha sido maravilloso poder trabajar con vosotros. A Guille y Nuri por el apoyo moral y maduro que siempre me dan. Y a Alba por su gran capacidad para arrimar el hombro y permitirme avanzar.

A mis compañeras *M&M*, Dra. Comas y Dra. Sanchez, que, aunque no podemos vernos todo lo que queremos, nos apoyamos todo lo que podemos.

Y por supuesto,

A mi familia, la que eliges, mi hermana postiza la Dra.Villar y Marc, y mis niños Oriol y Guillem, que siempre me hacen sentir como en casa.

A mi familia, mi padre, mi madre y mi hermana, los que no he escogido, pero que elegiría mil veces. Gracias por ayudarme a no perder el rumbo.

A mis *hijos*, por hacerme sentir bien siempre, sin condiciones.

A mi marido, por ponérmelo difícil para superarme y fácil cuando ya me lo ponía difícil yo misma. Parte de esta tesis y de lo que soy, es gracias a ti.

Al Hospital Universitario Vall d’Hebron y la Universidad Autònoma de Barcelona por permitirme avanzar en mi carrera profesional e investigadora.

Gracias por todo.

ABBREVIATIONS

AACE: American Association of Clinical Endocrinologists

ABCD: adiposity-based chronic disease

AEE: activity energy expenditure

AI: artificial intelligence

AMRA

ALM: appendicular lean mass

ASAT: abdominal subcutaneous adipose tissue

ASPEN: American Society for Parenteral and Enteral Nutrition

AT: adipose tissue

BIA: bioimpedance analysis

BIVA: bioimpedance vector analysis

BC: body composition

BEE: basal energy expenditure

BMC: body mass cell

BMI: body mass index

C3: third cervical

CT: computed tomography

CVD: cardiovascular disease

CUN-BAE : Clínica Universidad de Navarra-Body Adiposity Estimator

DIT: diet-induced thermogenesis

DLW: doubly labelled water

DXA: Dual-Energy X-ray Absorptiometry

EASO: European Association for the Study of Obesity

ECW: extracellular water

ESPEN: European Society for Clinical Nutrition and Metabolism

EWGSOP: European Working Group on Sarcopenia in Older People

FELANPE: Federación Latinoamericana de Nutrición Parenteral y Enteral

FM: fat mass

FFM: fat free mass

GLIM: Global Leadership Initiative on Malnutrition

HU: Hounsfield Units

IC: indirect calorimetry

ICW: intracellular water

Kg: kilograms

L3: third lumbar

LM: lean mass

M: metres

MF: multifrequency

MM: muscle mass

SAT: subcutaneous adipose tissue

SEEN: Spanish Society of Endocrinology and Nutrition

SF: single frequency

SMI: skeletal muscle index

SMM: skeletal muscle mass

SO: sarcopenic obesity

SOGLI: Sarcopenic Obesity Global Leadership Initiative

PAT: preperitoneal adipose tissue

PENSA: Parenteral and Enteral Nutrition Society of Asia

PwO: patients with obesity

R: resistance

RF: rectus femoris

RQ: respiratory quotient

REE: resting energy expenditure

ROI: region of interest

MRI: magnetic resonance image

VAT: visceral adipose tissue

T4: fourth thoracic

T2D: type 2 diabetes

TBW: total body water

TEE: total energy expenditure

US: ultrasound

VO₂: oxygen volume

VCO₂: dioxide volume

W: weight

Xc: reactance

INDEX OF CONTENTS

SUMMARY

RESUM

1. INTRODUCTION	13
1.1. Defining body composition	13
1.2. Clinical applications of measuring body composition	14
1.2.1. Muscle mass	14
1.2.2. Adipose tissue	16
1.2.3. Muscle mass and adipose tissue	17
1.2.4. Water compartment.	19
1.3. Current methods for the assessment of BC	19
1.3.1. Anthropometry	19
1.3.1.1. Body mass index	19
1.3.1.2. Perimeters and skin folds	20
1.3.1.3. Equations for BC estimations	21
1.3.2. Dual-Energy X-ray Absorptiometry (DXA)	23
1.3.3. Bioimpedance analysis (BIA)	25
1.3.4. Ultrasound (US)	27
1.3.5. Computed tomography (CT)	30
1.3.6. Magnetic resonance imaging (MRI).	33
1.3.7. Comparison and short of BC methods	35
1.4. Energy expenditure	36
1.4.1. Definition and clinical relevance.	36
1.4.2. Methods to estimate REE	38
1.4.2.1. Predictive equations	38
1.4.2.2. Empiric	39
1.4.2.3. BIA estimations	40
1.4.3. Methods to measure REE	40
1.4.3.1. Direct calorimetry	40
1.4.3.2. Indirect calorimetry	40
1.4.3.3. Other methods	41

2. JUSTIFICATION OF THE STUDY	42
3. HYPOTHESIS	43
4. OBJECTIVES	44
5. COMPENDIUM OF PUBLICATIONS	45
5.1. Clarifications regarding the methodology	45
5.2. First article	48
5.3. Second article	59
5.4. Third article	71
5.5. Intellectual property resulted from the studies of this thesis	92
6. OVERALL SUMMARY OF RESULTS	128
6.1. Study 1	128
6.2. Study 2	129
6.3. Study 3	130
7. OVERALL SUMMARY OF THE DISCUSSION	131
7.1. Clinical relevance	139
8. FUTURE PERSPECTIVES	141
9. GLOBAL CONCLUSIONS	144
10. BIBLIOGRAPHY	145

SUMMARY

Currently, the assessment of body composition (BC) is mandatory for a proper nutritional evaluation and for the optimization of specific treatments. There are many techniques that can be used to assess BC, although few can be considered precise techniques that provide quantitative and qualitative information. BC analysis by computed tomography (CT) is a reference technique, with high precision and high-value information on tissue quality and density. For the segmentation of the BC, the use of a marking tool is necessary. Our group has worked on the development of a semi-automatic tool trained with artificial intelligence for the simplest and most precise marking of the different tissues. In this thesis, the validity of this technique for the study of BC in patients with severe obesity is demonstrated for the first time. In addition, new equations are developed, with results superior to the previous ones and with greater applicability (including any body mass index) for the calculation of body composition, which demonstrate the influence of the tissue density in these models. On the other hand, muscle ultrasound (US) is a simple and accessible technique, which is presented as a good alternative to CT, when the latter is not available. However, one limitation of the US is the fact that the measurements are observer-dependent. Therefore, the application of an automatic or semi-automatic software tool can help improve the technique. In this thesis we confirm these data by developing a semi-automatic tool for analysing muscle US.

Finally, given the important association of muscle mass with energy requirements, and that CT is a technique that has proven to be a reference technique in BC, we propose for the first time the possibility of developing an AI model that estimates resting energy expenditure (REE). In this thesis we developed a model that is able to estimate REE better than any other current estimation method (predictive equations or BIA). It is worth noting that this AI based three-variable model ruled out the patient's gender as the main variable, an innovative discovery that goes beyond the classic recommendations for estimating requirements and has a great potential of changing the actual paradigm.

RESUM

Actualment, la valoració de la composició corporal (CC) és obligatòria per a una correcta avaluació nutricional i per a l'optimització de tractaments específics. Hi ha moltes tècniques que es poden emprar per valorar la CC, encara que poques es poden considerar tècniques precises que aportin informació quantitativa i qualitativa. L'anàlisi de la CC mitjançant tomografia computaritzada (TC) és una tècnica de referència, amb gran precisió i informació de gran valor sobre la qualitat i densitat tissular. Per a la segmentació de la CC és necessari fer servir una eina de marcatge. El nostre grup ha treballat en el desenvolupament d'una eina semiautomàtica entrenada amb intel·ligència artificial per a la segmentació més senzilla i precisa dels diferents teixits. En aquesta tesi es demostra per primera vegada la validesa d'aquesta tècnica per a l'estudi de la CC en pacients amb obesitat severa. A més, es desenvolupen noves equacions, amb resultats superiors a les anteriors i amb més aplicabilitat (incloent-hi qualsevol índex de massa corporal) per al càlcul de la composició corporal, que demostrin la influència de la densitat tissular en aquests models. D'altra banda, l'ecografia muscular (US) és una tècnica senzilla i accessible, que es presenta com una bona alternativa a la TC quan aquesta última no està disponible. Tot i això, una limitació de la US és el fet que les mesures són dependents de l'observador. Per tant, l'aplicació d'una eina de *software* automàtica o semiautomàtica pot ajudar a millorar la tècnica. En aquesta tesi confirmem aquestes dades desenvolupant una eina semiautomàtica per analitzar la US muscular.

Finalment, atesa la important associació de la massa muscular amb els requeriments energètics, i que la TC és una tècnica que ha demostrat ser una tècnica de referència per la CC, proposem per primera vegada la possibilitat de desenvolupar un model d'IA que estimi la despesa energètica en repòs (GER). En aquesta tesi desenvolupem un model capaç d'estimar el GER millor que qualsevol altre mètode d'estimació actual (equacions predictives o BIA). Cal destacar que aquest model de tres variables basat en IA va descartar el gènere del pacient com a variable principal, una troballa innovadora que va més enllà de les recomanacions clàssiques per a l'estimació dels requeriments i té un gran potencial de canvi del paradigma actual.

1. INTRODUCTION

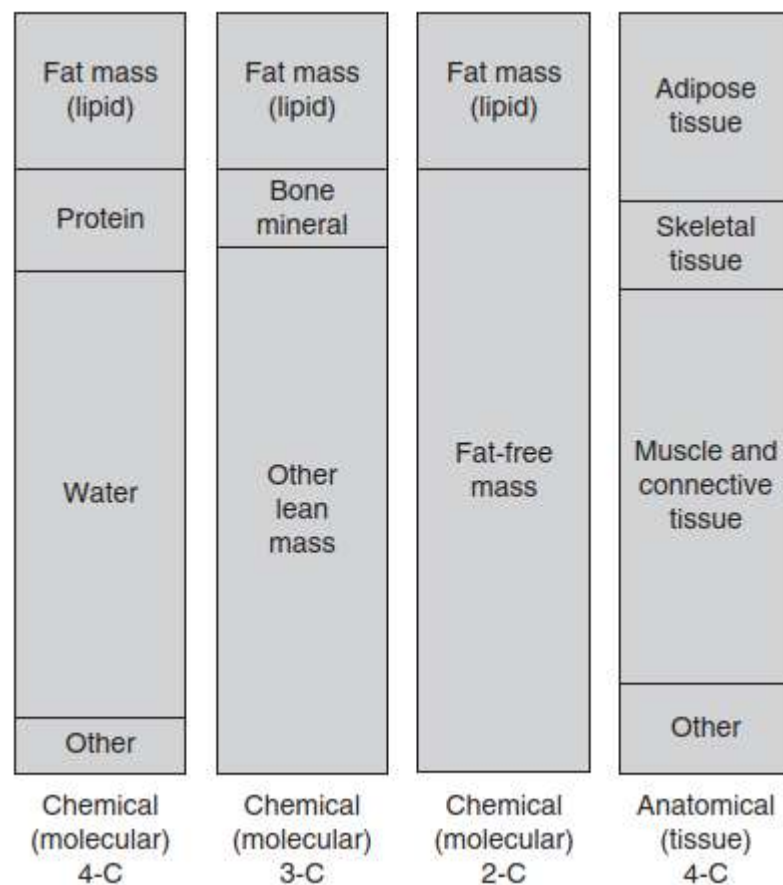
Currently, the assessment of body composition (BC) is mandatory for a proper nutritional evaluation and for the optimization of specific treatments. Knowledge of BC can allow us to design and implement a personalised weight control strategy (diet, physical exercise and pharmacological) as well as a more precise and better metabolically adjusted outcome assessment. Therefore, it is important that healthcare professionals have a critical understanding of currently available BC assessment techniques (1).

1.1. Defining body composition

BC can be analysed at different levels of complexity, from the atomic to tissue-system level, finding different categories (2). The most widely used method in clinical practice and clinical research is the tissue-system level. In this strategy, depending on the measurement method the results can be expressed based on two-compartment (2C), three-compartment (3C), four-compartment (4C) or multi-compartment models (3) (Figure 1). The more compartments it contains, the greater the accuracy of the body composition assessment (4). This categorization will also depend on the limitations of the method used, for example, some methods such as Dual-Energy X-ray Absorptiometry (DXA), at present considered a reference method for BC, will only permit to categorise at molecular level distinguishing the tissues in 3C: fat mass, lean tissue mass and bone (3)

A more advanced and precise study of BC provides more detailed information by segmenting the compartments of fat-free mass, and sometimes assessing tissue quality, hydration status, and also the distribution of adipose tissue within the body, as will be explained later (2,4).

Figure 1. Chemical and anatomical body composition models. T.R. Ackland et al. Current Status of Body Composition Assessment in Sport, 2012.



C = component

1.2. Clinical applications of measuring body composition:

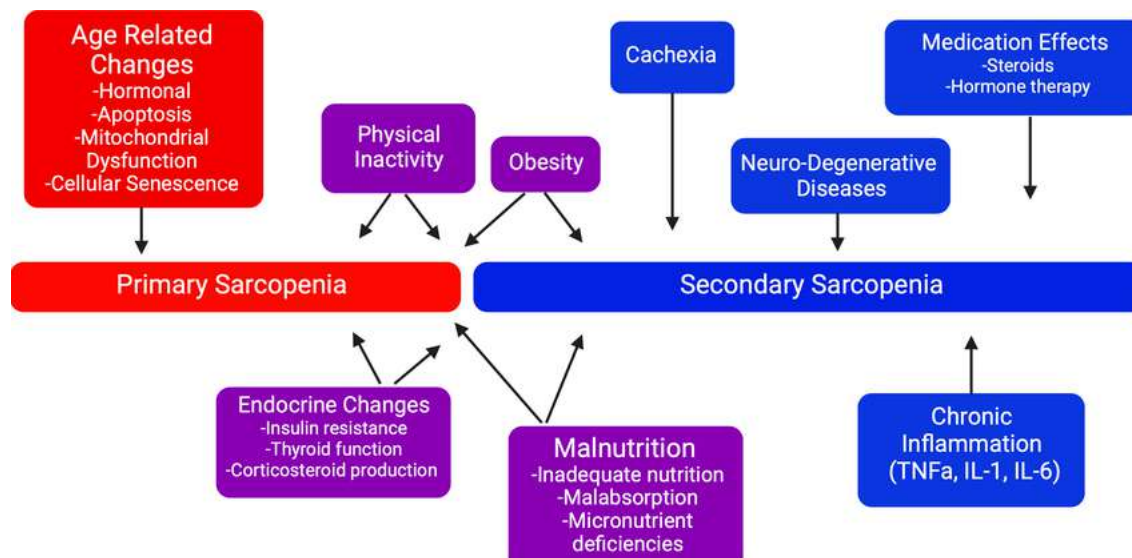
1.2.1. Muscle mass

Muscle mass represents around 30-40 % of total body mass, with significant differences between males and females, being the most important component of fat-free mass compartment (5) Sarcopenia is defined as a progressive and generalised loss of skeletal muscle mass, strength and/or physical function, which is associated with an increased risk of adverse outcomes, such as physical disability, poor quality of life, higher mortality (6) and metabolic syndrome (7–11).

Primary sarcopenia is a physiological situation that generally runs in parallel with ageing (12,13). It is estimated that the muscle mass physiologically decreases by approximately 6% per decade after mid-life (14) . This decrease will be more

accelerated and higher than expected in the case of associated pathology (acute or chronic), identified in this case as secondary sarcopenia (15,16) (Figure 2).

Figure 2. Pathophysiology of primary and secondary sarcopenia. Image: Stephanie L Gold et al. Putting some muscle into sarcopenia-the pathogenesis, assessment and clinical impact of muscle loss in patients with inflammatory bowel disease, 2023.



Skeletal muscle and lean body mass are important markers of prognosis and functional recovery in chronic and acute illness, particularly in conditions in which muscle atrophy is prevalent (17). For instance, at present, more than 600 original articles, including many meta-analyses report the impact of muscle and adipose tissue in relation to oncological outcomes such as survival, morbidity, surgical complications, chemotherapy toxicity and mortality (18,19), highlighting the importance of incorporating the BC assessment in the daily clinical practice.

Moreover, the assessment of muscle quality and not only the muscle mass is of growing interest and has been included in the last definitions and consensus of the European Working Group on Sarcopenia in Older People (EWGSOP) (20). Myosteatosis, defined as an ectopic fat depot within muscle (21–23) increases with ageing and obesity and negatively correlates with muscle mass, strength, and mobility and higher risk of metabolic complications (insulin resistance, type 2 diabetes) (22).

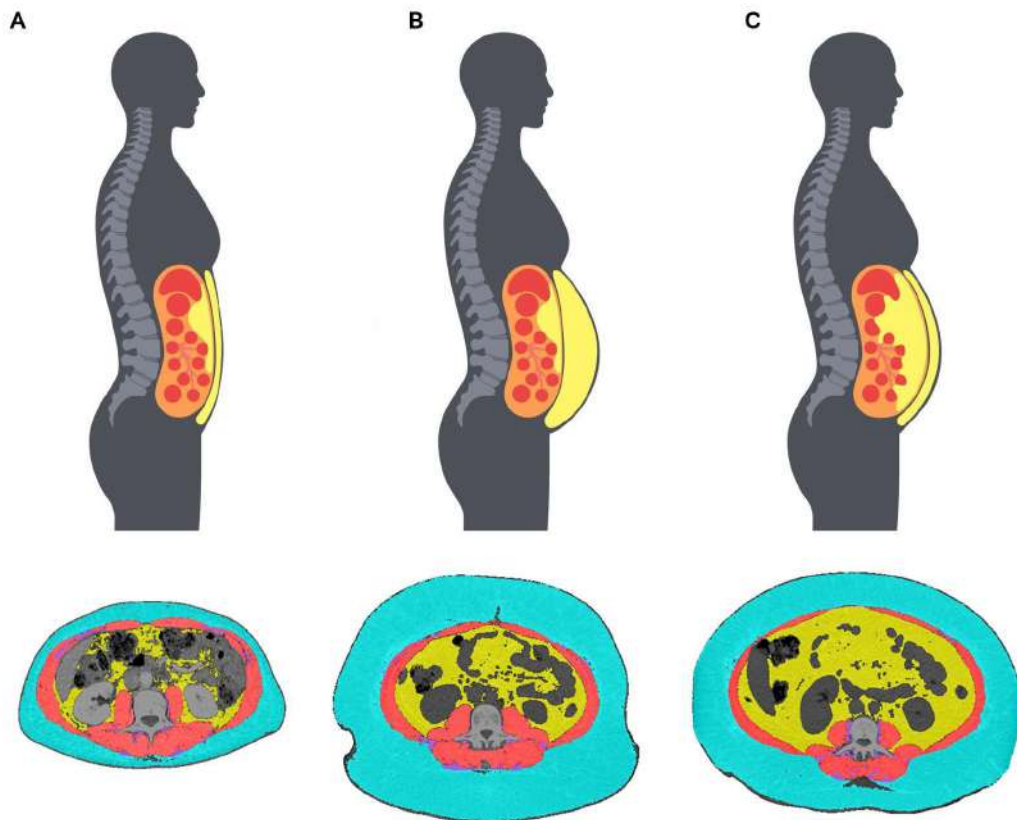
1.2.2. Adipose tissue

Classically, the definition of obesity and the amount of adipose tissue has been related to the body mass index (BMI). The BMI is the ratio of weight (kg) to height squared. Universally, obesity was diagnosed when the BMI was greater than 30 kg/m².

Recently, the American Association of Clinical Endocrinologists (AACE) proposed a new definition for obesity as a “adiposity-based chronic disease (ABCD)”, which has also been adopted by the European Association for the Study of Obesity (EASO) (24,25). This concept refers not only to the total amount of body fat, but also to its distribution and functionality (26). Besides the total amount of adipose tissue in the body, it is important to know its distribution and proportion, given its significant role in pathologies such as metabolic syndrome and associated complications.

Individuals with high body fat composition, particularly abdominal distribution, are at a greater risk of metabolic complications, mortality (27–31), higher rate of complications in abdominal surgery (32,33) and even worse prognosis in COVID-19 infection (34,35). Therefore, the assessment of BC should include a more detailed and accurate evaluation of adipose tissue by differentiating subcutaneous (SAT) and visceral tissue (VAT) (Figure 3).

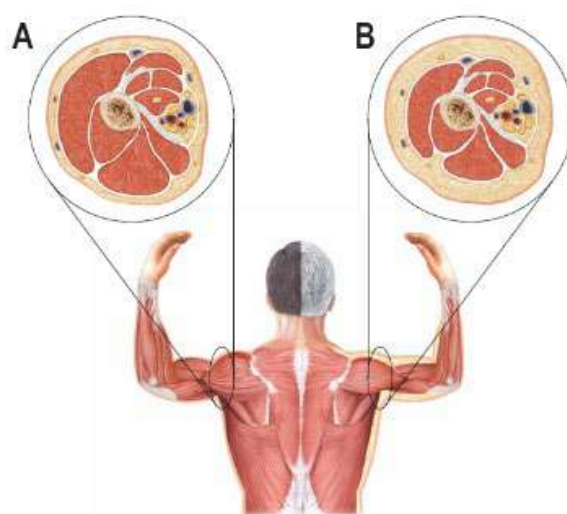
Figure 3. Types of obesity according to the distribution of abdominal adipose tissue: A. normal, B. Obesity with predominance of subcutaneous adipose tissue, C. Obesity with predominance of visceral adipose tissue.



1.2.3. Muscle mass and adipose tissue

In recent years was showed that the association between low muscle mass and high adipose tissue mass, represents a higher risk factor of metabolic complications and mortality than the two entities alone (36,37). In this regard, recently, the European Society for Clinical Nutrition and Metabolism (ESPEN) and EASO have agreed on a definition and diagnostic criteria for sarcopenic obesity (SO), a condition in which sarcopenia and obesity coexist and lead to a cumulative risk derived from the two clinical situations (38).

Figure 4. Graphic representation of normal adipose tissue and muscle mass distribution (A), and sarcopenic obesity (B). Benton MJ et al. Sarcopenic obesity: strategies for management, 2011.



More recently, these two societies (ESPEN and EASO) have launched the initiative the Sarcopenic Obesity Global Leadership Initiative (SOGLI), to reach expert consensus on definition criteria and management of sarcopenic obesity (38). They recommend diagnosing SO in two steps: firstly, a functional assessment of the muscle using hand grip strength; and secondly, an assessment of body composition, recommending BIA and DXA as first-choice techniques. They support the use of cut-points provided by Dodds et al. (39) for Caucasian populations, by Gallagher et al. for FM (40), by Janssen et al. for SMM/W (41).

Table 1. Cut points recommended by Sarcopenic Obesity Global Leadership Initiative.

Hand grip strength cut-off points	Adiposity cut- off points	Low muscle mass cut –off points
Dodds - Men <27 kg - Women: <16 kg	DXA (% FM according to Gallagher) - Age 20-39 years: - Men: >26% - Women: >39% - Age 40-59 years: - Men: >29% - Women: >41%	DXA (ALM/weight) according to Batsis - Men: <25,7% - Women: <19,4% BIA (SMM/weight) according to Janssen - Men: <31,5% - Women: <22,1%

1.2.4. Water compartment

Measuring the water compartment is a challenge in clinical practice due to its continuous and rapid change, especially in pathologies with frequent changes in blood volume such as heart or kidney failure (42,43). The use of variables such as absolute weight (kg) in these cases is not recommended because they do not represent the real changes produced at the BC level. Techniques that do not rely on variables affected by fluid variation, such as the Bioelectrical Impedance Vector Analysis (BIVA) are necessary to be able to carry out a more precise BC assessment and better adapt therapeutic measures (in pathologies such as heart failure or advanced kidney disease) (44,45).

1.3. Current methods for the assessment of BC

1.3.1. Anthropometry.

The anthropometric evaluation consists of a set of measures such as weight, height, body mass index, skin folds, perimeters and circumferences alone or combinations (1). These measures can be interpreted comparatively in an evolutionary process or can be interpreted based on reference values validated for a specific population (46).

1.3.1.1. Body mass index

Body mass index (BMI) is calculated by a mathematical formula based on the weight (kg) and the height (m). This parameter was proposed by a mathematician; Adolphe Quetelet (24,47), whose development was based on European population from France and Scotland as an anthropological method to identify "*l'homme moyen*" from a typological perspective rather than a health status biomarker (48). Despite that the BMI was not a parameter designed to evaluate the health status of the population and was based on data limited only to specific Caucasian population, in 1998 the World Health Organization includes the BMI as the main factor for the classification of the humans into underweight, normal weight, overweight and people with obesity (Report of a WHO Expert Committee 1995) (49).

Table 2. BMI classifications. Table: Volkan Yumuk. European Guidelines for Obesity Management in Adults, 2015.

Category	BMI, kg/m ²
Underweight	<18.5
Healthy weight	18.5–24.9
Pre-obese state	25.0–29.9
Obesity grade I	30.0–34.9
Obesity grade II	35.0–39.9
Obesity grade III	≥40

Several studies showed a direct relationship between BMI and obesity-related comorbidities (such as T2D) as well as with the increased mortality (50). These studies, added to the simplicity of obtaining BMI, resulted in the widespread use and acceptance of this index as the main criteria in the diagnosis and management of nutritional status (50). Given that the BMI only identifies how weight is adjusted for height, regardless of factors such as age, race or sex, and without informing us of the BC, it is now increasingly accepted that the BMI has serious limitations in daily clinical practice. (51–53). In addition, its use as the main morphological criterion has led to erroneous conclusions, such as the “obesity paradox in heart failure” which was recently withdrawn by the American Heart Association (54,55).

1.3.1.2. *Perimeters and skin folds*

Besides BMI, in the daily clinical practice the measurement of folds and perimeters, such as waist circumference has also been implemented to complete the information on BC (46). Some of the most widespread perimeters for estimating adipose tissue mass are the waist circumference and the waist-to-hip ratio (56,57). They were proven to be related to a predominantly abdominal fat distribution and have been correlated with an increased risk of metabolic complications such as type 2 diabetes, dyslipemia and cardiovascular risk, among others (56,58). In recent years, calf circumference has been gaining relevance thanks to the good correlations that it presents with skeletal muscle mass, especially in the context of sarcopenia assessment in the older adult and recent publications of adjustment factors that allow for the elimination of the confounding effects of obesity (8,59,60).

Skinfolds is a technique that measures a double fold of skin with subcutaneous fat in various sites of the body, using callipers (49). The usual measurement sites include triceps, biceps, subscapular, suprailiac, mid-calf, and anterior abdominal wall.

Measures of skinfolds and circumferences are a low-cost and simple technique. Its main limitations are related to the low reproducibility given the technical difficulties that require trained personnel, and its low precision to assess small changes in BC, as well as a very superficial assessment of the tissues (61). When BC assessment is not available, anthropometry can be used as a superficial surrogate, but always considering the limitations (60).

1.3.1.3. Equations for BC estimation

Multiple equations have been developed to estimate BC, with different main objectives: a) total body fat, b) abdominal fat and c) muscle mass. Multiple equations and indexes have been developed to offer a better approximation to CVD and metabolic diseases such as waist circumference (62,63). In some cases, they show to be better predictors of CVD, metabolic and premature death than BMI (64,65). Nevertheless, overall data so far is controversial on the usefulness of these equations for BC estimation.

Moderate to high levels of correlation with BC reference techniques (DXA or plethysmography) have been observed, and also significant association with increased cardiovascular risk or metabolic syndrome (62,63,66–69).

Two examples of formulas to calculate total body fat mass are the Deurenberg equation (69) and the CUN-BAE (Clínica Universidad de Navarra-Body Adiposity Estimator) (67). Both equations show a better estimation of fat mass than BMI, validated by plethysmography (CUN-BAE) and DXA or densitometry (Deurenberg) as the reference technique, and also show better association with increased risk of cardiovascular disease (CVD) (62,66,67,69,70).

However, technological progress has permitted us to demonstrate that these parameters are not accurate enough to make a correct approach to the patient's state of health, based on the different body compartments. They are only

estimations, based on limited populations, and some of them were created more than 100 years ago (53).

Table 3. Equations for anthropometry body mass estimations. Formula, year of development (bibliographic reference), reference method used and level of correlation.

<i>Equation</i>	<i>Year</i>	<i>Reference method</i>	<i>Correlation to reference method</i>
CUN-BAE (% Fat Mass) = [– 44,988 + (0,503 × age) + (10,689 × sex) + (3,172 × BMI) – (0,026 × BMI ²) + (0,181 × BMI × sex) – (0,02 × BMI × age) – (0,005 × BMI ² × sex) + (0,00021 × BMI ² × age)]	(2012) (66)	<i>Air displacement plethysmography</i>	r=0.9
Deurenberg (% Fat mass) = 1,20 × BMI + 0,23 × age – 10,8 × sex – 5,4	(1990) (69)	<i>Densitometry (underwater weighing)</i>	r=0.79
Waist to height ratio (WhtR) = $\frac{\text{waist circumference (cm)}}{\text{height (cm)}}$	(2010) (57)	<i>Clinical results</i>	None
Conicity index (CI) = $\frac{\text{waist circumference (m)}}{0,109 \times \sqrt{\frac{\text{weight (kg)}}{\text{height (m)}}}}$	(1991) (71)	<i>Clinical results</i>	None
Bonora men (cm) = –453.7 + (6.37 × waist circumference (cm)) Bonora women (cm) = –370.5 + (4.04 × waist circumference (cm)) + (2.62 × age)	(1995) (72)	<i>RMI– L4</i>	SAT área (both): r=0.89 VAT área: men 0.56 VAT área: women 0.68
Body adiposity index (BAI) = $\frac{\text{hip circumference (cm)}}{\text{height (m)}} - 1,8$	(2011) (73)	<i>DXA</i>	r=0.85
Body roundness index (BRI) = $= 364,2 - 365,5 \sqrt{1 - \frac{\left(\frac{\text{waist circumference (m)}}{2\pi}\right)^2}{(0,5 \times \text{height})^2}}$	(2013) (74)	<i>DXA and RMI</i>	r=0.88
Body shape index (ABSI) = $\frac{\text{waist circumference (m)}}{\text{BMI}^{\frac{2}{3}} \times \text{height}^{\frac{1}{2}} \text{ (m)}}$	(2012) (75)	<i>Clinical results</i>	None
Hume - men (kg) = (0,32818 × weight(kg)) + (0,33929 × height (cm)) – 29,5336 Hume – women (kg) = (0,29569 × weight(kg)) + (0,41813 × height (cm)) – 43,2933	(1966) (76) (2014) (77)	<i>Antipyrine space</i> <i>DXA(77)</i>	<i>Antipyrine space</i> Men: r= 0.58 Women: r=0.73 DXA: r=0.913

1.3.2. Dual-Energy X-ray Absorptiometry (DXA)

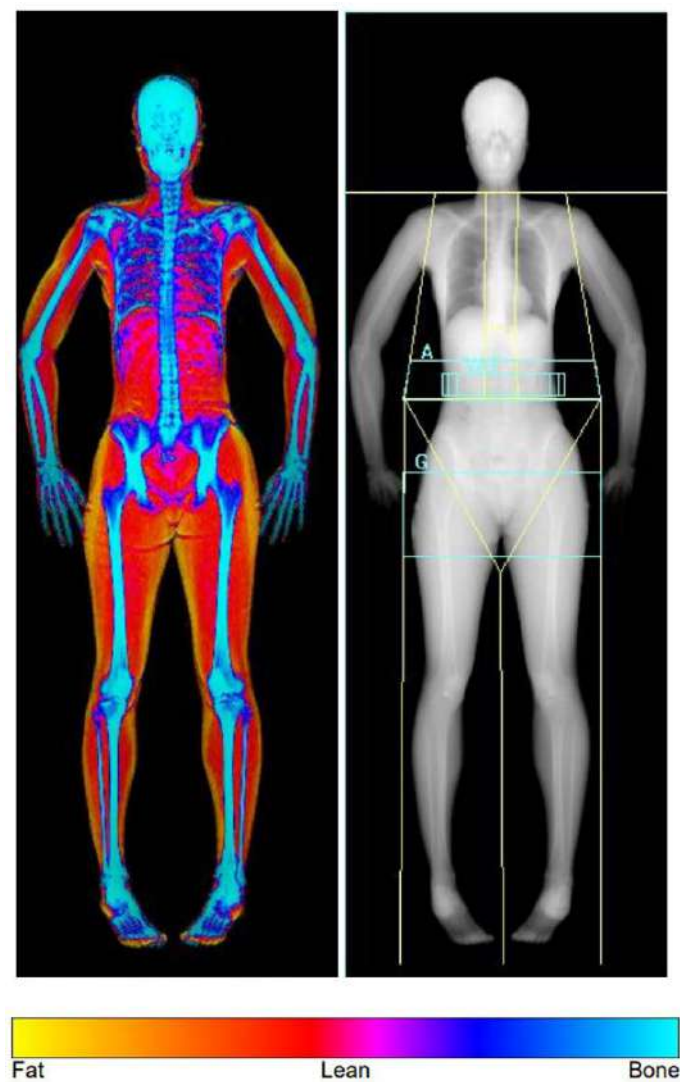
Dual energy X-ray absorptiometry (DXA) was originally developed to measure bone mineral density. Subsequently, with technical improvements and refined software, DXA became a reference technique for BC measurement, particularly for its accuracy in measuring fat mass. DXA discriminates three different compartments, based on their specific X-ray attenuation properties: bone mineral content (BMC), lipids (triglycerides, phospholipid membranes, etc.) which is the so-called "fat mass" (FM) and free of lipids. soft tissue that is the "lean mass" (LM) (78). It is important to point out that since there are only specific attenuation factors for bone and fat, the DXA technique measures two compartments (bone mass and fat mass) and estimates the third (lean mass) (79).

Despite not obtaining many direct measurements, technological improvements and software make it possible to estimate several variables such as the fat mass index (FMI), android/gynoid index (GA) and lipodystrophy indices (% trunk/leg fat, trunk mass/limb fat ratio) or estimation of visceral adipose tissue (79). The main advantage of this technique is that it allows us to know the BC of the whole body with little exposure to radiation (figure 1). In addition, said information on body composition can be obtained globally (whole body) or segmentally (arms, legs and trunk separately).

DXA is considered a precise technique and has a fast acquisition time (66). However, a special space is needed for the device and trained personnel, as well as exposure to X-ray radiation (even at low doses ($1-7 \mu\text{Sv}$), equivalent to 1-10% of a chest X-ray, should be taken into account (80). Another important limitation is due to its two-dimensional characteristic: DXA does not provide measurements on the distribution of adipose tissue at the abdominal level (only VAT or SAT estimates) nor on the state of hydration or quality of the tissue (81,82). The accuracy of DXA to measure BC depends on correct image preparation, which is crucial to keep the biological variability of LM and FM measurements as low as possible (79). In addition, as the thickness of a tissue increases, it loses accuracy, especially with thicknesses greater than 4 cm, therefore it is not a reference technique in cases of severe obesity (82,83). Furthermore, DXA cannot be performed on individuals with

more than 160 kilograms of total body weight. Despite its significant limitations, evidenced by comparison with new methods of BC assessment, DXA is still considered a reference method (requested for validation of most of the methods for BC assessment) and incorporated in practical guidelines (38,47).

Figure 5. DXA image body attenuation and android/gynoid measure. Image: UC Davis Health, DXA body composition analysis, 2023.



1.3.3. Bioimpedance analysis (BIA).

Bioelectrical impedance (BI) or bioimpedance analysis (BIA), is a simple, non-invasive, quick and not expensive method that estimates the BC by measuring the resistance to a low-power alternating current through the body (84).

There are two main methods of bioimpedance analysis (BIA): conventional (measured in kg or %) derived from estimated equations; and vectorial (Bioelectrical Impedance Vector Analysis or BIVA) which evaluates the tissues according to the electrical raw results. Main raw results are the resistance (R) which correlates negatively with body water content, and reactance (Xc) which is related to the capacitance of the cellular membrane (85–87).

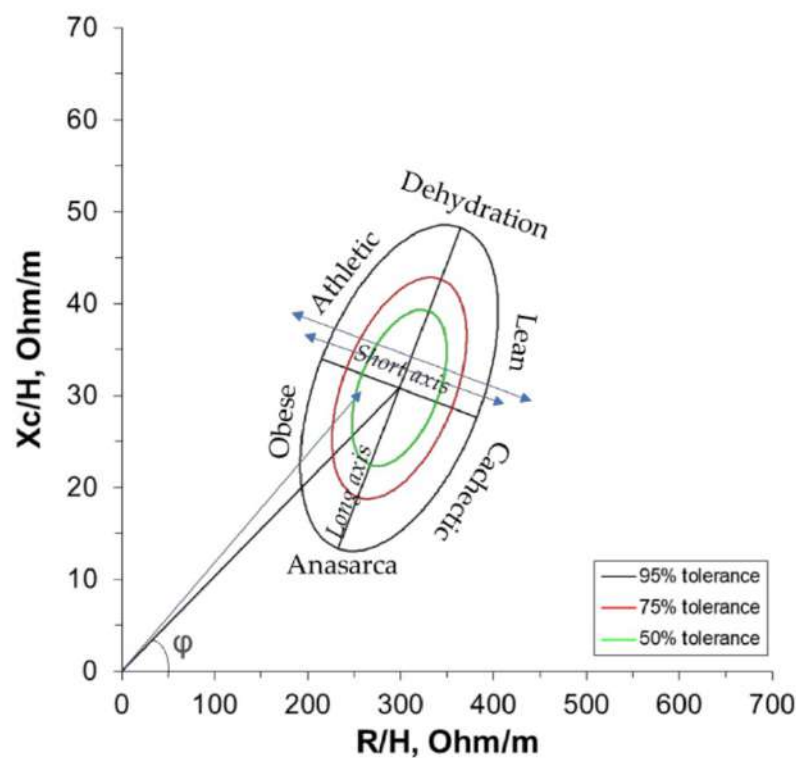
BIA quantifies mass by transforming electrical information through predictive equations (including the age, ethnicity, weight and the height of the subject (88) and estimates BC as bicompartamental model: fat free mass (FFM) and fat mass (FM) in kilograms and percentage (89). Specific equations have been validated for different ethnic groups (89). BIA also allows estimation of body hydration measuring total body water (TBW), extracellular water (ECW) and intracellular water (ICW) (85).

There are mainly two types of conventional BIA related to the electric frequency used: a) mono or single frequency BIA (SF-BIA) of 50Hz or b) multifrequency (MF-BIA). The application of more than one frequency or multifrequency BIA (MF-BIA), permits the assessment of the same variables as in the SF-BIA but with a higher level of precision since the high frequencies cross the cell membrane optimising the information of the intra and extracellular liquid.

The main limitation of conventional BIA in general, is that the equations usually assume a constant hydration of 73% of FFM, which will cause important limitations in the accuracy of the measurement in conditions such as critically ill or surgical patients, heart or kidney failure, among others (42,83,90).

The fact that the classical BIA uses algorithms based on predictive equations represents a significant limitation that can be overcome by using Bioelectrical Impedance Vector Analysis or BIVA. BIVA analyses raw bioelectrical data (resistance and reactance), normalised by height and plotted as bivariate in an easy graph interpretation, providing a semiquantitative evaluation of body mass cell (BMC) and body water (TBW) (Figure BIVA) (84,88,91–93). Since BIVA does not use weight, it allows the assessment of fluid pattern distribution especially useful in clinical situations that implies oedema or high-water content Figure (BIVA). (90,94). In the BIVA graphic representation vector moves along the minor axis of the ellipse according to the cell mass and moving to the right side if the cell mass is less(92).

Figure 6. Interpretation of BIVA graph. Resistance (R) and reactance (Xc) were normalized by the height (H, meter) Image: adapted from Piccoli and Pastore, 2002.



The raw BIA variable of the phase angle (a tangent of resistance to reactance), it is considered as an important marker of the integrity of body tissues and predictor of health cells (95). Phase angle has gained importance due to its strong correlation with the nutritional and health status and prognostic value, associated with muscle mass and function (87,95,96). Probably the phase angle

should be included in the future guidelines due to its high prognostic value as a parameter in the core values of surgical risk and mortality (60,97–99).

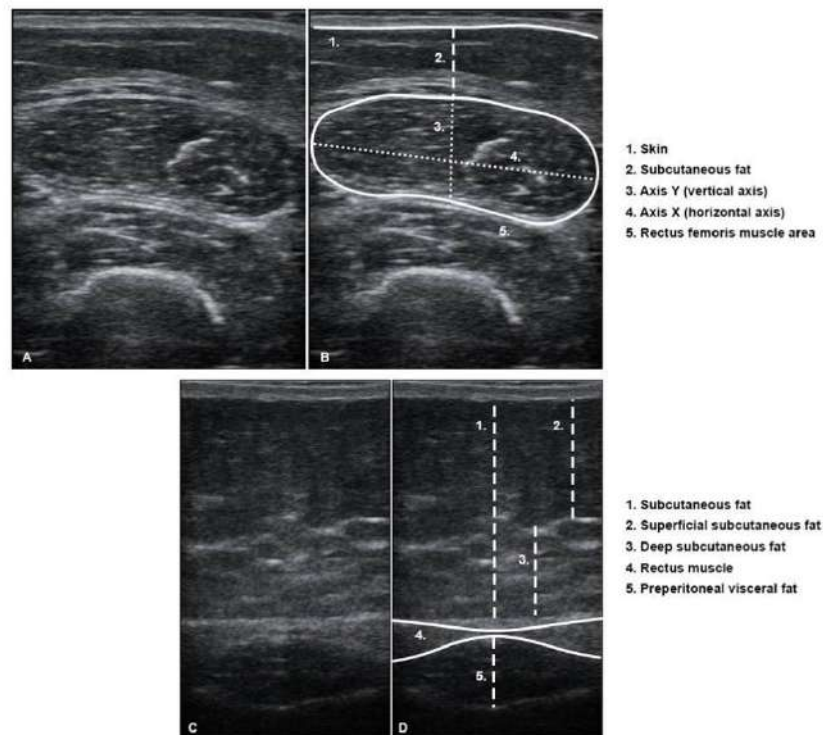
1.3.4. Ultrasound (US)

Ultrasound (US) is a non-invasive, simple, portable, reproducible and largely available tool, that can have been recently shown to be useful for the assessment of BC (both quantity and quality of muscle mass and adipose tissue).

Muscle mass can be estimated based on data from several accessible skeletal muscle groups (100). Several skeletal muscle groups have been studied with US, and most of them showed a strong correlation with total muscle mass measured by reference methods such as DXA (R value 0.7-0.9) (100,101). Quadriceps femoris is the most evaluated muscle group, especially the rectus femoris (100,102). Based on these recent data, the SARCUS consensus (100) includes recommendations on the mandatory quantitative parameters that muscle US evaluation should include in general: muscle thickness (cm), pennation angle, fascicle length (cm), echo-intensity and cross-sectional area of the muscle (cm²). Additionally, other measurements can be considered, such as: muscle volume, muscle microcirculation, muscle contraction and muscle stiffness (100). Moreover, to avoid changes in reliability, it is recommended to use the mean value of two or three measurements (100).

US is also useful for assessment of different AT compartments: subcutaneous, preperitoneal (PAT) or visceral tissue. These measures are usually taken on a central abdominal image (figure 1). PAT shows a direct correlation with other visceral deposits such as intrahepatic fat or renal fat (103) and after further validation could represent a simple method to evaluate VAT.

Figure 7. Ultrasound transverse section. (1A, 1B) Rectus femoris measures. Image and scheme of the anatomical structures. (1C, 1D) Abdominal area. Image and scheme of the anatomical structures.



The US image is recorded on a grey scale, ranging from 0= black to 255= white, depending on the echogenicity of the image. Currently, it can be quantified by identifying the area of interest using manual tools such as Photoshop or Image J (Figure 3) (104). Healthy muscle tissue tends to be echolucent (dark), interspersed with small, bright and curved echoes that represent epi- and perimysium (105). The appearance of greater hyperechogenicity and increased whiteness indicates an increase in fat infiltration (104,105).

Figure 8. Ultrasound rectus femoris qualitative analysis using *Photoshop CC 2020*. Image and grayscale histogram.



Furthermore, at present there is no standardised protocol nor clear cut-off points for different populations and clinical situations (82,83). In an attempt to standardise the US method, recent consensus guidelines have been published to further improve reproducibility and validity for the BC assessment by US (100).

Besides those inherent to the technique itself, related to the device and the experience of the explorer (13), we consider the lack of standardisation as the main current limitation of these techniques. In Spain, the Spanish Society of Endocrinology and Nutrition (SEEN) has established a measurement protocol for the lower third of the rectus femoris and the midpoint of the abdomen, which is currently widely used nationwide (105). Nevertheless, the US has a significant potential to become one of the most used techniques for BC assessment in the next few years, due to the simplicity and reproducibility which is stimulating growing interest in research and future studies.

1.3.5. Computed tomography (CT)

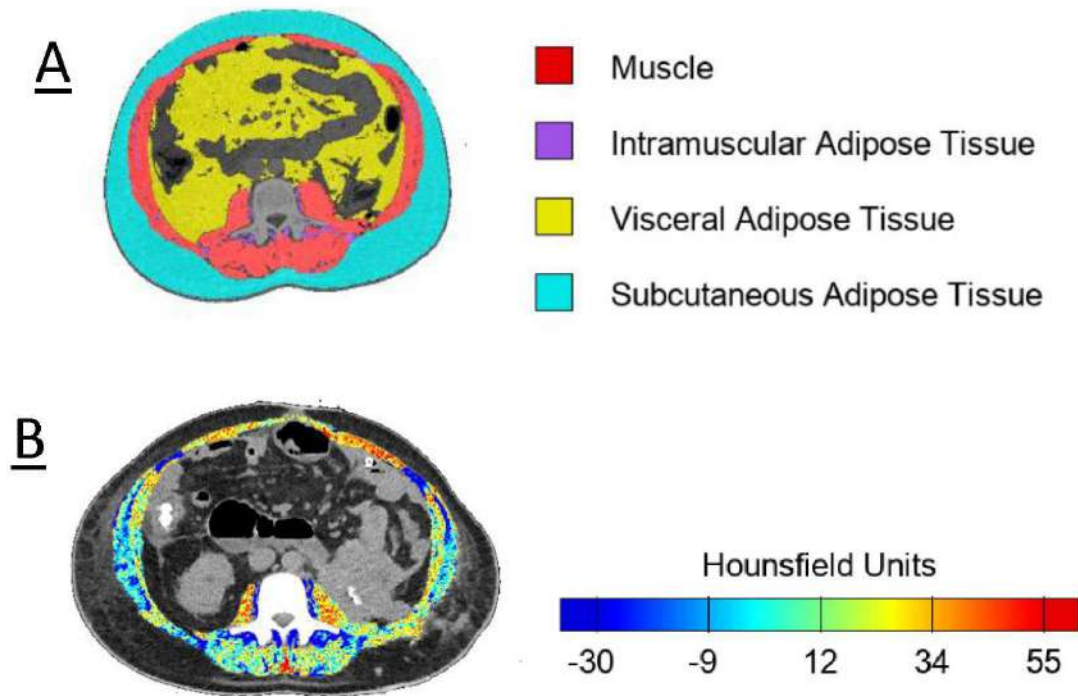
Computed tomography is a multi-compartmental method that provides an accurate quantitative and qualitative assessment as well as segmentation of adipose tissue (SAT, VAT) and skeletal muscle (Figure 9). Currently, computed tomography (CT) and magnetic resonance imaging (MRI) (explained further) are the most accurate methods available for the analysis of BC (106,107).

CT analysis of BC can be performed with a single or various slices of the same vertebra. Currently, the L3 vertebrae has shown more accurate results and with good correlations with BC assessed by whole-body MRI (108,109). However, CT BC has been evaluated at different vertebrae levels as T4, C3, and L3 (110–115).

The CT obtains the images in spiral and through multiple slices, therefore permits to collect volumetric information from the human body, even to complete reconstruction of internal organs if needed (116), allowing a more precise assessment of the BC evaluation. Regardless, the explored body region (T4, C3, L3, etc) the areas of interest are usually measured in cm^2 and in most studies adjusted by height and expressed also in cm^2/m^2 (38,109,117,118).

Furthermore, images obtained from the CT are presented on a computer screen with grayscale values, corresponding to Hounsfield units (HU). Recently, the HU parameter was incorporated in the BC assessment which allowed us to differentiate between tissue types (119). The reference ranges of these tissues may vary depending on the study, but in general, adipose tissue presents negative HU ranging from (-190 to -30) for subcutaneous and intramuscular adipose tissue and (-50 to -150) for visceral tissue, and (-29 to 150) HU for skeletal muscle mass (83,119,120). Furthermore, the use of HU permits to assess the amount of fat within the muscle mass (myoesteatosis), providing an accurate qualitative evaluation, not only quantitative. This concept has gained interest and the quantification of muscle quality measured by HU has shown a high prognostic correlation in cancer or hepatic disease, even when the correlations with the muscle mass (measured in cm^2) were not significant (119,121,122).

Figure 9. CT segmentation of BC in a slice at the L3 level analysed with the semi-automatic software FocusedOn BC. A. Information on quantitative segmentation. B. Qualitative evaluation of muscle mass.



Until recently, the assessment of the BC through CT image was performed by manual outlining of the area of interest causing the analysis to be subjected to inter-reader variability and time-consuming (107). Current software and computer-assisted diagnostic tools categorised as manual and semi-automatic, make analysis easier and reduce time expended (123) and provide a complete BC segmentation at “a glance” (23,119,124,125).

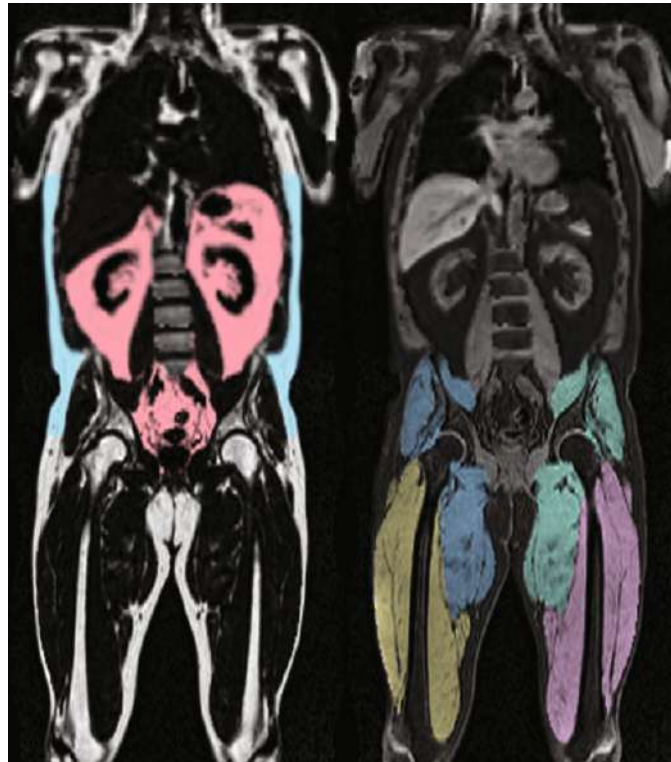
However, the BC assessment by CT imaging has at present some limitations such as high doses of radiation, expensive devices that require special place and trained personnel limiting its indication at larger scale in the daily clinical practice (78,82). In recent years, technological advances are helping to overcome these limitations. For instance, some centres are starting to perform a single CT slice for the BC assessment only, making this technique easier, cheaper, less exposure to

radiation and less time-consuming (60). However, its large applicability is still limited at large scale. Currently, significant data can be obtained in an “opportunistic manner” in those pathologies where CT-scan is indicated as per protocol in the daily clinical practice, such as cancer, abdominal pathology, surgical complications, critically ill patients, where BC assessment is also of high interest for a proper personalised approach and management (107,126).

1.3.6. Magnetic resonance imaging (MRI).

At present, body-MRI is one of the most accurate methods for BC assessment (78,82). The image acquisition depends on the application of a pulse of radiofrequency, leading to energy absorption by the hydrogen protons and release energy which is detected by a receptor used to create the whole body or regional images (127). The difference between tissues and organs is related to the tissue specific magnetic resonance properties (82). BC based on MRI uses the different magnetic properties of the nuclei of certain chemical elements (usually hydrogen in water and fat), and the resonance chemical phase shifts between fat and water to calculate images of only fat and water from a single acquisition (128). The fundamental principles on which the quantitative determination is based using the technique of "fat and water images" or Dixon method, is based on the fact that the different magnetic resonance frequencies of the protons in the fat and the water are used to separate the two signals into a fat image and a water image, allowing a first approximation of BC separating these two compartments very precisely (Figure 6) (51,128). Common MRI-based body composition metrics are visceral adipose tissue (VAT) volume, abdominal subcutaneous adipose tissue (ASAT) volume, thigh muscle volume, thigh muscle fat infiltration (MFI), and liver fat (51). Taking these measurements allows a profiling of the patient's BC and metabolic risk. There are some tools that facilitate this process, such as the AMRA Profiler (AMRA Medical AB, Linköping, Sweden), which is the tool for BC profiling that was used in the validation studies of fat-referenced MRI (51,60,128).

Figure 10. MRI. Fat and water image (Dixon method). Segmentation of abdominal subcutaneous AT (ASAT), visceral (VAT) and muscle groups from fat water separated. To the left is the fat image with ASAT (blue) and VAT (red). To the right is the water image with the different muscle groups coloured. Image: Nayak et al., Body composition profiling at 0.55T: Feasibility and precision, 2023.



A feasibility and precision study in a patient with obesity is needed to elucidate the value of low field wide bore MRI as a tool in body composition profiling in patients with obesity and bariatric patient populations (128).

As in the case of CT-scan, the most frequently used is the L3 vertebrae level, for quantitative analysis of body composition is still in a single slice, mainly in L3 vertebrae level, as in the case of the CT-scan. The advantage compared with the CT is that it provides similar information but without emitting radiation. However, the main limitations are that it is time consuming, requires breath-holding for a few seconds, limited by claustrophobia and tolerance to noise, and expensiveness. MRI is a technique with more limited indications in daily clinical practice, therefore is less likely to take advantage of the MRI images performed as part of clinical protocols in several pathologies. These limitations make MRI less attractive than CT-scan despite its accuracy.

1.3.7. Comparison and short of BC methods

All the currently available methods are summarised in **Table 4**.

Table 4. Comparison and short of body composition methods.

Technique	PROS	CONS
Anthropometry	<ul style="list-style-type: none"> - Low cost or inexpensive. - Safe - Portable - High accessibility 	<ul style="list-style-type: none"> - Low accuracy and low sensitivity. - No quality evaluation - Results are highly dependent on operators.
BIA/BIVA	<ul style="list-style-type: none"> - Low cost. - Safe - Fast. - Portable - High accessibility. - Useful for longitudinal comparison - Useful for fluid status using BIVA - Quality evaluation (phase angle, BIVA). 	<ul style="list-style-type: none"> - BIA: use regression equations (indirect method) and low accuracy for BC measures. - BIA: need specific and constant conditions for reproducibility - Limited applicability when BMI>35 kg/m2.
US	<ul style="list-style-type: none"> - Low cost. - Safe - Portable - Real time visualisation. - High accessibility - Useful for longitudinal comparison - Quality evaluation (grey scale) 	<ul style="list-style-type: none"> - Lack of standardised protocol or cut off. - Requires specific technical skills and operator experience. - Results (reliability and accuracy) dependent on operators. - No raw imagen. - Quality evaluation is limited by edema or severe obesity. - Quality evaluation high acquisition time
DXA	<ul style="list-style-type: none"> - Safe for repeat measures (low radiation exposure). - Good accuracy. - Simultaneous measurement of whole-body fat mass and bone mass. - Regional and whole-body measurements - Reference method so far for most of the studies 	<ul style="list-style-type: none"> - Use of radiation (low dose). - High cost. - Requires specific technical skills and operator experience. - Inability to quantify adipose compartments (no differentiation between subcutaneous and visceral fat). - Measurements are influenced by thickness (lost accuracy in obesity) or alterations in the fluid status. - No quality evaluation
CT	<ul style="list-style-type: none"> - High quantitative and qualitative accuracy - Standardised quality assessment - Differentiate abdominal adipose compartments - No influenced by high level of adipose tissue - Indicated as per protocol in many pathologies “ 	<ul style="list-style-type: none"> - Radiation exposure - High cost - Requires technical skill for image analysis (use of software for BC measure) or payment software. - Absence of normal cut-off
MRI	<ul style="list-style-type: none"> - Safe - High accuracy - High image resolution - Differentiate adipose compartments - Quality evaluation - No influenced by high level of adipose tissue 	<ul style="list-style-type: none"> - Expensive. - Long imagen acquisition time - Uncomfortable - Requires technical skill for image analysis (use of software for BC measure) or payment software.

FM: fat mass; FFM: fat free mass; BIA: bioimpedance analysis; BIVA: bioimpedance vectorial analysis, BMI: body mass index; US: ultrasound; DXA: Dual-Energy X-ray Absorptiometry; CT: computed tomography; MRI: Magnetic resonance imaging; BC: body composition.

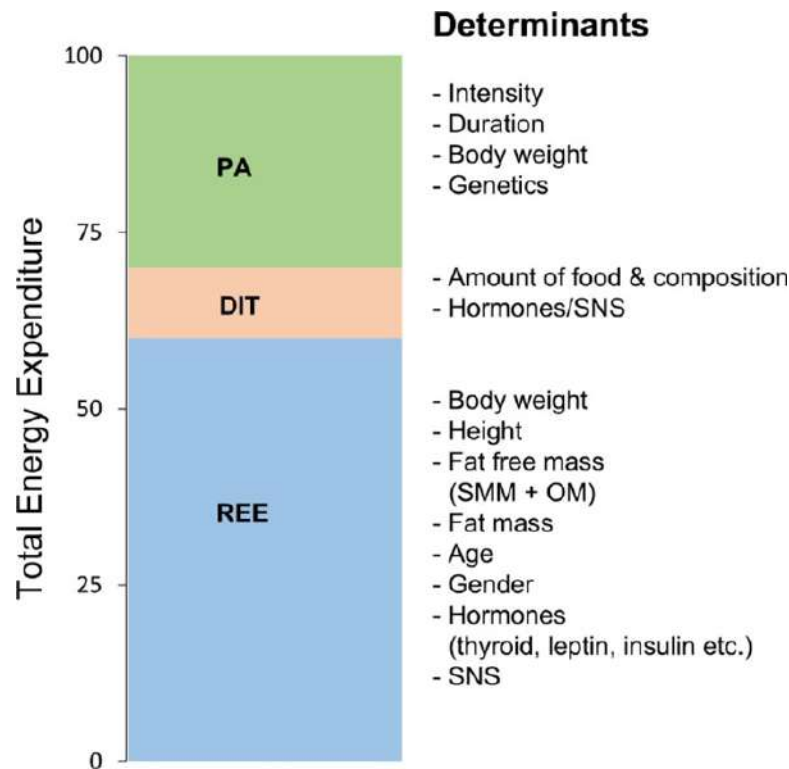
1.4. Energy expenditure

1.4.1. Definition and clinical relevance.

Energy and weight homeostasis need a balance between energy intake and energy expenditure. Total energy expenditure (TEE) is defined as the amount of heat energy used by the human body daily functioning. TEE can be divided into three main components: basal or resting energy expenditure (BEE or REE), diet-induced thermogenesis (DIT) and activity (AEE). The main component of TEE is REE and refers to the energy needed to sustain vital functions at rest in absence of recent food intake, physical activity and psychological stress. (129–131).

REE is influenced by multiple factors such as age, gender, weight, height and body composition (129,132).

Figure 11. Three main components of total energy expenditure (TEE): basal or resting energy expenditure (BEE or REE), diet-induced thermogenesis (DIT) and activity (AEE). Some of the main variables that affect each section are broken down. Image: M.J.Soaes, M.J. Muller, Resting energy expenditure and body composition: critical aspects for clinical nutrition, 2018.



REE is especially variable in disease people according to level of injury, severity and duration of the disease, nutritional status, lean body mass among others (133). Optimal nutrition support, defined as energy prescription based on measured REE, has been associated with better clinical outcomes (133). To achieve the highest quality of patient care, we should strive for patient-specific nutrition support regimens, to avoid complications associated with under- or over-feeding (130). For this reason, most of the latest ESPEN guidelines recommend measuring energy expenditure by indirect calorimetry whenever it is available (134–138).

1.4.2. Methods to estimate REE

1.4.2.1. *Predictive equations*

Due to the limited access to equipment that measures REE, predictive equations have been developed like a simple method to estimate REE using readily variables known to affect metabolism such as gender, weight, height or age without the need to use specialised equipment and appliances (129,130).

Predictive equations are derived according to a specific patient population and different clinical situations as hospitalised, critical or patients with obesity, with the aim of optimising their accuracy. They represent an accessible, simple and inexpensive method but with low correlation with reference techniques (IC) (around 60%), even when BC parameters are included in the algorithm (139).

Table 5. Description of some of the most commonly used predictive equations in clinical practice.

Equation	Factors used for calculation	Use of gender	Formula
Harris- Benedict (1919) (140)	Biological Sex, WT (kg), HT (cm), age (year)	Yes	M: $13.75 \times WT + 5.00 \times HT - 6.75 \times \text{age} + 66.47$ F: $9.56 \times WT + 1.85 \times HT - 0.67 \times \text{age} + 655.09$
Mifflin – St Jeor (1990) (141)	Biological Sex, WT (kg), HT (cm), age (year)	Yes	M: $9.99 \times WT + 6.25 \times HT - 5 \times \text{age} + 5$ F: $9.99 \times WT + 6.25 \times HT - 5 \times \text{age} - 161$
Ireton – Jones (2022) (142)	Biological Sex, WT (kg), age (year), BMI (obesity)	Yes	$629 - (11 \times \text{age}) + (25 \times WT) - (609 \times 1 \text{ if obesity};$ $\times 0 \text{ if normal BMI})$
25 kcal/kg (ESPEN) (143)	WT (kg)	No	$25 \times WT$
30 kcal/kg (ESPEN) (143)	WT (kg)	NO	$30 \times WT$

1.4.2.2. Empiric calculations

One of the alternatives recommended by clinical nutrition guidelines is the empirical use of weight by a correction factor according to the state of the disease, which usually ranges from 25 kcal to 40 kcal per kg of weight per day (Table 6). This option, although widely used in daily practice due to its simplicity, has a low correlation with the real requirements of patients.

Table 6. Short of the last ESPEN guidelines on the calculation of energy requirements and their contributions.

ESPEN Guidelines (EG)	IC recommendation	Estimated energy requirements
EG on chronic intestinal failure in adults (2023)(144)	×	1.4 times the resting energy expenditure (REE) or about 30 kcal/kg/d
EG on nutritional support for polymorbid medical inpatients (2023)(145)	✓	25-30 kcal/kg/dia
EG on Clinical Nutrition in inflammatory bowel disease (2023)(146)	✓	30-35 kcal/kg/dia
EG on obesity care in patients with gastrointestinal and liver diseases e Joint ESPEN/UEG guideline (2022)(147)	✓	25 (reference body weight)
EG on hospital nutrition (2021)(143)	×	25-35 kcal/kg/dia
EG on clinical nutrition in hospitalized patients with acute or chronic kidney disease (2021)(137)	✓	30-35 kcal/kg/dia
EG clinical nutrition in acute and chronic pancreatitis (2020)(136)	×	1.49 (1.08-1.78) the predicted resting energy expenditure
EG on clinical nutrition in liver disease (2019)(148)	✓	32 kcal/kg/dia
EG clinical nutrition in neurology (2018)(149)	✓	25-30 kcal/kg/dia
EG Clinical nutrition in surgery (2017)(150)	✓	25-30 kcal/kg/dia
EG on nutrition in cancer patients (2017)(151)	✓	25-30 kcal/kg/dia

1.4.2.3. *BIA estimations.*

BIA has recently emerged as an easily accessible tool for the BC assessment in clinical practice due to its simplicity, portability and low cost. Although this technique does not directly measure REE, some advanced BIA devices include algorithms that estimate the REE using variables such as age, biological sex, and BC, with higher accuracy when compared with the mathematical equations (152). Generally, each device uses its own equation, and these are not usually published.

1.4.3. Methods to measure REE

1.4.3.1. *Direct calorimetry.*

Direct calorimetry measures body heat produced during metabolic processes to quantify total energy expenditure (TEE). It is done in a thermally sealed chamber, maintaining a complete resting state (133). Conditions are unrealistic for clinical use and availability very limited for clinical measure. Although highly accurate is an expensive method that requires technical expertise and more specific devices (131).

1.4.3.2. *Indirect calorimetry.*

Carbon-based nutrients are converted into CO₂, H₂O and heat in the presence of oxygen. Energy expended can be calculated by measuring the amount of oxygen used (VO₂) and carbon dioxide released (VCO₂) using Weir's equation, a controlled environment (130,153). In spontaneous breathing subjects, a ventilated canopy hood is usually used to collect the inspired and expired gas (129). Air leaks of respiratory gases alter the accuracy of the measurement and should be avoided (133). It should be noted that if it is performed in a resting state, IC will allow the measurement of REE, not TEE. IC is considered the gold standard for REE measure (133,154).

Measurements must be conducted with strict adherence to resting conditions for accurate results (154). Should be performed in a quiet environment, under "resting conditions" (resting 10-15 min before starting the test), fasting at least 5

hours before the test, avoid exercise for at least 4 h and avoid nicotine, caffeine, and stimulatory nutritional supplements for at least 4 h before the calorimetric assessment (129,130).

Respiratory Quotient (RQ) is the relation of VCO_2 and VO_2 ($RQ = VCO_2 / VO_2$) and reflects the composition of oxidised substrates (129,130,155). The RQ within the physiologic range of 0.67-1.3 validates the IC measurements. Moreover, a valid test requires a “steady state” period of gas exchange defined by a 5-min interval during which VO_2 and VCO_2 vary by <10% (131). REE can also measure in hospitalised patients receiving continuous feeding, because the metabolic rate change from continuous feeding (DIT) is minimal (129) RQ is helpful to tailor the prescription of the nutrition regimen.

Conventionally, IC has been underused, mostly due to costs, shortage of personnel, and lack of education or training. With recent advances in technology, indirect calorimeters are easier to operate and more portable (156) but a number of factors could change measured REE and act as a potential error and still need an important quantity of time for each test.

1.4.3.3. *Other methods*

Doubly labelled water (DLW). Water containing non-radioactive isotope labelled hydrogen and oxygen atoms is given orally, after a baseline body liquids evaluation. This evaluation is repeated after 7-12 days to calculate the variations and then energy expenditure can be estimated. This method allows the calculation of EE, but the delay to obtain the results and the high cost limits its use in clinical practice. (133).

Fick method. Thermodilution method is used in this technique to measure the O_2 content in arterial and mixed venous blood from a pulmonary artery. VO_2 can be calculated using the Fick equation, assuming a fixed RQ. Requires a pulmonary artery catheter to measure the cardiac output, infrequent or not very feasible situation, especially in non-critical patients (133)

2. JUSTIFICATION OF THE STUDY

Currently, segmentation of two different tissues by CT is a technique considered a reference for the study of BC. This determination has been validated at the level of the third lumbar vertebra. However, questions such as the superiority of choosing a specific point of the L3 or analysing several slices remain unanswered.

Obesity represents one of the population phenotypes with greatest technical difficulty for the study of BC. In part, due to the presence of large amounts of adipose tissue. There are no studies carried out in patients with severe obesity with CT. In addition, the equations that serve to compare the results of CT with those obtained by DXA (technique with cut-off points), were developed in patients with normal BMI or overweight.

Muscle ultrasound is a technique with great advantages such as being simple, accessible, low cost and can be performed at the bedside. However, as limitations we find that its results are operator dependent, both for obtaining the image and the results (measurements). Automation using AI or image analysis tools has been shown to reduce human-dependent error. Today, there are tools to measure muscle quality using ultrasound, but there are no automatic tools that reduce interobserver variability.

The calculation of energy requirements is a fundamental aspect of the nutritional treatment plan and a challenge given the current tools. The most frequently used approach is that provided by predictive equations. Muscle mass plays a significant role in energy requirements. Techniques such as bioimpedance offer estimates based on calculations that include muscle mass quantification. However, it is not always possible to perform or have a BIA and there are no other body quantification methods that provide estimates of energy requirements.

This thesis offers three works that offer solutions to these different clinical questions, until now unanswered.

3. HYPOTHESIS

Techniques such as CT and ultrasound provide images that, when analysed by software trained by AI models, are useful for the assessment of BC and REE. Furthermore, the results obtained using these software tools, validated against reference techniques, have surpassed the currently validated surrogates widely used for the assessment of BC and REE.

4. OBJECTIVES

4.1. Main objective

To validate the usefulness of assessing muscle mass at the third lumbar vertebra in a Computed Tomography image, using semi-automatic software, compared to the standard method (body composition densitometry).

4.2. Secondary objectives

To explore the usefulness of studying body composition using CT in patients with severe obesity, and the impact of segmenting other tissues such as intramuscular adipose tissue.

To evaluate the accuracy of the pre-existing equations (based on cm² provided by CT images), to estimate in Kg the BC in PwO, by comparison with DXA.

To determine the clinical value of the mean Hounsfield Units obtained by studying a lumbar CT section.

5. COMPENDIUM OF PUBLICATIONS

5.1. Clarifications regarding the methodology

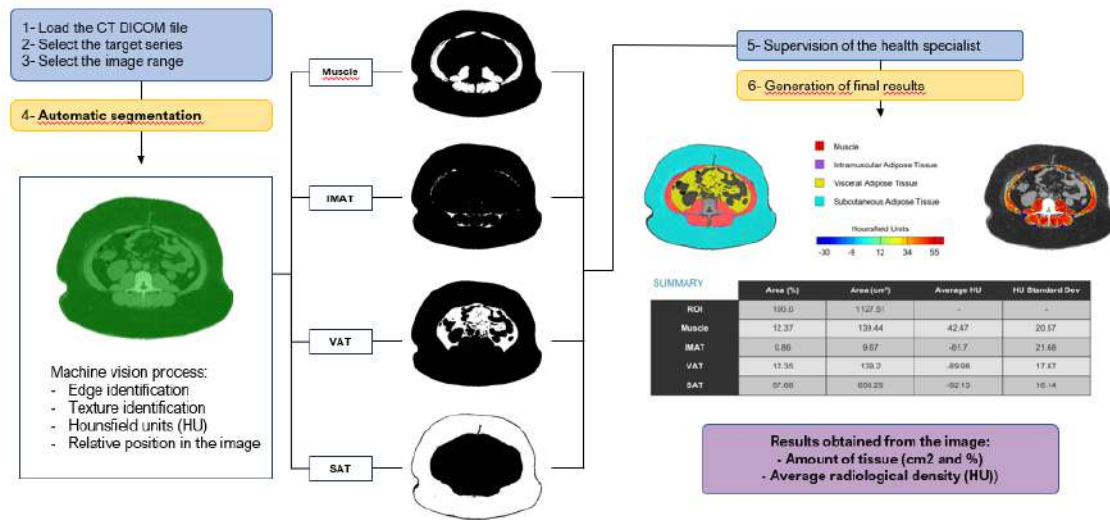
To carry out the projects that comprise the thesis, it was necessary to have a tool that could segment abdominal CT images efficiently and reliably. As there was no existing tool that met the desired characteristics, a collaboration with ARTIS Development was initiated to develop the FocusedON® software tool. The development and validation process of FocusedON® has undergone multiple stages since then.

The initial phase took place between 2017 and 2019. During these early stages of development, about 80 abdominal CT images from patients with various pathologies were used. The images were manually segmented by two radiology specialists using the Horos® program. Different tissues (visceral fat, subcutaneous fat, and muscle tissue) were manually marked on a random cross-section at the L3 level, which allowed for training the first model included in FocusedON® for the automatic segmentation of body composition in CT images. Some of the first images were simultaneously marked by both radiologists (randomly) to confirm that inter-observer differences were not significant.

The automatic segmentation performed by this first model included in FocusedON® was far from perfect, as the number of images used to train the model was very limited. However, ARTIS Development included a tool that allows for the manual correction of the segmentation performed by the software easily and quickly. Combining the initial approach of segmentation performed by the software, and the ease of making manual corrections, it became possible to segment images much more efficiently.

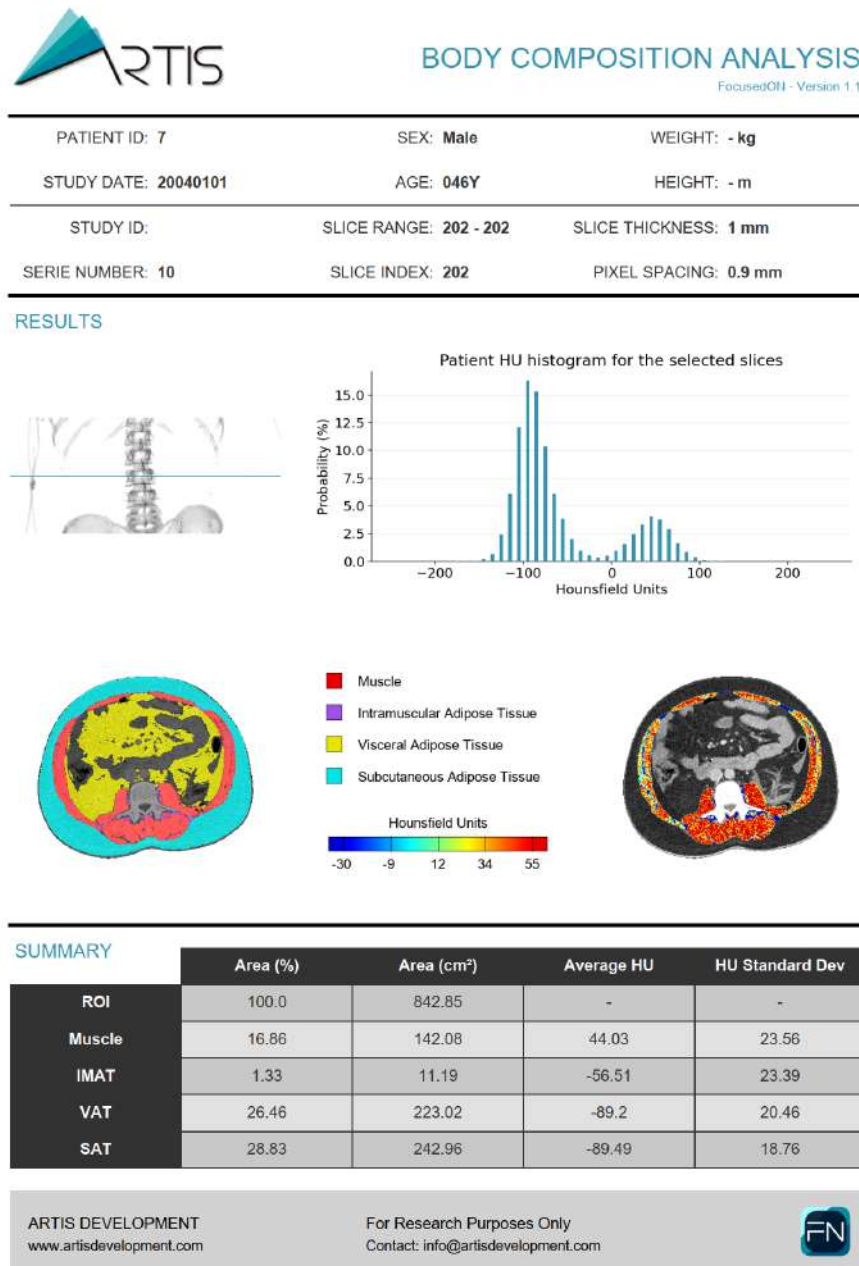
Thus, a tool was already available that could be used to conduct the studies, providing precise and reliable results with less human effort. Additionally, ARTIS Development also introduced into the software the ability to "learn" from manual corrections made by the user. As new images are marked and manual corrections are made, these corrections can be used to retrain the segmentation models integrated into the software, enhancing their accuracy. In this way, by early 2024, FocusedON® had been trained with over 3000 CTs.

Figure 12. Processing and segmentation of a section at the level of the 3rd lumbar vertebra, analyzed using FocusedON-BC software.



Currently, the algorithm is capable of automatically and accurately identifying and measuring the different components of body composition previously mentioned, as well as intra/intermuscular fat, executing the tissue segmentation in just a few seconds. The software imports the results into a PDF and Excel report for easier data management (Figure 13).

Figure 13. Model report generated by FocusedOn-BC software after TC segmentation



5.2. First article

Palmas, F., Ciudin, A., Guerra, R., Eiroa, D., Espinet, C., Roson, N., Burgos, R., & Simó, R. (2023). Comparison of computed tomography and dual-energy X-ray absorptiometry in the evaluation of body composition in patients with obesity. *Frontiers in Endocrinology*, 14. <https://doi.org/10.3389/fendo.2023.1161116>



OPEN ACCESS

EDITED BY
Manuel Gil-Lozano,
Helmholtz Center München, Helmholtz
Association of German Research Centres
(HZ), Germany

REVIEWED BY
Luiz Guilherme Kraemer-Aguilar,
Rio De Janeiro State University, Brazil
Diego Bellido Guerrero,
Servicio Gallego De Salud, Spain

*CORRESPONDENCE
Andreea Ciudin
✉ andreea.ciudin@vallhebron.cat
Rafael Simó
✉ rafael.simo@vhr.org

RECEIVED 07 February 2023
ACCEPTED 17 April 2023
PUBLISHED 26 June 2023

CITATION
Palmas F, Ciudin A, Guerra R, Eiroa D,
Espinete C, Roson N, Burgos R and Simó R
(2023) Comparison of computed
tomography and dual-energy X-ray
absorptiometry in the evaluation of body
composition in patients with obesity.
Front. Endocrinol. 14:1161116.
doi: 10.3389/fendo.2023.1161116

COPYRIGHT
© 2023 Palmas, Ciudin, Guerra, Eiroa,
Espinete, Roson, Burgos and Simó. This is an
open-access article distributed under the
terms of the [Creative Commons Attribution
License \(CC BY\)](https://creativecommons.org/licenses/by/4.0/). The use, distribution or
reproduction in other forums is permitted,
provided the original author(s) and the
copyright owner(s) are credited and that
the original publication in this journal is
cited, in accordance with accepted
academic practice. No use, distribution or
reproduction is permitted which does not
comply with these terms.

Comparison of computed tomography and dual-energy X-ray absorptiometry in the evaluation of body composition in patients with obesity

Fiorella Palmas¹, Andreea Ciudin^{1,2,3,4*}, Raul Guerra⁵,
Daniel Eiroa⁶, Carina Espinete⁷, Nuria Roson⁶, Rosa Burgos^{1,2,3}
and Rafael Simó^{1,2,3,4*}

¹Endocrinology and Nutrition Department, Hospital Universitari Vall d'Hebron, Barcelona, Spain,
²Diabetes and Metabolism Research Unit, Vall d'Hebron Institut de Recerca (VHIR), Barcelona, Spain,
³Department of Medicine, Universitat Autònoma de Barcelona, Barcelona, Spain, ⁴Centro De
Investigación Biomédica En Red De Diabetes y Enfermedades Metabólicas Asociadas (CIBERDEM),
Instituto De Salud Carlos III (ISCIII), Madrid, Spain, ⁵ARTIS Development, Las Palmas, Spain,
⁶Department of Radiology, Institut De Diagnòstic Per La Imatge (IDI), Hospital Universitari Vall
d'Hebron, Barcelona, Spain, ⁷Nuclear Medicine Department, Vall Hebron Hospital, Barcelona, Spain

Objective: a) To evaluate the accuracy of the pre-existing equations (based on cm² provided by CT images), to estimate in kilograms (Kg) the body composition (BC) in patients with obesity (PwO), by comparison with Dual-energy X-ray absorptiometry (DXA). b) To evaluate the accuracy of a new approach (based on both cm² and Hounsfield Unit parameters provided by CT images), using an automatic software and artificial intelligence to estimate the BC in PwO, by comparison with DXA.

Methods: Single-centre cross-sectional study including consecutive PwO, matched by gender with subjects with normal BMI. All the subjects underwent BC assessment by Dual-energy X-ray absorptiometry (DXA) and skeletal-CT at L3 vertebrae. CT images were processed using FocusedON-BC software. Three different models were tested. Model 1 and 2, based on the already existing equations, estimate the BC in Kg based on the tissue area (cm²) in the CT images. Model 3, developed in this study, includes as additional variables, the tissue percentage and its average Hounsfield unit.

Results: 70 subjects (46 PwO and 24 with normal BMI) were recruited. Significant correlations for BC were obtained between the three models and DXA. Model 3 showed the strongest correlation with DXA ($r = 0.926$, CI95% [0.835–0.968], $p < 0.001$) as well as the best agreement based on Bland – Altman plots.

Conclusion: This is the first study showing that the BC assessment based on skeletal CT images analyzed by automatic software coupled with artificial

intelligence, is accurate in PwO, by comparison with DXA. Furthermore, we propose a new equation that estimates both the tissue quantity and quality, that showed higher accuracy compared with those currently used, both in PwO and subjects with normal BMI.

KEYWORDS

obesity, morbid obesity, body composition, computed tomography, dual-energy X-ray absorptiometry

Introduction

Obesity is a chronic and relapsing disease which prevalence is significantly increasing worldwide and its related comorbidities suppose a high cost for healthcare system (1–3).

At present body mass index (BMI) remains a categorical diagnostic criterion for obesity. Nevertheless, BMI has serious limitations and do not provide information on the body composition (BC) and the metabolic condition of the subjects (4). Recently, efforts have focused to identify more specific prognostic factors and biomarkers of obesity and its metabolic complications (5–7). The American Association of Clinical Endocrinologists (AACE) proposed a new definition for obesity: “adiposity-based chronic disease (ABCD)”, which has also adopted by the European Society of Obesity (EASO) (8, 9). The concept “adiposity-based” refers not only to the total quantity of body fat, but also to its distribution and/or functionality (4, 10).

Furthermore, besides body fat, the muscle mass has a very relevant and complex role in the BC and body homeostasis and metabolic condition (11–13). Sarcopenia, which is the loss of muscle mass and strength of physical function synergistically worsen the adverse effects of obesity (14). However, the study of BC is crucial for identifying sarcopenia, especially in PwO, where body volume can mask low muscle mass if only anthropometric data is used for the clinical assessment (15). Recently, the European Society for Clinical Nutrition and Metabolism (ESPEN) and EASO have agreed a definition and diagnostic criteria for sarcopenic obesity, a condition in which sarcopenia and obesity coexists and leads to a cumulative risk derived from the two clinical situations (15, 16). In addition to measure the amount of adipose tissue or muscle mass, it is important to know its distribution and proportion, given its significant role in pathologies such as metabolic syndrome and associated complications (17–20). However, methods to assess BC are not taken into consideration in the daily clinical practice in the obesity management due to the lack of simple and reliable tests.

Dual-energy X-ray absorptiometry (DXA) has long been considered a reference technique to assess BC and it is still a reference method (14). It provides the mass of the different tissues, measured in kilograms. However, DXA does not provide information on the distribution of adipose tissue at the abdominal level (SAT or VAT) (21). Furthermore, in many clinics, accessibility to DXA is limited and except for the assessment of bone density, it is not a test that is performed in the usual clinical routine (22, 23).

In this scenario, CT emerges as a technique widely used in clinical practice that contains very precise information for assessing BC (24–28). Regional analysis of fat and fat-free mass at the third lumbar vertebra was shown to have a high correlation with total BC, and provides significant additional information of tissue quality and myosteatosis, based on the Hounsfield units (HU) (29–32). To obtain the CT image, the emission of radiation is necessary (approximately 10 mSv). Nonetheless, at present the assessment of BC by means of a CT image is been largely used in clinical research, especially in those pathologies in which the CT evaluation is part of the protocol, such as some types of cancer or abdominal pathologies (33).

Currently, BC assessment by CT is obtained by manual or semi-automatic marking software that provide an area parameter (cm^2) and average of Hounsfield Units of the of target tissue (34). The use of this type of software requires trained staff able to manually correct the images, therefore, the evaluation of these results is time consuming and unfeasible in the current clinical practice at large scale. However, emerging technologies, such as artificial intelligence (AI), have promoted the development of new software tools able to rapidly and precisely analyze the images obtained by CT resulting in qualitative and quantitative information (24, 25, 27, 35). As far as we know at present no such tool coupled with AI is used for the BC assessment based on CT scan images in PwO.

The accuracy of the BC assessment by CT image was evaluated by comparison with DXA, as the reference method (36, 37). For this purpose, equations were developed (i.e., those described by Mourtzakis et al) (24) to convert the cm^2 information provided by the CT-scan into Kg provided by DXA. It should be noted that these equations have been validated in subjects with mean BMI < 27 kg/m^2 , most of them with cancer and malnutrition. At present there is no data regarding the accuracy of these equations in PwO. Furthermore, these equations were based only on the area parameter (cm^2) provided by the CT-scan and did not take into the account the HU.

On this basis, we designed the present study aimed to a) evaluate the accuracy of the pre-existing equations (based on cm^2 provided by CT images), to estimate in Kg the BC in PwO, by comparison with Dual-energy X-ray absorptiometry (DXA). b) evaluate the accuracy of a new approach (based on both cm^2 and HU parameters provided by CT images), using an automatic software and AI to estimate the BC in kg in PwO, by comparison with DXA.

Materials and methods

Patient selection

We performed a single-centre cross-sectional study including consecutive patients with morbid obesity, matched by gender with normal BMI subjects at Vall d'Hebron University Hospital, between April and September 2021. Control group was randomly drawn from patients with DXA performed in our centre with normal BMI (20–25 kg/m²).

The study was approved by the local Ethics Committee (PR (AG)510/2021) and carried out in accordance with the Declaration of Helsinki. All the patients signed the informed consent form before the participation in the study.

Inclusion criteria: a) age between 18 and 60 years; b) morbid obesity (BMI >40 kg/m² or BMI > 35 kg/m² with at least one comorbidity related to obesity).

Exclusion criteria: a) any condition except obesity that can affect the body composition, (ex. myopathy, neurodegenerative disease, renal, liver and heart failure etc); b) any treatment that can affect the body composition as per investigator criteria (ex. corticosteroids, growth hormone, etc); c) unable to perform both DEXA and CT scan; d) anthropometric data above the usual CT-scan machines (such as body weight >205kg or the presence of an abdominal circumference greater than the ability to obtain an image in a cut (>200cm corresponding to CT-scan gantry diameter, usually of 70cm); e) metal plates or artifacts that can affect the radiodensity measurements (Hounsfield Units).

Clinical data collection

All the subjects underwent within a maximum of 30 days from the inclusion in the study: complete medical history, anthropometric data (weight-kg, height-m), biochemical analysis, body composition DXA and skeletal CT centered at L3 vertebrae.

BMI was calculated using the following formula: weight (kg)/height² (m²).

DXA analysis

Body composition DXA was performed using GE Lunar Prodigy dual-energy X-ray absorptiometry (DXA) scanner (GE Healthcare, Madison, WI, USA) by a certified technician. The software used for the total and regional body composition estimation was Encore (GE Healthcare) version 15. Each region was automatically analysed and then supervised by a Nuclear Medicine Physician. The following variables were registered: fat mass (Kg), fat free mass (Kg), appendicular skeletal muscle mass (Kg), appendicular skeletal muscle mass index (Kg/m²).

CT data extraction

Skeletal CT images focused at L3 vertebrae were obtained using a multidetector computed tomography scanner (Aquilion Prime SP,

Canon Medical Systems, Japan), using the following technical parameters: 135 kV (tube voltage), 1mm 80 row (detector configuration), tube current modulation, and 0.8 sec/rotation (gantry rotation). The following variables were registered: skeletal muscle mass area or SMA (cm² and %), skeletal muscle mass index or SMI (cm²/m²), intramuscular adipose tissue area or IMAT (cm² and %), intramuscular adipose tissue index or IIMAT (cm²/m²), area of visceral fat mass (VFA) (cm² and %), subcutaneous fat (SFA) (cm² and %), visceral fat mass index (VFI) (cm²/m²), and subcutaneous fat (SFI)(cm²/m²), and average Hounsfield Units (HU) value per each segmented tissue.

The CT images centered at the third lumbar vertebra (L3) were analysed using FocusedON-BC software. This software presents a user-friendly interface and includes a semiautomatic labeling tool that allows the user to modify the body mass segmentation automatically carried out by the software. To determine skeletal muscle and abdominal adipose tissue area we analysed the cross-sectional CT images at the third lumbar vertebra (L3) using FocusedON-BC software. A total of 16 slices for each patient were assessed. The muscles involved in the analysis were: psoas, erector spinae, quadratus lumborum, transversus abdominis, external and internal obliques, and rectus abdominis muscles. Adipose tissue was classified as subcutaneous, visceral, and infiltrating the muscles. All areas were measured in cm² and normalized for height. Tissue quality was assessed based on its average Hounsfield Units (HU) value. Standard thresholds were employed as follows: -29 to 150 HU for skeletal muscle, -190 to -30 for subcutaneous adipose tissue and -150 to -50 for visceral adipose tissue (32, 38).

Models used for the body composition evaluation

The research works carried out so far have demonstrated the good correlation between the muscle and fat tissues area, measured in cm² at the L3 vertebral level, with the total amount of muscle and body fat mass, measured in kg by DXA. Mourtzakis et al. (24) has proposed a linear regression model, referred in this work as Model 1, which has also been used by Tewari et al. (39). However, these research works have been carried out using a relatively short number of patients with similar BMI values, and none of them have included people living with morbid obesity. For these reasons, the first goal of this work is to evaluate the suitability of Model 1 to assess muscle mass for patients with a wider range of BMI values, include people living with obesity.

Model 1: This is the most widely used in clinical practice (24) and estimates the fat mass (FM) and fat-free mass (FFM) using the area labelled as fat (visceral and subcutaneous) and muscle in a CT slice at L3 vertebral level (measured in cm²).

This model is described by Equation 1 (Mourtzakis et al. model) (24):

$$FM_{(kg)} = 0.042 \cdot FM_CT_L3_{(cm^2)} + 11.2 \quad (\text{eq 1.a})$$

$$FFM_{(kg)} = 0.3 \cdot Muscle_CT_L3_{(cm^2)} + 6.06 \quad (\text{eq 1.b})$$

Values of $FM_{CT_L3(cm^2)}$ and $Muscle_{CT_L3(cm^2)}$ for each patient are directly obtained from the FocusedON-BC software. These values were used to estimate the FM and FFM in kilograms using this model.

Model 2: This model has been generated to evaluate if Model 1 methodology is suitable to estimate muscle and fat mass in kg for patients with different BMI values, including people living with obesity. Concretely, least squared method has been used to adjust the linear regression model described in Model 1 (24) to better fit our patient's data, and hence, better results are expected. This model is described by Equation 2:

$$FM_{(kg)} = 0.058 \cdot FM_{CT_L3(cm^2)} + 7.35 \quad (\text{eq 2.a})$$

$$FFM_{(kg)} = 0.27 \cdot Muscle_{CT_L3(cm^2)} + 13.31 \quad (\text{eq 2.b})$$

FocusedON Model: is a new model proposed by our group based on the present study, using FocusedON software. The goal of this approach is to provide a solution that can be used to precisely estimate the body fat mass and fat free mass (in kg) based on the data extracted from a CT scan with independence of the patient BMI. This approach takes in consideration both the tissue area, measured in percentage, and its average density, measured in HU. These data are directly obtained from FocusedON-BC software. This model is described by Equation 3:

$$\rho \approx \frac{HU}{1000} + 1 \rightarrow \left(\frac{kg}{cm^3} \right) \quad (\text{eq 3.a})$$

$$FM_{(kg)} = 0.0069 \cdot \frac{Weight}{\rho_{ROI}} \cdot FAT(\%) \cdot \rho_{FAT} + 4.53 \quad (\text{eq 3.b})$$

$$FFM_{(kg)} = Weight_{(kg)} - FM_{(kg)} \quad (\text{eq 3.c})$$

First, this model considers the tissue density according to its HU average value, as shown in Equation 3.a. This equation estimates the tissue density in kilograms per cubic centimeter based on its radiodensity measured in HU. As FocusedON-BC provides the average patient radiodensity (for the analyzed images), the patient volume can be extrapolated based on this value and the patient weight as $V_{total} = Weight / \rho_{ROI}$. Then, since FocusedON-BC provides each tissue quantity measured in area percentage, we can extrapolate to estimate the total tissue volume as $V_{tissue} = (V_{total} \cdot Tissue\ percentage) / 100$. Finally, tissue mass measured in kilograms can be estimated according to its density as $M_{tissue} = V_{tissue} \cdot \rho_{tissue}$. Following this procedure for fat tissue we obtained $FM_{(kg)} = m \cdot (Weight / \rho_{ROI}) \cdot FAT(\%) \cdot \rho_{FAT} + n$. If we replace the weight, density and tissue percentage with our patient data and apply least squared method to calculate m and n we obtain Equation 3.b. Since we already know patients' weight and we are estimating the amount of fat mass in kilograms, we can directly know the amount of fat free mass as the difference (Equation 3.c).

Statistical analyses

Statistical analysis was performed using Python 3.8. Continuous variables are presented as mean \pm standard deviation (SD) for normal distributed variables and median \pm interquartile range (IQR) for non-normal distributed variables. Categorical variables are presented using percentages. Statistical significance was accepted at $p < 0.05$. Quantile-Quantile Plot (QQ) has been used to assess the normal distribution of the dataset. The correlation between analysed methods and the DXA was assessed using linear correlation coefficient (Pearson). Bland-Altman plots were used to estimate agreement between analysed methods and DXA. Additionally, simplified error grid plots have been also used to assess the error obtained in the estimations. The error ($<10\%$, $10-20\%$ or $>25\%$) was measured as the difference between the estimated value and the reference value provided by DXA.

Sample size calculation: At present there is no data regarding the use of equations based on CT-scan images for the BC assessment in PwO therefore we were not able to calculate a sample size based on this population. Nevertheless, we took into the account the previous data reported by Mourtzakis (24) for estimating the whole-body fat mass of the subject, measured in kg, based on the fat area quantified in a CT scan image at L3 in cm^2 was also useful for subjects with a wider range of BMI values, including patients living with obesity. This study obtained the next correlation model using 51 subjects (oncological patients reported by the study with an BMI = 26.9 ± 6.2 kg/m²):

$$FM_{whole\ body\ (kg)} = 0.042 \cdot FML3\ (cm^2) + 11.2 \cdot r = 0.88, p < 0.001$$

Due to the high correlation obtained, and the fact that it has been further validated in other studies (Tewari et al. (39)), we assume that 51 patients should be enough to carry out this proof of concept. However, as we pretended to test the model for subjects with a wider range of BMI values (higher variability), we increased the sample size by 35%, resulting a sample size of $51 \times 1.35 = 68.85$ patients.

Furthermore, we carried out the next calculation (based on Cohen equation) to verify that the sample-size is correct for our goal:

$$N = Z^2 \cdot S^2 / d^2$$

N is the sample size; Z is the critical value of the standard normal distribution at the 5% significance level (1.96); S² is the estimated standard deviation of the estimating variable ($284\ cm^2$ of fat tissue measured at L3); d is the desired precision in the outcome variable (whole-body fat mass measured in kg). Based on this equation, if we expect a precision of 4 kg ($d=4$), the obtained N value would be also 68 subjects. We included in our study 70 subjects.

Results

A total of 70 subjects were included in this study: 46 PwO and 24 with normal BMI. The baseline characteristics are shown in Table 1. The BMI of all the subjects, both PwO and normal BMI showed a normal distribution as reflected in the QQ plot displayed in Figure 1.

The correlations and agreement between the reference method, DXA, with the three models that were created for the study are displayed in Table 2. Multiple conclusions can be drawn from these results.

First, the correlation and agreement obtained with each model when using only 1 CT slice is very close to the one obtained when using 16 slices. This suggests that a single slice may be representative enough for the BC assessment based on CT scan images.

Secondly, it can also be observed that all models present high correlation values (higher than 0.75 in all the tests), being **FocusedON Model** the one providing the highest correlation (0.93). It should be noted that a high correlation value does not necessarily imply a good agreement between the reference method, DXA, and the tested model. In this regard, Figures 2, 3 graphically show a scatter plot with the trendlines, correlation values and confidence intervals corresponding to each model. In Figure 2, where points corresponding to **Model 1** and **Model 2** are

considerably far from the tendency, reflects that these two models based on currently used equations, present bad agreement with respect to DXA in PwO. Figure 3, that corresponds to **FocusedON Model**, the points are closer to the trendline, showing that the newly proposed model presents a good agreement with respect to DXA.

Furthermore, for a better accuracy, data was confirmed by two additional statistical analyses (agreement Bland-Adman plots- Figure 4 and error grid- Figure 5). In both analysis, **FocusedON Model** still presented the best agreement with DXA in comparison with Model 1 and Model 2. The numerical values corresponding to these plots are also summarized in Table 2.

Discussion

This is the first study showing that the BC assessment based on skeletal CT images analyzed by automatic software coupled with artificial intelligence, is accurate in PwO, by comparison with DXA. Furthermore, we propose a new equation that estimates both the tissue quantity and quality, that showed higher accuracy compared with those currently used, both in PwO and subjects with normal BMI.

At present, the model most widely used in the clinical practice was developed by Mourtzakis et al. (24). This model estimates the FM and FFM using the area labelled as fat (visceral and

TABLE 1 Demographic and clinical characteristics of the subjects included in the study.

N	All	Patients with MO	Control group	p- value
	70	46	24	
Gender, females, %(n)	59 (41)	70 (32)	38 (9)	0.02
Age (years), mean (SD)	47.37 ± 12.8	43.17 ± 10.35	55.42 ± 13.37	<0.001
Weight (kg), mean (SD)	101.41 ± 23.78	114.37 ± 14.49	76.57 ± 17.5	0.00007
BMI (kg/m ²), mean (SD)	37.63 ± 9.52	43.56 ± 4.69	26.27 ± 4.86	0.00007

BMI, body mass index; SD, standard deviation.

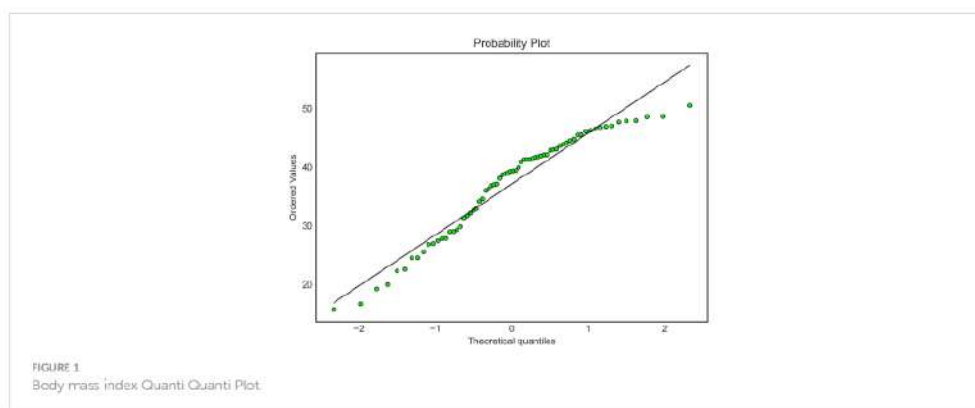
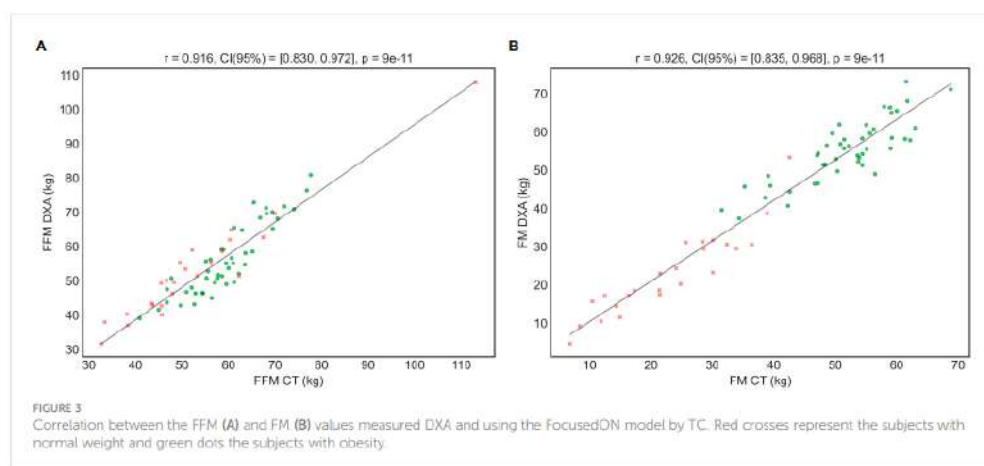
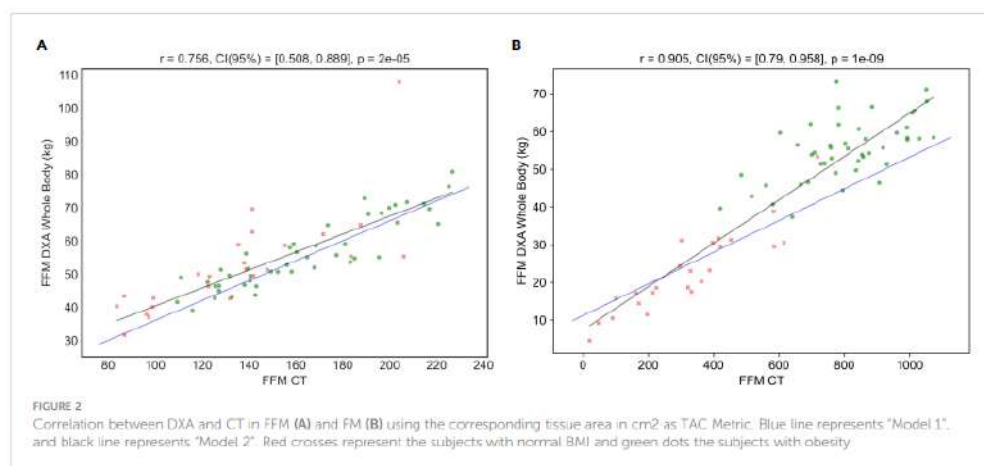
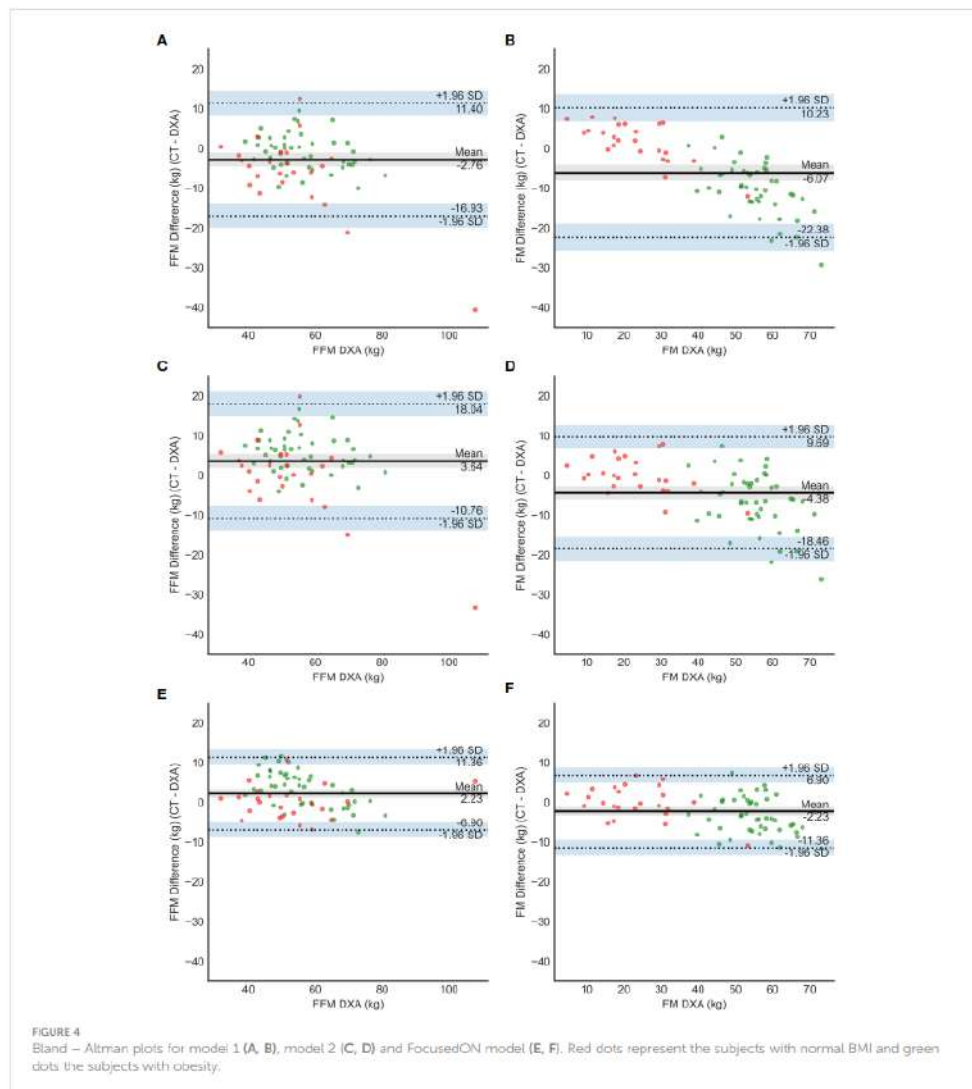


TABLE 2 Correlation and agreement between the different models with DXA.

		Fat free mass				Fat Mass			
		Pearson	Error (kg)			Pearson	Error (kg)		
			-1.96 SD	Mean	+1.96 SD		-1.96 SD	Mean	+1.96 SD
1 slice	Model 1	0.75	-17.08	-2.76	11.56	0.91	-22.31	-6.03	10.25
	Model 2	0.75	-11.1	3.26	17.62	0.91	-18.56	-4.48	9.59
	FocusedON model	—	-6.77	2.42	11.61	0.93	-11.61	-2.42	6.77
16 slices	Model 1	0.76	-16.93	-2.76	11.4	0.90	-22.38	-6.07	10.23
	Model 2	0.76	-10.76	3.64	18.04	0.90	-18.46	-4.38	9.69
	FocusedON model	—	-6.9	2.23	11.36	0.93	-11.36	-2.23	6.9

— indicates that the fat free mass has not been directly estimated by the FocusedON model, and so, the Pearson coefficient has not been calculated. Instead, the fat free mass has been calculated as the difference between patient weight and the fat mass estimated by the FocusedON model.

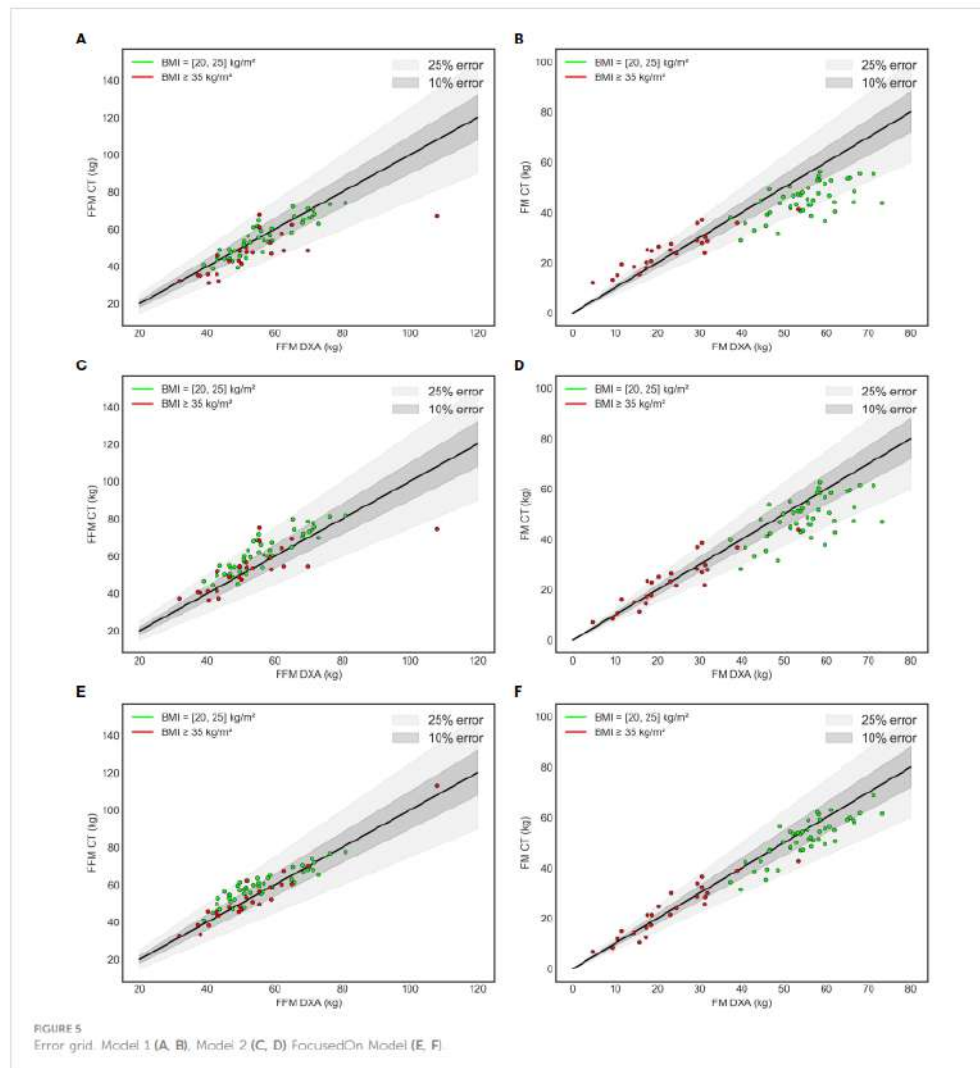




subcutaneous) and muscle in a CT slice at L3 vertebral level (measured in cm^2). These authors evaluated 51 patients diagnosed of lung or colorectal cancer with a BMI of $26.9 \pm 6.2 \text{ kg/m}^2$ and obtained a high correlation with DXA, $r=0.88$ (MRE $3.49 \pm 2.31 \text{ kg}$, $p<0.001$) for FM and $r=0.94$ (MRE $5.23 \pm 3.54 \text{ kg}$, $p<0.001$) for FFM. Few years later Tewari et al. (39) validated the results using the same model, based on 47 patients with esophagogastric cancer with a mean BMI $27.65 \pm 5.31 \text{ kg/m}^2$. They obtained a correlation with DXA of 0.66 (IC 0.451–0.9.964, $p<0.0001$) for FM and 0.76 (IC

95% -0.8621 – 0.8325, $p<0.0001$) for FFM. It should be noted that, to the best of our knowledge, most of the studies using this model have been performed in the oncological setting or in critical care units but not in patients with obesity (40–42).

We tested the model proposed by Mourtzakis (24), defined as Model 1, and an adjusted version defined as Model 2 (see Methodology). Bland-Altman plots showed that both models had low agreement with DXA. Both models underestimate the FM for the subjects with obesity and overestimate it in the subjects with



normal BMI. In the case of Model 2 the errors were lower but still they remained significant. These findings suggest that these 2 models, based only in the tissue area, measured in cm^2 , cannot be generalized for a wide range of BMIs to accurately estimate body FM and FFM in kg. Additionally, these models are less precise for subjects with obesity.

The CT image also provides the HU of the tissues. The HU is a quantitative measurement of radio density. The absorption/

attenuation coefficient of radiation within a tissue is used during CT reconstruction to produce a grayscale image (43). The absorption of X-ray is proportional to the density of the tissue. The use of HU allows to evaluate the tissue quality and estimate its density. In this study we have created a new model that considers, for the first time, both the percentages of adipose and muscle tissue and their average HU, instead of just each tissue area in cm^2 as in the models used so far in the literature. This new model (Model 3 –

FocusedON Model) has provided results that are more accurate and the data was confirmed by three different statistical analysis methods. The correlation between Model 3 and DXA was the strongest. It also showed better agreement with DXA based on Bland-Atman plots, also without under or overestimating the FM and FFM in any of the two groups.

This study proposes a new model, FocusedON model, for estimating body composition based on CT data in PwO and normal BMI. This new model has demonstrated to be superior in accuracy to those presented in previous studies, which only take into account the quantity of tissue measured in cm^2 . Our model uses parameters of tissue quantity (%) and quality (HU) to create more accurate equations. These findings underlie the importance of revisiting the traditional equations and models where they only used CT measurements expressed in cm^2 .

In addition, it should be noted that the cut-off points commonly used today for the diagnosis of sarcopenia have been developed in oncological population groups, with a small sample size that did not significantly include the overweight or people living with obesity. We have shown in our study that these models are not optimal for the assessment of PwO, so the present cut-off levels should be reevaluated. Another novelty resulted from our study is that we propose a simplified method using single-slice CTscan image. Previous study recommends that multiple slices should be analyzed (44). In our study, using multiple slices in the analysis of BC was not significantly superior to use a single slice for the CT-scan image.

Nevertheless, our study has some limitations: First, patient's weight limit: The method cannot be applied in subjects with severe obesity that cannot undergo CT-scan, such as weight > 200 kg. However, these patients represent <3% of the PwO. Small sample size, it should be noted that we performed a proof-of-concept study with a strong agreement between the model and the reference method. We consider that this apparent limitation has no significant influence on the results of the study due to several arguments: a) the sample size of our study is higher (70 subjects) than the study published by Mourtzakis et al. (24) (51 subjects) as previously explained, which is the currently used model to estimate BC based on CT-scan; b) the proposed model includes not only quantitative but also qualitative variables, allowing a better approximation to the clinical and metabolic reality of the patients. Actually, the combination of these variables will be used in future studies with a larger sample size to produce more complex and precise models (i.e., using non-linear machine learning methods).

In summary, in this proof-of-concept study we demonstrated for the first time that the equations currently used for BC assessment based on CT images are not accurate in PwO. Additionally, we proposed a new simplified model, based on single-slice approach of CT-scan image, including both quantitative and qualitative data of BC, that showed better results than the ones being widely used at present in the clinical practice. Further studies are needed to validate and refine this new methodology, which could open a new avenue in the study and management of obesity, by accurately assess the BC "at a glance" with simple and automatic methods.

Ethical Approval

All procedures performed in studies involving human participants were in accordance with the ethical standards of the institutional and/or national research committee and with the 1964 Helsinki declaration and its later amendments or comparable ethical standards. This study protocol was reviewed and approved by Comité de Ética de Investigación con Medicamentos del Hospital Universitario Vall d'Hebron, approval number PR(AG)510/2021. The study has been granted an exemption from requiring written informed consent.

Data availability statement

The original contributions presented in the study are included in the article/supplementary material. Further inquiries can be directed to the corresponding authors.

Author contributions

Conceptualization: AC, FP, RS. Data curation FP, RG. Formal analysis FP, AC, RG. Funding acquisition RS. Investigation: FP, RG, DE, NR, CE, RB. Methodology FP, RG, AC. Project administration: AC, RS; Resources FP, AC. Software RG. Supervision RS, RB. Validation AC, RS. Visualization AC, RG, DE, CE, NR, RB, RS. Roles/Writing - original draft: FP, RG; Writing - review & editing AC, RS. All authors contributed to the article and approved the submitted version.

Funding

This study was supported by grants from the Instituto de Salud Carlos III (Fondo de Investigación Sanitaria, PI20/01806). The funders had no role in study design, data collection and analysis, decision to publish, or preparation of the manuscript.

Conflict of interest

The authors declare that the research was conducted in the absence of any commercial or financial relationships that could be construed as a potential conflict of interest.

Publisher's note

All claims expressed in this article are solely those of the authors and do not necessarily represent those of their affiliated organizations, or those of the publisher, the editors and the reviewers. Any product that may be evaluated in this article, or claim that may be made by its manufacturer, is not guaranteed or endorsed by the publisher.

References

1. Iyedi A, Soltani S, Motlagh SZT, Emadi A, Shahinfar H, Moosavi H, et al. Anthropometric and adiposity indicators and risk of type 2 diabetes: systematic review and dose-response meta-analysis of cohort studies. *BMJ* (2022) 376(1). doi: 10.1136/bmj.2021.067516
2. Di Angelantonio E, Bhupathiraja SN, Wormser D, Gao P, Kaptoge S, de Gonzalez AB, et al. Body-mass index and all-cause mortality: individual-participant-data meta-analysis of 239 prospective studies in four continents. *Lancet* (2016) 388(10046):776–86. doi: 10.1016/S0149-6736(16)30175-1
3. Blüher M. Obesity: global epidemiology and pathogenesis. *Nat Rev Endocrinol* (2019) 15(5):288–98. doi: 10.1038/s41574-019-0176-8
4. Gómez-Ambrosi J, Silva C, Galefré JC, Escalada J, Santos S, Millán D, et al. Body mass index classification misses subjects with increased cardiometabolic risk factors related to elevated adiposity. *Int J Obes* (2012) 36(2):286–94. doi: 10.1038/ijo.2011.100
5. Borgia M, West J, Bell JD, Harvey NC, Romu T, Heymsfield SB, et al. Advanced body composition assessment: from body mass index to body composition profiling. *J Invest Med* (2018) 66:887–95. doi: 10.1136/ijim-2018-000722
6. Yokum S, Ng J, Stice E. Relation of regional grey and white matter volumes to current BMI and future increases in BMI: a prospective MRI study. *Int J Obes (Lond)* (2012) 36(5):656. doi: 10.1038/1102.011.175
7. Garvey WT. New horizons, a new paradigm for treating to target with second-generation obesity medications. *J Clin Endocrinol Metab* (2022) 107(4):1339–47. doi: 10.1210/clinem/dgab848
8. Mechanick JL, Hurler DL, Garvey WT. Adiposity-based chronic disease as a new diagnostic term: the American association of clinical endocrinologists and American college of endocrinology position statement. *Endocrine Pract* (2017) 23(3):372–8. doi: 10.4158/EP161688.PS
9. Frühbeck G, Busetto L, Dicker D, Yumuk V, Goossens GH, Hebebrand J, et al. The ABCD of obesity: an EASO position statement on a diagnostic term with clinical and scientific implications. *Obes Facts* (2019) 12:131–6. www.karger.com/ofa. doi: 10.1159/000497124
10. Ballesteros Pomar MD, Vilarrasa García N, Rubio-Herrera MA, Barahona MJ, Bueno M, Caxías A, et al. Abordaje clínico integral SEN de la obesidad en la edad adulta: resumen ejecutivo. *Endocrinol Diabetes Nutr* (2021) 68(2):130–6. doi: 10.1016/j.endinu.2020.05.003
11. Janssen I, Heymsfield SB, Wang ZM, Ross R. Skeletal muscle mass and distribution in 468 men and women aged 18–88 yr. *J Appl Physiol* (2000) 89(1):81–8. doi: 10.1152/jappl.2000.89.1.81
12. Hunter GR, Singh H, Carter SJ, Bryan DR, Fisher G. Sarcopenia and its implications for metabolic health. *J Obes* (2019) 2019. doi: 10.1155/2019/8031705
13. Argiles JM, Campos N, Lopez-Pedrosa JM, Rueda R, Rodriguez-Mañas L. Skeletal muscle regulates metabolism via interorgan cross-talk: roles in health and disease. *J Am Med Dir Assoc* (2016) 17(9):789–96. doi: 10.1016/j.jamda.2016.04.019
14. Cruz-Jentoft AJ, Bahat G, Bauer J, Boirie Y, Bruyère O, Cederholm T, et al. Sarcopenia: revised European consensus on definition and diagnosis. *Age Ageing* (2019) 48(1):16–31. doi: 10.1093/ageing/afy169
15. Cappellari GG, Guillet C, Poggiogalle E, Pomar MDB, Batis JA, Boirie Y, et al. Sarcopenic obesity research perspectives outlined by the sarcopenic obesity global leadership initiative (SOGLI) – proceedings from the SOGLI consortium meeting in Rome November 2022. *Clin Nutr* (2023) 42(5):687–99. doi: 10.1016/j.clnu.2023.02.018
16. Donini LM, Busetto L, Bischoff SC, Cederholm T, Ballesteros-Pomar MD, Batis JA, et al. Definition and diagnostic criteria for sarcopenic obesity: ESPEN and EASO consensus statement. *Obes Facts* (2022) 15(3):321–35. doi: 10.1159/000521241
17. Shen W, Middleton MS, Cunha GM, Delgado TI, Wolfson T, Gums A, et al. Changes in abdominal adipose tissue deposits accessed by MRI correlate with hepatic histologic improvement in non-alcoholic steatohepatitis. *J Hepatol* (2023) 78(2):238–46. doi: 10.1016/j.jhep.2022.10.027
18. Covassin N, Sert-Kunoyoshi FH, Singh P, Romero-Corral A, Davison DE, Lopez-Jimenez F, et al. Experimental weight gain increases ambulatory blood pressure in healthy subjects: implications of visceral fat accumulation HHHS public access author manuscript. *Mayo Clin Proc* (2018) 93(5):618–26. doi: 10.1016/j.mayocp.2017.12.012
19. Vasamsetti SB, Natarajan N, Sadaf S, Florentin I, Dutta P. Regulation of cardiovascular health and disease by visceral adipose tissue-derived metabolic hormones. *J Physiol* (2022), 10.1111/JP282728
20. Chen Q, Wu Y, Gao Y, Zhang Z, Shi T, Yan B. Effect of visceral adipose tissue mass on coronary artery disease and heart failure: a mendelian randomization study. *Int J Obes* (2022) 1–5. doi: 10.1038/s41366-022-01216-x
21. Kaul S, Rothney MP, Peters DM, Wacker WK, Davis CE, Shapiro MD, et al. Dual-energy X-ray absorptiometry for quantification of visceral fat. *Obesity* (2012) 20(6):1313–8. doi: 10.1038/oby.2011.393
22. Gupta N, Balasekaran G, Victor Govindaswamy V, Yong Hwa C, Meng Shan L. Comparison of body composition with bioelectric impedance (BIA) and dual energy X-ray absorptiometry (DEXA) among Singapore Chinese. *J Sci Med Sport* (2011) 14:33–5. doi: 10.1016/j.jsams.2010.04.005
23. Toombs RJ, Ducher G, Shepherd JA, De Souza MJ. The impact of recent technological advances on the trueness and precision of DXA to assess body composition. *Obesity* (2012) 20(1):30–9. doi: 10.1038/oby.2011.211
24. Mourtzakis M, Prado CMM, Lieffers JR, Reiman T, McCargar LJ, Baracos VE. A practical and precise approach to quantification of body composition in cancer patients using computed tomography images acquired during routine care. *Appl Physiol Nutr Metab* (2008) 33(5):997–1006. doi: 10.1139/H08-075
25. Dabiri S, Popuri K, Cespedes Feliciano EM, Cuan BJ, Baracos VE, Faisal Beg M. Muscle segmentation in axial computed tomography (CT) images at the lumbar (L3) and thoracic (T4) levels for body composition analysis. *Comput Med Imaging Graph* (2019) 75:47–55. doi: 10.1016/j.compmedimag.2019.04.007
26. Shi W, Grainger AT, Justison NJ, Qing K, Roy R, Berr SS. Deep learning-based quantification of abdominal fat on magnetic resonance images. *PloS One* (2018) 13(9). doi: 10.1371/journal.pone.0294071
27. Wang K, Manidipalli A, Retson T, Bahrami N, Hasenstab K, Blansit K, et al. Automated CT and MRI liver segmentation and biometry using a generalized convolutional neural network. *Radiol Artif Intell* (2019) 1(2):180022. doi: 10.1148/ryai.2019180022
28. Hamer OW, Aguirre DA, Casola G, Lavine JE, Woenckhaus M, Sirlin CB. Fatty liver: imaging patterns and pitfalls. *Radiographics* (2006) 26(6):1637–53. doi: 10.1148/rf.266065004
29. Shen W. Total body skeletal muscle and adipose tissue volumes: estimation from a single abdominal cross-sectional image. *J Appl Physiol* (2004) 97(6):2333–8. doi: 10.1152/japplphysiol.00744.2004
30. Albano D, Messina C, Vitale J, Scofield LM. Imaging of sarcopenia: old evidence and new insights. *Eur Radiol* (2020) 30(4):2199–208. doi: 10.1007/s00330-019-06573-2
31. Lee JW, Ban MJ, Park JH, Lee SM. Visceral adipose tissue volume and CT-attenuation as prognostic factors in patients with head and neck cancer. *Head Neck* (2019) 41(6):1605–14. doi: 10.1002/hed.25605
32. Aubrey J, Esfandiari N, Baracos VE, Buteau FA, Frenette J, Putman CT, et al. Measurement of skeletal muscle radiation attenuation and basis of its biological variation. *Acta Physiologica* (2014) 210(3):489–97. doi: 10.1111/apha.12224
33. Tolonen A, Pakarinen T, Sassi A, Kyttä J, Canciano W, Rinta-Kiikka I, et al. Methodology, clinical applications, and future directions of body composition analysis using computed tomography (CT) images: a review. *Eur J Radiol* (2021) 145. doi: 10.1016/j.ejrad.2021.109943
34. Barbalho ER, da Rocha IMG, de Medeiros GOC, Friedman R, Fayh APT. Agreement between software programmes of body composition analyses on abdominal computed tomography scans of obese adults. *Arch Endocrinol Metab* (2020) 64(1):24–9. doi: 10.20945/2359-397000000174
35. Wu X, Kim GH, Salisbury ML, Barber D, Bartholmai RJ, Brown KK, et al. *Pulmonary Perspective computed tomographic biomarkers in idiopathic pulmonary fibrosis: the future of quantitative analysis* (2019). Available at: www.atsjournals.org.
36. Bredella MA, Ghomi RH, Thomas BJ, Torriani M, Brick DJ, Gerweck AV, et al. Comparison of DXA and CT in the assessment of body composition in premenopausal women with obesity and anorexia nervosa. *Obesity* (2010) 18(11):2227–33. doi: 10.1038/oby.2010.5
37. Kroll L, Mathew A, Baldini G, Hosch R, Koitka S, Kleesiek J, et al. CT-derived body composition analysis could possibly replace DXA and BIA to monitor NET-patients. *Sci Rep* (2022) 12(1). doi: 10.1038/s41598-022-17611-3
38. Mitsopoulos N, Baumgartner RN, Heymsfield SB, Lyons W, Gallagher D, Ross R. Cadaver validation of skeletal muscle measurement by magnetic resonance imaging and computerized tomography. *J Appl Physiol* (1998) 85(1):115–22. doi: 10.1152/jappl.1998.85.1.115
39. Tewari N, Awad S, Macdonald IA, Lobo DN. A comparison of three methods to assess body composition. *Nutrition* (2018) 47:1–5. doi: 10.1016/j.nut.2017.09.005
40. Sandini M, Patiño M, Ferrone CR, Alvarez-Perez CA, Honselmann KC, Paiella S, et al. Association between changes in body composition and neoadjuvant treatment for pancreatic cancer (2018). Available at: <https://jannetnetwork.com/>.
41. Mundi MS, Patel JJ, Martindale R. Body composition technology: implications for the ICU. *Nutr Clin Pract* (2019) 34(1):48–58. doi: 10.1002/ncp.10230
42. Leoniard WCPM, McIninger J, Weijs PJM. C CURRENT OPINION measuring and monitoring lean body mass in critical illness. Available at: www.co-criticalcare.com.
43. Hounsfield unit - StatPearls - NCBI bookshelf. Available at: <https://www.ncbi.nlm.nih.gov/books/NBK547721/>.
44. Barazzoni R, Bischoff S, Boirie Y, Busetto L, Cederholm T, Dicker D, et al. Sarcopenic obesity: time to meet the challenge. *Obes Facts* (2018) 11(4):294–305. doi: 10.1159/000490361

5.3. Second article

Palmas, F., Mucarzel, F., Ricart, M., Lluch, A., Zabalegui, A., Melian, J., Guerra, R., Rodriguez, A., Roson, N., Ciudin, A., & Burgos, R. (2024). Body composition assessment with ultrasound muscle measurement: optimization through the use of semi-automated tools in colorectal cancer. *Frontiers in Nutrition*, 11. <https://doi.org/10.3389/fnut.2024.1372816>



OPEN ACCESS

EDITED BY
Rodolfo Espinoza,
Hospital Copa Star, BrazilREVIEWED BY
Zahra Vahdat Shariatpanahi,
Shahid Beheshti University of Medical
Sciences, Iran
Hugo Boechat Andrade,
Instituto Nacional de Infectologia Evandro
Chagas (INI), Brazil*CORRESPONDENCE
Fiorella Palmas
✉ fiorellaximena.palmas@vallhebron.cat
Fernanda Mucarzel
✉ fernanda.mucarzel@vhir.org

RECEIVED 18 January 2024

ACCEPTED 09 April 2024

PUBLISHED 17 April 2024

CITATION
Palmas F, Mucarzel F, Ricart M, Lluch A,
Zabalegui A, Melian J, Guerra R, Rodríguez A,
Roson N, Ciudin A and Burgos R (2024) Body
composition assessment with ultrasound
muscle measurement: optimization through
the use of semi-automated tools in colorectal
cancer.
Front. Nutr. 11:1372816.
doi: 10.3389/fnut.2024.1372816COPYRIGHT
© 2024 Palmas, Mucarzel, Ricart, Lluch,
Zabalegui, Melian, Guerra, Rodríguez, Roson,
Ciudin and Burgos. This is an open-access
article distributed under the terms of the
[Creative Commons Attribution License](https://creativecommons.org/licenses/by/4.0/)
(CC BY). The use, distribution or reproduction
in other forums is permitted, provided the
original author(s) and the copyright owner(s)
are credited and that the original publication
in this journal is cited, in accordance with
accepted academic practice. No use,
distribution or reproduction is permitted
which does not comply with these terms.

Body composition assessment with ultrasound muscle measurement: optimization through the use of semi-automated tools in colorectal cancer

Fiorella Palmas^{1,2*}, Fernanda Mucarzel^{1*}, Marta Ricart¹,
Amador Lluch¹, Alba Zabalegui¹, Jose Melian³, Raul Guerra³,
Aitor Rodriguez⁴, Nuria Roson⁴, Andreea Ciudin^{1,2,5} and
Rosa Burgos^{1,2,5}¹Endocrinology and Nutrition Department, Hospital Universitari Vall d'Hebron, Barcelona, Spain,
²Centro de investigación Biomédica en Red de Diabetes y Enfermedades Metabólicas Asociadas (CIBERDEM), Instituto de Salud Carlos III (ISCIII), Madrid, Spain, ³ARTIS Development, Las Palmas de
Gran Canaria, Spain, ⁴Department of Radiology, Institut De Diagnòstic Per La Imatge (IDI), Hospital
Universitari Vall d'Hebron, Barcelona, Spain, ⁵Department of Medicine, Universitat Autònoma de
Barcelona, Barcelona, Spain

Colorectal cancer (CRC) is a disease with a high prevalence and major impact on global health. Body composition (BC) data are of great importance in the assessment of nutritional status. Ultrasound (US) is an emerging, accessible and non-invasive technique that could be an alternative when it is not feasible to perform computed tomography (CT). The aim of this study is to evaluate the correlation between CT, as a reference technique, and US of the rectus femoris (RF) as a "proof of concept," in a cohort of patients with CRC and assess the optimisation of results obtained by US when performed by our new semi-automated tool. A single-centre cross-sectional study including 174 patients diagnosed with CRC and undergoing surgery was carried out at the Vall d'Hebron Hospital. We found a strong correlation between CT and US of the RF area ($r = 0.67$; $p < 0.005$). The latter, is able to discriminate patients with worse prognosis in terms of length of hospital stay and discharge destination (AUC-ROC = 0.64, $p = 0.015$). These results improve when they are carried out with the automatic tool (area AUC-ROC = 0.73, $p = 0.023$), especially when normalised by height and eliminating patients who associate overflow. According to our results, the US could be considered as a valuable alternative for the quantitative assessment of muscle mass when CT is not feasible. These measurements are improved when measuring software is applied, such as "Bat" software.

KEYWORDS

ultrasound, rectus femoris, computed tomography, colorectal cancer, body composition

1 Introduction

Muscle plays a fundamental role in the patient's prognosis and its measurement is now necessary to make a correct nutritional assessment (1). Body composition (BC) evaluation is fundamental for the identification of hidden muscle abnormalities despite adequate, excess or stable weight (2–4). As stated in several recent clinical guidelines, body composition assessment is emphasised as an integral part of daily clinical practise in nutritional assessment (1, 5–7).

In the context of two highly prevalent conditions, such as malnutrition related to the disease (MRD) and sarcopenia, measurement of muscle mass is critical for optimal assessment and identification (1, 7).

Malnutrition related to the disease (MRD) is defined as a subacute or chronic nutritional state in which a combination of varying degrees of over- or undernutrition and inflammatory activity has resulted in altered body composition and reduced function (8, 9).

Sarcopenia is defined as a progressive and generalised loss of skeletal muscle mass, strength and/or physical function, which is associated with an increased risk of adverse outcomes, such as physical disability, poor quality of life, increased mortality (7) and metabolic syndrome (10–14). The presence of sarcopenia at diagnosis or its onset during treatment has been widely associated with poorer outcomes in terms of prognosis, higher rates of surgical complications, poorer response to chemotherapy and greater toxicity, longer hospital stay, and mortality (15–17).

Malnutrition and sarcopenia are very common in patients with oncological pathology (18). Their presence is closely associated with poor clinical outcomes and prognosis. Therefore, the study of BC is important to facilitate diagnoses and allow early intervention (19, 20).

Nowadays, there are several techniques to assess BC and muscle mass, and it is important to recognise the strengths and limitations for an optimal application. Currently, bioelectrical impedance analysis (BIA), muscle ultrasound (US), dual-energy X-ray absorptiometry (DXA), magnetic resonance image (MRI) and computed tomography (CT) are recognised as diagnostic methods for sarcopenia (5, 7).

On the one hand, BIA is a simple, non-invasive, fast and inexpensive method that estimates the BC by measuring the resistance to a low-power alternating current through the body (21). BIA estimates BC as a bicompartimental model: fat free mass (FFM) and fat mass (FM) in kilogrammes and percentage (22). The use of predictive equations is the main limitation of the BIA as it requires a constant hydration and population references that do not always correspond to the clinical reality of the patient (23–25).

Furthermore, DXA is considered to be a precise technique that provides results from three compartments. It is important to note that since there are only specific attenuation factors for bone and fat, the DXA technique measures only two compartments (bone mass and fat mass) and estimates the third (lean mass) (26, 27). The need for dedicated space for the equipment, trained personnel and exposure to X-ray radiation (even at low doses) are some of the limitations (28).

In addition, US is an emerging accessible bedside, portable, and non-invasive technique as it does not involve ionising radiation for the patient (29, 30). It is able to provide not only quantitative information but also qualitative information by grey scale (31–33). Several skeletal muscle groups have been studied with US, and most of them showed a strong correlation with total muscle mass (32, 34). The quadriceps femoris is the most studied muscle group, especially the rectus femoris (32, 35). Quantitative analysis shows a strong correlation with reference techniques such as MRI or CT (36–38).

CT is emerging as a widely used technique in clinical practise, providing very accurate information for the assessment of BC (39–41). Regional analysis of adipose tissue and muscle at the third lumbar vertebra has been shown to have a high correlation with total BC, and provides significant additional information on tissue quality based on the Hounsfield units (HU) (26, 40, 42).

The assessment of BC by CT image has been widely used in clinical research, especially in those pathologies where CT evaluation is part of the protocol, such as some types of cancer or abdominal pathologies (43). Colorectal cancer (CRC) is a disease of high prevalence and great impact on global health, being the third most commonly diagnosed cancer worldwide and the second leading cause of cancer death (44). Abdominal CT must be routinely performed in colorectal cancer for diagnosis, staging and follow-up (17, 45, 46).

It is crucial to highlight the fluctuations of BC during the evolution of the disease, especially during the active treatment process, which indicates the importance of monitoring its evolution (45, 46). Therefore, an easy to perform and accessible technique is needed to allow us to study BC at any time during the patient's evolution, taking into account that it does not cause any harm or discomfort to the patient. In this scenario, the US could be a good alternative to CT when the latter is unfeasible to carry out.

In this context, this study is proposed with the aim of assessing: (a) the strength of correlation between the measurements made by ultrasound at the level of the rectus femoris in relation to abdominal CT (as a reference technique) and clinical variables of evolution; (b) to determine which ultrasound variables are significantly associated with clinical evolution; (c) the use of our semi-automated tool would optimise the results obtained by US; (d) whether the use of semi-automatic tools in ultrasound better represents the patient's clinical reality than manual measurements.

2 Materials and methods

2.1 Patient selection

We performed a single-centre cross-sectional study including consecutive patients diagnosed with colorectal cancer who underwent oncological surgery at the Vall d'Hebron University Hospital, between May 2021 and September 2023.

The study was approved by the local ethics committee PR (AG) 489/2021 and was conducted in accordance with the Declaration of Helsinki.

All the patients signed the informed consent form before participating in the study. Inclusion criteria: (a) more than 18 years of age; (b) diagnosis of colorectal cancer confirmed by biopsy; (c) patients recruited 48 h after colorectal oncology surgery; (d) acceptance and return of the signed informed consent form signed after clarification of doubts. Exclusion criteria: (a) unable to perform CT scan; (b) unable to undergo ultrasound in the rectus femoris (i.e., amputations); (c) abdominal CT scan performed 30–40 days before recruitment.

2.2 Clinical data collection

Patients were recruited 48 h after colorectal oncology surgery. At this time, anthropometric measurements of current weight and height

were performed, and anthropometric history (usual weight and weight loss in the previous 6 months) was obtained. Patients' performance status was assessed using the Eastern Cooperative Oncology Group (ECOG) scale. The remaining demographic and oncological variables were obtained from the clinical history. At the time of recruitment, a tetrapolar bioimpedance was performed using the Bodystat quadscan 4,000.

In this study, we evaluated the potential use of rectus femoris muscle measurement, via ultrasound, as a prognostic criterion for clinical outcomes in patients, specifically considering length of hospital stay and discharge destination.

After discharge, return home from the hospital was considered a natural progression. The need for hospitalisation at home, referral to a social health centre or death was considered an unfavourable outcome with a poor prognosis.

The hospital stay considered favourable in our centre for this type surgery is 3–5 days. Therefore, two hospital stay groups were identified, those with a normal or expected hospital stay (less than 5 days) and those with a prolonged hospital stay (>10 days). The exclusion of patients with stays between 6 and 9 days was a deliberate methodological choice. This decision was informed by the clinical observation that within this range, the reasons for prolonged hospitalisation can vary widely, encompassing both medical complications and non-medical, logistical factors (such as weekend discharge policies, availability of the discharging physician, or unexpected systemic demands on hospital resources). As such, including this group in either the positive or negative outcome categories could introduce significant variability and potential bias into the analysis, undermining the clarity and interpretability of our findings. Our approach aligns with the principle of maximising the interpretability of the study's outcomes by focusing on patient groups with clear clinical trajectories.

We scored these two prognostic variables together as "good" (good outcome) or "poor" (poor outcome). In this way, those individuals who have a "normal" stay (up to 5 days) and who return home upon discharge are considered to have a good prognosis. This allows for biases such as those patients with a short stay who end up dying.

2.3 Rectus femoris ultrasound

Ultrasound measurements of the unilateral right quadriceps rectus femoris (RF) were performed in all patients. Ultrasound imaging and manual measurements were performed by an experienced medical sonographer on the same day of recruitment. A linear portable ultrasound transducer (UProbe L6C Ultrasound Scanner, Guangzhou Sonostar Technologies Co., China) was used, and all the images were acquired with 10 kHz.

Thigh muscle measurements were performed with the patient in the supine position with knees extended and relaxed. The acquisition site was located two-thirds of the way along the femur length, measured between the anterior superior iliac spine and the upper edge of the patella (29). The transducer was placed perpendicular to the long axis of the thigh with abundant use of contact gel and minimal pressure to avoid muscle compression (Figure 1A).

All parameters were taken as the average of two consecutive measurements in the dominant leg. We took an image in a transversal

section, and then measured the cross-sectional area (CSA) in cm^2 , the X-axis and Y-axis in cm, which corresponded to the linear measurement of the distance between the muscle limits of the rectus femoris (lateral and anteroposterior), and the total fat subcutaneous tissue in cm (Figure 1B). All US parameters were also standardised by the height squared (in cm^2 for the rectus femoris) (29).

In order to optimise the measurements obtained manually from the US, our group has developed a semi-automatic tool called "Bat." All the images in crude format (".dcm"), obtained from the US were first manually marked with the "Bat" tool. Later, the tool generated the same metrics of the RF area obtained manually, adding the grayscale value (0: Black, 255: white) (31, 32).

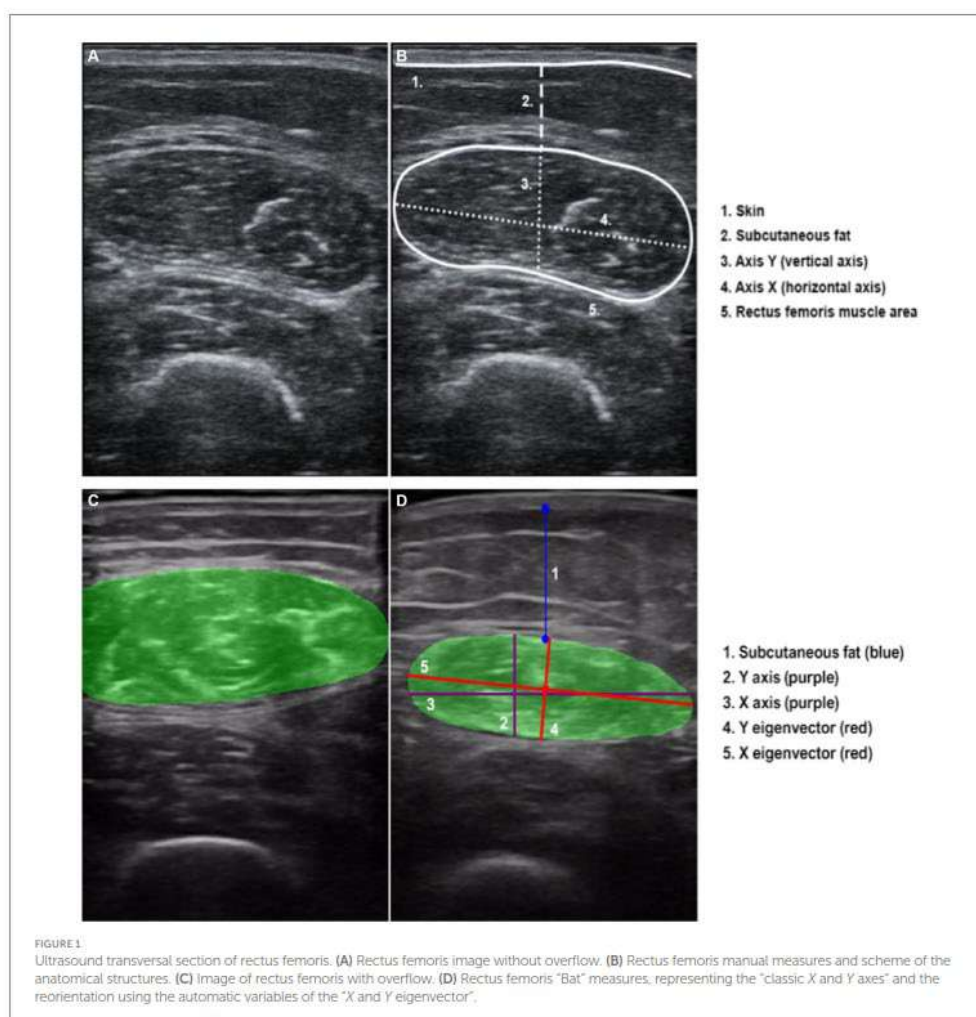
To analyse these images, a combination of advanced digital techniques, including pixel labelling, Principal Component Analysis (PCA) and centroid identification were used. The latter involves calculating the "centre" of the labelled pixels, similar to determining the equilibrium point of the muscle's shape within the image. Besides, PCA is also a sophisticated statistical method used to identify patterns in data. Its purpose is to express data in a way that highlights both its similarities and its differences. In simple terms, envisioning the muscle as an ellipse, these axes can be visualised as lines passing through its centre. The first principal axis (major eigenvector) is the direction with the highest variance in the data (pixels) and corresponds to the "longest" diameter of the ellipse. The second principal axis (minor eigenvector) is perpendicular to the first and represents the direction with the next highest variance, corresponding to "shortest" diameter of the ellipse (Figure 1D).

Manual area marking using "Bat" tool was performed by a different researcher to the one who initially measured the image (Figure 1C). It is important to note that both researchers remained blind to any additional clinical or body composition data during both the image acquisition and analysis stages.

In addition, occasionally, the image of the rectus femoris exceeds the dimensions of the transducer, making it impractical to include the entire area in a single image. This circumstance, referred to as "overflow" (Figure 1C), presents a challenge at the image analysis level. When the image has overflow, the area calculation is estimated according to the trajectory of the rectum. As it is not possible to fully analyse the area completely manually or automatically, the level of precision or adjustment of this variable to the reality of the patient is artefactual. Therefore, we categorised the sample into two groups based on the presence or absence of image overflow to assess its potential impact on clinical outcomes.

2.4 Computed tomography analysis

Skeletal computed tomography (CT) images focused on the L3 vertebrae were obtained using a multidetector computed tomography scanner (Aquilion Prime SP, Canon Medical Systems, Japan), with the following technical parameters: 135 kV (tube voltage), 1 mm 80 row (detector configuration), tube current modulation, and 0.8 s/rotation (gantry rotation). The following variables were recorded: skeletal muscle mass area or SMA (cm^2 and %), skeletal muscle mass index or SMI (cm^2/m^2), intramuscular adipose tissue area or IMAT (cm^2 and %), intramuscular adipose tissue index or IIMAT (cm^2/m^2), area of visceral fat mass (VFA) (cm^2 and %), subcutaneous fat (SFA) (cm^2 and %), visceral fat mass index (VFI) (cm^2/m^2), and subcutaneous fat (SFI)



(cm^2/m^2), and average Hounsfield Units (HU) for each segmented tissue. The CT images centred on the third lumbar vertebra (L3) were analysed using FocusedON-BC software. Tissue quality was assessed based on its average Hounsfield Units (HU) value. Standard thresholds were used as follows: -29 to 150 HU for skeletal muscle, -190 to -30 for subcutaneous adipose tissue and -150 to -50 for visceral adipose tissue (41, 42, 47).

2.5 Statistical analyses

Statistical analyses were performed using Python 3. Continuous variables are presented as mean \pm standard deviation (SD) for normally distributed variables and median \pm interquartile range (IQR) for

non-normally distributed variables. Categorical variables are presented as percentages. Statistical significance was accepted at $p < 0.05$.

To assess whether a given numerical variable can be used as a predictive criterion for a patient's clinical outcome, the separability of groups associated with treatment success or failure was assessed. Treatment success or failure was determined on the basis of several clinical variables, such as length of hospital stay or discharge destination. Group separability was assessed using the Student's *t*-test when the two groups had a normal distribution and equivalent variances. The Mann-Whitney *U* test was used when neither condition applied. The Anderson-Darling method was used to evaluate the normality of the distribution of the numerical variables. The Levene's test was used to confirm the equivalence of variances.

In addition, ROC curves were used to quantify the overall precision of each method by measuring the area under the curve (AUC).

Given the innovative nature of the methodology being tested, our study was designed as a proof-of-concept (PoC) investigation. Primarily to explore the feasibility and potential efficacy of this new approach, rather than to provide definitive evidence of its effectiveness. This inherent uncertainty in the expected outcomes and effect sizes made traditional sample size calculation methods challenging to apply effectively. In this context, the sample size for our PoC study was determined based on practical considerations, including the availability of subjects and resources, with an emphasis on obtaining a preliminary assessment of the methodology's feasibility and potential signals of effectiveness.

Moreover, various graphs and images were generated to better illustrate the statistical results.

3 Results

3.1 Study population

We recruited 174 patients (see Table 1), predominantly male, with a mean age of 68.91 ± 11.52 years old. All participants had colorectal neoplasia, with the colon and sigmoid colon being the most commonly affected sites. Notably, 65% of the recruited patients presented with stage II-III disease at the time of diagnosis, although an overwhelming 95% maintained a good baseline functional status (ECOG ≤ 1). According to the GLIM criteria (assuming that all patients have an etiologic criteria + at least 1 phenotypic criteria including weight loss $>5\%$ during the last 6 months, BMI $< 20 \text{ kg/m}^2$ if < 70 years old or $< 22 \text{ kg/m}^2$ if > 70 years old and a reduction in muscle mass measured by BIA), 21% of the patients met the criteria for malnutrition, although the average BMI was above the normal range (BMI 26 kg/m^2) (5). Sarcopenia was screened screening using the SARC-F questionnaire, which showed a 9% risk of sarcopenia within in the sample.

3.2 Quantifying muscle mass: US vs. CT

The amount of muscle measured by the rectus femoris present a strong and statistically significant correlation with the results of the CT muscle area, especially in the variables "Y axis" and "area" (Table 2). In Figure 2 a graphical representation illustrates the correlation between the results of the RF ultrasound area and the results of the abdominal CT muscle area. The graphic presentation clearly shows a remarkable correlation between both CT and US findings. In particular, patients without overflow (represented by blue dots) are closer to 0, indicating a smaller muscle mass. The graph also highlights a noticeable clustering of the samples within a narrower numerical range, which represents a challenge in separating patients based on their clinical evolution.

3.3 US quantification of muscle mass and clinical evolution

The averages of the main variables obtained by ultrasound have been obtained and presented in Table 3. It can be seen that the

TABLE 1 Patients' demographic, clinical and anthropometric characteristics.

Characteristics	Study population (n = 174)
Sex	
Female	64 (37%)
Male	105 (60%)
Age (years)	68.91 ± 11.52
Tumour location	
Colon	78 (45%)
Sigmoid	53 (30%)
Rectum	23 (13%)
Cecum	15 (9%)
Anus	1 (1%)
TNM stage	
I	31 (18%)
II	54 (31%)
III	60 (34%)
IV	10 (6%)
ECOG	
0	141 (81%)
1	25 (14%)
2	4 (2%)
3	1 (1%)
4	1 (1%)
BMI (kg/m^2)	26.27 ± 4.61
Malnutrition by GLIM criteria	36 (21%)
Suspicion sarcopenia by SARC-F	16 (9%)
Ultrasound RF area (cm^2)	3.89 ± 1.35
CT muscle area – SMA (cm^2)	112.59 ± 28.52
Discharge destination	
Home	160 (92%)
No home	14 (8%)
Length hospital stay (days)	
≤ 5 (n = 112)	7.72 ± 10.12
≥ 10 (n = 31)	22.35 ± 15.44

BMI, body mass index; GLIM: Global leadership Initiative of Malnutrition, ECOG, Eastern Cooperative Oncology Group scale; RF, rectus femoris; CT, computed tomography; SMA, skeletal muscle area.

possibility of having a good or bad prognosis is related to the manual area ($p = 0.041$), and especially when we normalise this measurement by the square of the height (m^2), improving the ability to predict the patient's outcome. In addition, other manual and automatic variables also improve their prognosis capabilities when normalised by patient's height. In example, muscle area improves its AUC from 0.62 to 0.64 and Y axis from 0.59 to 0.61.

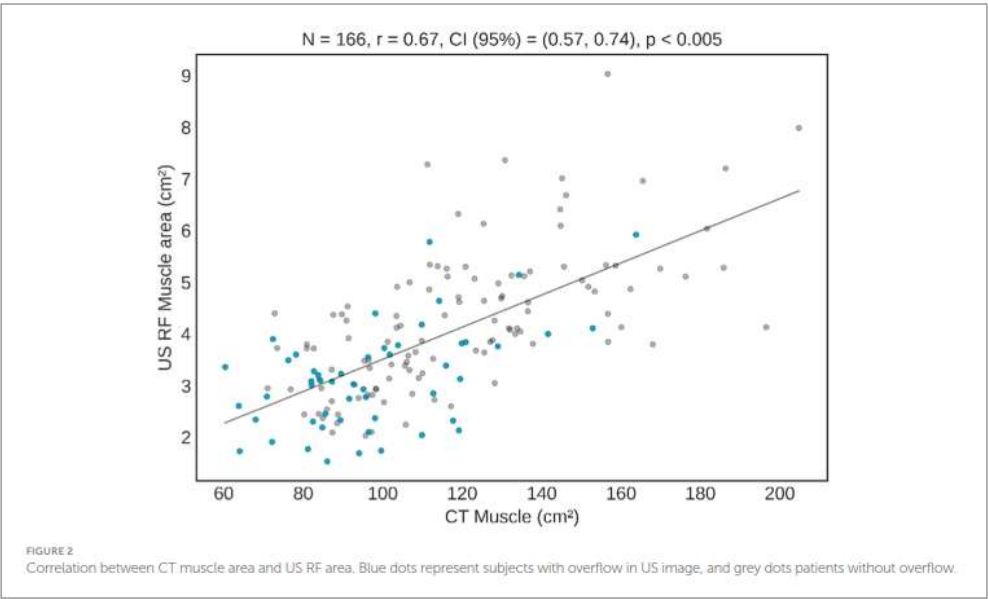
Similarly, when the patient's whit overflow was removed from the sample, muscle area improves its AUC from 0.64 to 0.71.

On the other hand, the use the software tool, which allows carrying the analysis in a more automatic and user independent way,

TABLE 2 Correlation between CT muscle area and US RF variables (area, X and Y axis).

CT variable	US variable	N	R ²	IC (95%)	p value
CT Muscle area (cm ²)	US RF Muscle area (cm ²)	166	0.67	(0.57, 0.74)	p < 0.005
CT Muscle area (cm ²)	US RF Muscle X (cm)	166	0.53	(0.41, 0.63)	p < 0.005
CT Muscle area (cm ²)	US RF Muscle Y (cm)	166	0.66	(0.56, 0.74)	p < 0.005

CT, computed tomography; US, ultrasound; RF, rectus femoris.



also increases the performance of the different metrics. For instance, muscle Y axis improves from 0.56 to 0.68, and even to 0.72 when using the y-eigenvector. Similarly, muscle area improves from 0.71 (after normalised by height and remove overflow) to 0.73 using semiautomatic tool. This improvement can be observed in the ROC curves displayed in Figure 3.

Although this trend can be clearly seen in the results, the difference between the manual and automatic metrics is not statistically significant (p -value > 0.05).

4 Discussion

This study is, to our knowledge, the first to use a semi-automatic tool in the evaluation of muscle ultrasound (US) in rectus femoris.

US has gained widespread acceptance and is nowadays included in several influential body composition guidelines (1, 7, 48). Positioned as the “stethoscope of body composition,” US is valued for its accessibility, cost-effectiveness, and bedside applicability (49). In our study, measurement of muscle mass using US at the RF showed a robust correlation when compared to quantification using CT as the reference technique ($r = 0.67$, IC 0.57–0.74, $p < 0.001$). These results are similar or superior to those reported in other studies, such as Paris

et al. shows ($r = 0.45$, $p < 0.01$) or Lambell et al. (0.7 , $p < 0.01$) (50, 51). However, the paucity of published evidence comparing ultrasound with CT is probably due to the logical challenge of synchronising both tests at clinically comparable times.

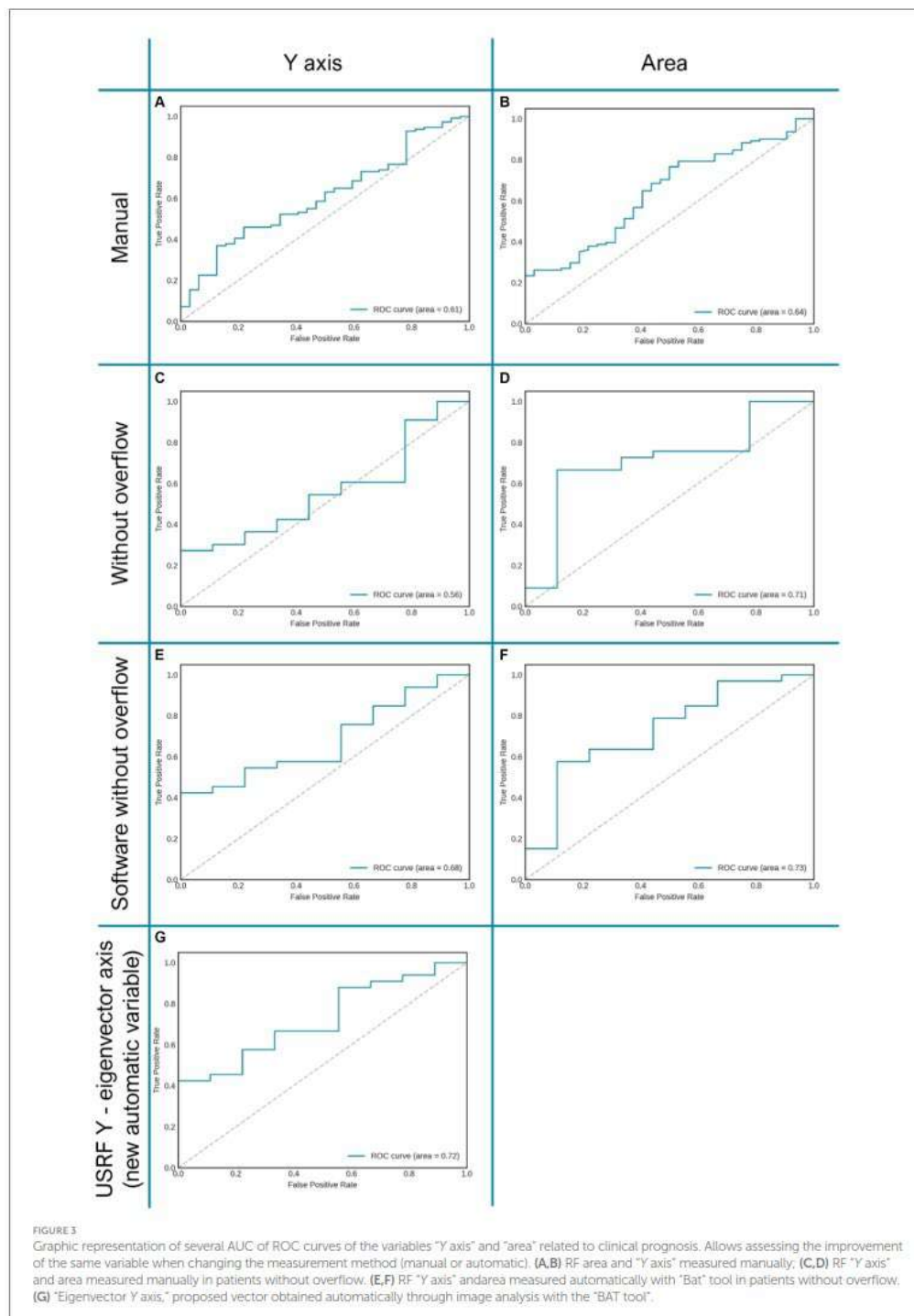
Taking into account the previously presented information, patients with colorectal cancer emerge as particularly suitable candidates, as they require CT scans as part of their follow-up, staging and overall assessment (45, 52). This positioning allows CT to be used as an “opportunistic” technique to analyse BC with a high degree of precision, thus providing a valuable validation platform for emerging techniques, such as US (53, 54). The results derived from this study contribute significantly to our understanding, endorsing US as a technique with acceptable results for screening and diagnosis of muscle alterations, validated against CT, in patients with colorectal cancer. Thus, it would be an alternative tool for use in the future when TC is not feasible.

It should be noted that muscle ultrasound is a technique that provides us quantitative (area and Y axis) and qualitative muscle information (grey scale) (29). This information is obtained directly from muscle mass and has been shown to have a very good correlation with the patient’s functional capacity and prognosis (55, 56). In the case of bioimpedance, a doubly indirect method of assessing body composition, quantitative information on muscle

TABLE 3 Clinical evolution using US RF variables using all the image, and separating those with and without overflow, normalised or not by height.

Manual metrics	With overflow		Unnormalized by height						Normalised by height (/m ²)					
	US variable	All (n=143)	Good outcomes (n=111)	Poor outcomes (n=32)	p value	ROC (AUC)	SE	All (n=143)	Good outcomes (n=111)	Poor outcomes (n=32)	p value	ROC (AUC)	SE	
	US RF muscle area (cm ²)	3.92	4.06	3.45	0.041	0.62	0.06	1.4	1.45	1.22	0.015	0.64	0.05	
	US RF muscle x (cm)	3.65	3.67	3.56	0.315	0.56	0.06	1.32	1.33	1.28	0.095	0.57	0.06	
	US RF muscle y (cm)	1.32	1.35	1.24	0.087	0.59	0.06	0.47	0.49	0.44	0.064	0.61	0.05	
	Without overflow													
Software metrics	US variable	All (n=42)	Good outcomes (n=33)	Poor outcomes (n=9)	p value	ROC (AUC)	SE	All (n=42)	Good outcomes (n=33)	Poor outcomes (n=9)	p value	ROC (AUC)	SE	
	US RF muscle area (cm ²)	3.12	3.24	2.7	0.178	0.65	0.1	1.16	1.21	0.99	0.099	0.71	0.1	
	US RF muscle x (cm)	3.32	3.37	3.14	0.19	0.68	0.1	1.25	1.28	1.15	0.065	0.68	0.12	
	US RF muscle y (cm)	1.18	1.2	1.13	0.522	0.55	0.11	0.44	0.45	0.41	0.248	0.56	0.1	
	US RF muscle area-s (cm ²)	3	3.12	2.52	0.061	0.7	0.1	1.12	1.17	0.93	0.023	0.73	0.1	
	US RF muscle y-s (cm ²)	1.15	1.18	1.04	0.152	0.66	0.09	0.43	0.44	0.38	0.053	0.68	0.09	
	US RF x-eigenvector (cm)	3.29	3.33	3.16	0.374	0.6	0.13	1.24	1.26	1.16	0.253	0.59	0.14	
	US RF Muscle y-eigenvector (cm)	1.16	1.19	1.03	0.085	0.69	0.08	0.43	0.45	0.38	0.024	0.72	0.09	

US, ultrasound; RF, rectus (emerie; SE, standard error.



mass can be obtained through fat free mass, but not qualitative information on muscle mass (22). The phase angle is a parameter that we can obtain from the BIA that has a highly impactful prognostic value (57, 61). However, it is a parameter that comes from a complete body evaluation, not from muscle mass in particular. On the other hand, DXA is a highly accurate technique for evaluating body composition, but it is not a particularly good technique for evaluating muscle status since it does not provide information on muscle quality (26). Furthermore, it is an expensive and inaccessible technique.

Reduction in muscle mass (MM) is strongly associated with a prognosis in terms of postoperative complications, prolonged hospital stays, discharge outcomes, treatment response and mortality (61). Consistent with this premise, our study results confirm that lower MM, as measured by US, associated with longer hospital stays and decreased likelihood of discharge home, essentially indicating a more difficult prognosis for the patient. Given the accessibility of US as a technique, serious consideration should be given to its more frequent incorporation into protocols for prevention and clinical optimization in patients with colorectal cancer. Furthermore, the results obtained can play a key role in tailoring multimodal treatments in cases where low muscle mass is evident or its deterioration is observed over time.

On the other hand, one of the weaknesses of muscle ultrasound is its operator-dependent nature, requiring skilled personnel to perform it accurately (39, 59, 60). It is also necessary to implement standardised protocols so that their results are comparable (32). A key factor contributing to the variability of findings is the manual nature of quantitative measurements, such as the area or the X and Y axes, which are subject to the operator interpretation. There are various software programmes that allow us to obtain the grey scale through manual measurements, but currently, there are no tools for the rest of the ultrasound metrics at the RF level that are automatic (31).

In this study, we begin to develop a near automatic tool that simplifies the process by requiring only the manual marking of the RF area. This innovative approach facilitates the automatic derivation of other variables from the initial manual marking. Several processes in medicine have shown that the automation of measurements and the use of software that reduces the intervention of the “researcher’s hand” is superior and optimises results (61–63). When performing ultrasound imaging, for example of the rectus femoris muscle, there’s a common challenge related to the orientation of the ultrasound probe. Even a slight rotation or tilt of the probe can alter the appearance of the muscle in the image. However, the described method, based on principal axes (eigenvectors), significantly mitigates this problem by incorporating principal component analysis (PCA) to identify the principal axes of the muscle image effectively addresses this challenge. Regardless of the probe’s orientation, the principal axes of the muscle’s image will consistently adjust. This means that the major and minor axes of the ellipse representing the muscle are consistently aligned with the directions of maximum variance in the image, regardless of how the ultrasound probe is held.

This technique featly reduces the reliance on the operator skill or consistency in probe placement. Different observers can perform the scan, and the main axes will remain consistent for the same anatomical structure, ensuring more objective and reproducible measurements. By focusing on the intrinsic geometric properties of the muscle tissue, as represented by the ellipse in the image, measurements become

more reflective of the actual dimensions of the muscle and less dependent on the probe positioning. Consequently, this approach leads to more accurate and objective assessments of muscle size, shape, and potentially its health status.

Firstly, we carefully analysed the correlation between our measurements and those performed manually, and found robust and statistically significant associations for all variables (refer to Table 3). RF area (cm²) emerged as the variable with the strongest correlation with CT, although results were also noted for the Y axis (see Table 2). This may be related to the fact that the favourable performance of the axis due to its vertical measurement, which is not affected by possible image displacement from the screen. In this sense, we observed that a significant percentage of the images (62%) acquired according to our protocol in the lower third of the leg showed an area that extended beyond the edges of the screen. This overflow situation, where the area extends beyond the edges of the screen, introduces a potential source of imprecision in area measurements compared to situations where the area is fully displayed. We therefore, stratified the sample into two groups, with and without overflow. We re-run the clinical correlation in the group without overflow, and observed an improvement in the ROC curves, indicating a lower rate of false positives and false negatives. An increase in the correlation with clinical complications, discharge destination and hospital stay were also observed. However, it is recognised that these results may be influenced by the fact that many patients without overflow generally have worst muscle mass.

A limitation of our tool is its partial automation, which requires a manual measurement by a researcher. However, it has been shown that a reduction in manual measurement leads to significantly better results. It is necessary to carry out studies with a larger sample size to fully automate the tool. In addition, it would have been interesting to measure the RF area a few centimetres closer to the patella to see if this would provide an improvement that we should definitely include in our protocols when eliminating the overflow. Furthermore, assessing the usefulness of these measurements in patient follow-up and exploring other prognostic variables such as post-operative complications or mortality is an interesting avenue for further research. Our ongoing studies are designed to a comprehensively address these issues.

5 Conclusion

In conclusion, the significant correlation levels observed in our study prompt led to consider the US as an alternative for the quantitative assessment of muscle mass when CT is not feasible. It is noteworthy to highlight the pioneering role of “Bat,” the first software to allow semi-automatic derivation of metrics in rectus femoris measurements. The application of principal axis analysis in ultrasound imaging is proving to be a powerful approach to standardising muscle tissue measurements. This methodology effectively overcomes the challenges associated with variable probe orientation, thereby improving the accuracy, objectivity, and reproducibility of measurements. Such improvements are of paramount importance in clinical settings, contributing significantly to accurate diagnosis and monitoring. In addition, the approach reduces inter and intra-observer dependencies, further enhancing the precision and objectivity of the results. This not only improves their separability but

also partially compensates for one of the recognised weaknesses of muscle ultrasound.

Whilst acknowledging these advances, it is prudent to emphasise the need for additional studies to fully automate the “Bat” tool and thoroughly reassess its clinical utility. This ongoing research is critical for refining and optimising muscle assessment methodologies, and ensuring continued progress in the field.

Data availability statement

The original contributions presented in the study are included in the article/supplementary material, further inquiries can be directed to the corresponding authors.

Ethics statement

The studies involving humans were approved by Comité de Ética de la Investigación con medicamentos del Instituto de Investigación Vall d'Hebron. The studies were conducted in accordance with the local legislation and institutional requirements. The participants provided their written informed consent to participate in this study.

Author contributions

FP: Conceptualization, Methodology, Supervision, Writing – original draft, Writing – review & editing, Validation, FM: Investigation, Writing – review & editing, MR: Investigation, Writing

– review & editing, AL: Investigation, Writing – review & editing, AZ: Investigation, Writing – review & editing, JM: Investigation, Software, Writing – review & editing, RG: Formal analysis, Software, Writing – review & editing, AR: Resources, Writing – review & editing, NR: Resources, Writing – review & editing, AC: Writing – review & editing, RB: Conceptualization, Funding acquisition, Writing – original draft, Writing – review & editing.

Funding

The author(s) declare that no financial support was received for the research, authorship, and/or publication of this article.

Conflict of interest

The authors declare that the research was conducted in the absence of any commercial or financial relationships that could be construed as a potential conflict of interest.

Publisher's note

All claims expressed in this article are solely those of the authors and do not necessarily represent those of their affiliated organizations, or those of the publisher, the editors and the reviewers. Any product that may be evaluated in this article, or claim that may be made by its manufacturer, is not guaranteed or endorsed by the publisher.

References

- Cederholm T, Jensen GL, Correia MITD, Gonzalez MC, Fukushima R, Higashiguchi T, et al. GLIM criteria for the diagnosis of malnutrition – a consensus report from the global clinical nutrition community. *Clin Nutr.* (2019) 38:1–9. doi: 10.1016/j.clnu.2018.08.002
- Xiao J, Caan BJ, Cespedes Feliciano EM, Meyerhardt JA, Peng PD, Baracos VE, et al. Association of Low Muscle Mass and Low Muscle Radiodensity with morbidity and mortality for Colon Cancer surgery. *JAMA Surg.* (2020) 155:942–9. doi: 10.1001/jamasurg.2020.2497
- Carneiro IP, Mazurak VC, Prado CM. Clinical implications of Sarcopenic obesity in Cancer. *Curr Oncol Rep.* (2016) 18:62. doi: 10.1007/s11912-016-0546-5
- Prado CM, Cushman SJ, Orsso CE, Ryan AM. Sarcopenia and cachexia in the era of obesity: clinical and nutritional impact. *Proc Nutr Soc.* (2016) 75:188–98. doi: 10.1017/S0029665115004279
- Barazzoni R, Jensen GL, Correia MITD, Gonzalez MC, Higashiguchi T, Shi HP, et al. Guidance for assessment of the muscle mass phenotypic criterion for the global leadership initiative on malnutrition (GLIM) diagnosis of malnutrition. *Clin Nutr.* (2022) 41:1425–33. doi: 10.1016/j.clnu.2022.02.001
- Donini LM, Busetto L, Bischoff SC, Cederholm T, Ballesteros-Pomar MD, Batsis JA, et al. Definition and diagnostic criteria for Sarcopenic obesity: ESPEN and EASO consensus statement. *Obes Facts.* (2022) 15:321–35. doi: 10.1159/000521241
- Cruz-Jentoft AF, Bahat G, Bauer J, Boirie Y, Bruyère O, Cederholm T, et al. Sarcopenia: revised European consensus on definition and diagnosis. *Age Ageing.* (2019) 48:16–31. doi: 10.1093/ageing/afy169
- Soeters PB, Reijnen PLM, van Bokhorst-de van der Schueren MAE, Schols JMGA, Halfens RJG, Meijers JMM, et al. A rational approach to nutritional assessment. *Clin Nutr.* (2008) 27:706–16. doi: 10.1016/j.clnu.2008.07.009
- Arends J, Baracos V, Bertz H, Bozzetti F, Calder PC, Deutz NEP, et al. ESPEN expert group recommendations for action against cancer-related malnutrition. *Clin Nutr.* (2017) 36:1187–96. doi: 10.1016/j.clnu.2017.06.017
- Merz KE, Thurmond DC. Role of skeletal muscle in insulin resistance and glucose uptake. *Compr Physiol.* (2020) 10:785–809. doi: 10.1002/cphy.c190029
- Landi F, Camprubi-Robles M, Bear DE, Cederholm T, Malafarina V, Welch AA, et al. Muscle loss: the new malnutrition challenge in clinical practice. *Clin Nutr.* (2019) 38:2113–20. doi: 10.1016/j.clnu.2018.11.021
- Bell KE, Paris MT, Avrutin E, Mourtzakis M. Altered features of body composition in older adults with type 2 diabetes and prediabetes compared with matched controls. *J Cachexia Sarcopenia Muscle.* (2022) 13:1087–99. doi: 10.1002/jcsm.12957
- Liu AW, Song SO, Hayashi T, Sato KK, Kahn SE, Leonetti DL, et al. Change in CT-measured abdominal subcutaneous and visceral but not thigh fat areas predict future insulin sensitivity. *Diabetes Res Clin Pract.* (2019) 154:17–26. doi: 10.1016/j.diabetes.2019.06.008
- Bauer J, Morley JE, Schols AMWJ, Ferrucci L, Cruz-Jentoft AF, Dent E, et al. Sarcopenia: a time for action. An SCWD Position Paper. *J Cachexia Sarcopenia Muscle.* (2019) 10:956–61. doi: 10.1002/jcsm.12483
- Chen WZ, Shen Z-L, Zhang FM, Zhang XZ, Chen WH, Yan XL, et al. Prognostic value of myosteatosis and sarcopenia for elderly patients with colorectal cancer: a large-scale double-center study. *Surgery.* (2022) 172:1185–93. doi: 10.1016/j.surg.2022.05.031
- Besson A, Deftereos I, Gough K, Taylor D, Shannon R, Yeung JM. The association between sarcopenia and quality of life in patients undergoing colorectal cancer surgery: an exploratory study. *Support Care Cancer.* (2021) 29:3411–20. doi: 10.1007/s00520-021-06025-y
- Nunes GD, Cardenas LZ, Miola TM, Souza JO, Carniatio LN, Bitencourt AGV. Preoperative evaluation of sarcopenia in patients with colorectal cancer: a prospective study. *Rev Assoc Med Bras.* (2023) 69:222–7. doi: 10.1590/1806-9282.20220339
- Brown JC, Cespedes Feliciano EM, Caan BJ. The evolution of body composition in oncology—epidemiology, clinical trials, and the future of patient care: facts and numbers. *J Cachexia Sarcopenia Muscle.* (2019) 9:1200–8. doi: 10.1002/jcsm.12379
- Bozzetti F. Forcing the vicious circle: sarcopenia increases toxicity, decreases response to chemotherapy and worsens with chemotherapy. *Ann Oncol.* (2017) 28:2107–18. doi: 10.1093/annonc/mdx271

20. Prado CM, Anker SD, Coats AIS, Laviano A, von Haehling S. Nutrition in the spotlight in cachexia, sarcopenia and muscle: avoiding the wildfire. *J Cachexia Sarcopenia Muscle*. (2021) 12:3–8. doi: 10.1002/jcsm.12673
21. Buffa R, Saragat B, Cabras S, Rinaldi AC, Marini E. Accuracy of Specific BIVA for the Assessment of Body Composition in the United States Population. *PLoS One*. (2013) 8:e58533. doi: 10.1371/journal.pone.0058533
22. Kyle UG, Bosaeus I, de Lorenzo AD, Deurenberg P, Elia M, Gómez JM, et al. Bioelectrical impedance analysis—part I: review of principles and methods. *Clin Nutr*. (2004) 23:1226–43. doi: 10.1016/j.clnu.2004.06.004
23. Cenicola GD, Castro MG, Piovacari SMF, Horie LM, Corrêa FG, Barrere APN, et al. Current technologies in body composition assessment: advantages and disadvantages. *Nutrition*. (2019) 62:25–31. doi: 10.1016/j.nut.2018.11.028
24. Thanapholsart I, Khan E, Lee GA. A current review of the uses of bioelectrical impedance analysis and bioelectrical impedance vector analysis in acute and chronic heart failure patients: an under-valued resource? *Biol Res Nurs*. (2022) 25:240–9. doi: 10.1177/10998004221132838
25. Piccoli A, Brunani A, Savia G, Pillon L, Favaro E, Berselli ME, et al. Discriminating between body fat and fluid changes in the obese adult using bioimpedance vector analysis. *Int J Obes*. (1998) 22:97–104. doi: 10.1038/sj.ijo.0800551
26. Albano D, Messina C, Vitale I, Scorfienza LM. Imaging of sarcopenia: old evidence and new insights. *Eur Radiol*. (2020) 30:2199–208. doi: 10.1007/s00330-019-06573-2
27. Messina C, Albano D, Gatto S, Tofanelli L, Bazzocchi A, Olivieri FM, et al. Body composition with dual energy X-ray absorptiometry: from basics to new tools. *Quant Imaging Med Surg*. (2020) 10:1687–98. doi: 10.21037/qims.2020.03.02
28. Lee SY, Gallagher D. Assessment methods in human body composition. *Curr Opin Clin Nutr Metab Care*. (2008) 11:566–72. doi: 10.1097/MCO.0b013e32830b5f23
29. García-Almeida JM, García-García C, Vegas-Aguilar IM, Ballesteros Pomar MD, Cornejo-Pareja IM, Fernández Medina B, et al. Nutritional ultrasound®: conceptualisation, technical considerations and standardisation. *Endocrinol Diabetes Nutr*. (2022) 70:74–84. doi: 10.1016/j.endinu.2022.03.008
30. Fischer A, Hertwig A, Hahn R, Anwar M, Siebenrock T, Pesta M, et al. Validation of bedside ultrasound to predict lumbar muscle area in the computed tomography in 200 non-critically ill patients: the USVALID prospective study. *Clin Nutr*. (2022) 41:829–37. doi: 10.1016/j.clnu.2022.01.034
31. Pillen S, Van Dijk JP, Weijers G, Rajimann W, De Korte CL, Zwarts MJ. Quantitative gray-scale analysis in skeletal muscle ultrasound: a comparison study of two ultrasound devices. *Muscle Nerve*. (2009) 39:781–6. doi: 10.1002/mus.21285
32. For the full SARCUS working group/Perkisas S, Bastijns S, Sanchez-Rodriguez D, Piotrowski K, de Cock AM. Application of ultrasound for muscle assessment in sarcopenia: 2020 SARCUS update: reply to the letter to the editor. *Eur Geriatr Med*. (2021) 12:427–8. doi: 10.1007/s41999-021-00462-y
33. Sanz-Paris A, González-Fernández M, Hueso-del Río LE, Ferrer-Lahuerta E, Monge-Vazquez A, Losafios-Callau F, et al. Muscle thickness and echogenicity measured by ultrasound could detect local sarcopenia and malnutrition in older patients hospitalized for hip fracture. *Nutrients*. (2021) 13:2401. doi: 10.3390/nu13072401
34. Berger J, Bunout D, Barrera G, de la Maza MP, Henríquez S, Leiva L, et al. Rectus femoris (RF) ultrasound for the assessment of muscle mass in older people. *Arch Gerontol Geriatr*. (2015) 61:33–8. doi: 10.1016/j.archger.2015.03.006
35. Perkisas S, Baudry S, Bauer J, Beckwee D, de Cock AM, Hobbelen H, et al. Application of ultrasound for muscle assessment in sarcopenia: towards standardized measurements. *Eur Geriatr Med*. (2018) 9:739–57. doi: 10.1007/s41999-018-0104-9
36. Thomaes T, Thomis M, Onkelinx S, Coudyzer W, Cornelissen V, Vanhees L. Reliability and validity of the ultrasound technique to measure the rectus femoris muscle diameter in older CAD-patients. *BMC Med Imaging*. (2012) 12:7. doi: 10.1186/1471-2342-12-7
37. Tandon P, Low G, Mourtzakis M, Zenith L, Myers RP, Abrahams JG, et al. A model to identify sarcopenia in patients with cirrhosis. *Clin Gastroenterol Hepatol*. (2016) 14:1473–1480.e3. doi: 10.1016/j.cgh.2016.04.040
38. Sanada K, Kearns CE, Midorikawa T, Abe T. Prediction and validation of total and regional skeletal muscle mass by ultrasound in Japanese adults. *Eur J Appl Physiol*. (2006) 96:24–31. doi: 10.1007/s00421-005-0061-0
39. Prado CMM, Heymsfield SB. Lean Tissue Imaging. *J Parenter Enter Nutr*. (2014) 38:940–53. doi: 10.1177/0148607114550189
40. Shen W. Total body skeletal muscle and adipose tissue volumes: estimation from a single abdominal cross-sectional image. *J Appl Physiol*. (2004) 97:2333–8. doi: 10.1152/japplphysiol.00744.2004
41. Tolonen A, Pakarinen T, Sassi A, Kytä J, Cancino W, Rinta-Kiikka I, et al. Methodology, clinical applications, and future directions of body composition analysis using computed tomography (CT) images: a review. *Eur J Radiol*. (2021) 145:109943. doi: 10.1016/j.ejrad.2021.109943
42. Aubrey J, Esfandiari N, Baracos VE, Buteau FA, Frenette J, Putman CT, et al. Measurement of skeletal muscle radiation attenuation and basis of its biological variation. *Acta Physiol*. (2014) 210:489–97. doi: 10.1111/apha.12224
43. Ahn H, Kim DW, Ko Y, Ha J, Shin YB, Lee J, et al. Updated systematic review and meta-analysis on diagnostic issues and the prognostic impact of myosteatosis: a new paradigm beyond sarcopenia. *Ageing Res Rev*. (2021) 70:101398. doi: 10.1016/j.arr.2021.101398
44. Sung H, Ferlay J, Siegel RL, Laversanne M, Soerjomataram I, Jemal A, et al. Global Cancer statistics 2020: GLOBOCAN estimates of incidence and mortality worldwide for 36 cancers in 185 countries. *CA Cancer J Clin*. (2021) 71:209–49. doi: 10.3322/caac.21660
45. Chung E, Lee HS, Cho ES, Park EJ, Baik SH, Lee KY, et al. Changes in body composition during adjuvant folfox chemotherapy and overall survival in non-metastatic colon cancer. *Cancers*. (2020) 12:12. doi: 10.3390/cancers12010060
46. Zhang L, Guan J, Ding C, Feng M, Gong L, Guan W. Muscle loss 6 months after surgery predicts poor survival of patients with non-metastatic colorectal cancer. *Front Nutr*. (2022) 9:9. doi: 10.3389/fnut.2022.1047029
47. Palmas F, Ciudin A, Guerra R, Eiroa D, Espinet C, Roson N, et al. Comparison of computed tomography and dual-energy X-ray absorptiometry in the evaluation of body composition in patients with obesity. *Front Endocrinol*. (2023) 14:14. doi: 10.3389/fendo.2023.1161116
48. Gortan Cappellari G, Guillet C, Poggiogalle E, Ballesteros Pomar MD, Batsis JA, Boirie Y, et al. Sarcopenic obesity research perspectives outlined by the sarcopenic obesity global leadership initiative (SOGIL) – proceedings from the SOGIL consortium meeting in Rome November 2022. *Clin Nutr*. (2023) 42:687–99. doi: 10.1016/j.clnu.2023.02.018
49. Ponti F, de Cinque A, Fazio N, Napoli A, Guglielmi G, Bazzocchi A. Ultrasound imaging, a stethoscope for body composition assessment. *Quant Imaging Med Surg*. (2020) 10:1699–722. doi: 10.21037/qims-19-1048
50. Paris MT, Mourtzakis M, Day A, Leung R, Watharkar S, Kozar R, et al. Validation of bedside ultrasound of muscle layer thickness of the quadriceps in the critically ill patient (VALIDUM study). *J Parenter Enter Nutr*. (2017) 41:171–80. doi: 10.1177/0148607116637852
51. Lambell KI, Tierney AC, Wang JC, Nanjajya V, Forsyth A, Goh GS, et al. Comparison of ultrasound-derived muscle thickness with computed tomography muscle cross-sectional area on admission to the intensive care unit: a pilot cross-sectional study. *J Parenter Enter Nutr*. (2021) 45:136–45. doi: 10.1002/jpen.1822
52. Golder AM, Sin LKE, Alani F, Alasadi A, Dolan R, Mansouri D, et al. The relationship between the mode of presentation, CT-derived body composition, systemic inflammatory grade and survival in colon cancer. *J Cachexia Sarcopenia Muscle*. (2022) 13:2863–74. doi: 10.1002/jcsm.13097
53. Aduse-Poku L, Gopireddy DR, Hernandez M, Lall C, Divaker J, Falzarano SM, et al. Intraindividual reliability of opportunistic computed tomography-assessed adiposity and skeletal muscle among breast cancer patients. *JNCI Cancer Spectr*. (2022) 6:6. doi: 10.1093/jncics/pkac068
54. Bates DDR, Pickhardt PJ. CT-derived body composition assessment as a prognostic tool in oncologic patients: from opportunistic research to artificial intelligence-based clinical implementation. *Am J Roentgenol*. (2022) 219:671–80. doi: 10.2214/AJR.22.27749
55. Joaquín C, Bretón I, Ocon Bretón MI, Burgos R, Gillis C, Bellido D, et al. Nutritional and Morphofunctional Assessment of Post-ICU Patients with COVID-19 at Hospital Discharge: NutriEcoMuscle Study. *Nutrients*. (2024) 16:886. doi: 10.3390/nu16060886
56. Salim SY, Al-Khathiri O, Tandon P, Baracos VE, Churchill TA, Warkentin LM, et al. Thigh Ultrasound Used to Identify Frail Elderly Patients with Sarcopenia Undergoing Surgery: A Pilot Study. *J. Sur. Res*. (2020) 256:422–432. doi: 10.1016/j.jss.2020.06.043
57. Fernández-Jiménez R, Dalla-Rovere L, García-Olivares M, Abuin-Fernández J, Sánchez-Torralvo FJ, Doulatram-Gangaram VK, et al. Phase angle and handgrip strength as a predictor of disease-related malnutrition in admitted patients: 12-month mortality. *Nutrients*. (2022) 14:1851. doi: 10.3390/NU14091851
58. Prado CM, Ford KL, Gonzalez MC, Murnane LC, Gillis C, Wischmeyer PE, et al. Nascent to novel methods to evaluate malnutrition and frailty in the surgical patient. *J Parenter Enter Nutr*. (2023) 47:554–68. doi: 10.1002/jpen.2420
59. Moreira OC, Alonso-Aubin DA, Patrocinio De Oliveira CE, Candia-Luján R, De Paz JA. Methods of assessment of body composition: an updated review of description, application, advantages and disadvantages. *Arch Med Deport*. (2015) 32:387–94.
60. Teigen LM, Kuchnia AJ, Mourtzakis M, Earthman CP. The use of Technology for Estimating Body Composition: strengths and weaknesses of common modalities in a clinical setting. *Nutr Clin Pract*. (2017) 32:20–9. doi: 10.1177/0884533616676264
61. Lenchik L, Heacock L, Weaver AA, Boutin RD, Cook TS, Itri J, et al. Automated segmentation of tissues using CT and MRI: a systematic review. *Acad Radiol*. (2019) 26:1695–706. doi: 10.1016/j.acra.2019.07.006
62. Paris MT, Tandon P, Heyland DK, Furberg H, Premji T, Low G, et al. Automated body composition analysis of clinically acquired computed tomography scans using neural networks. *Clin Nutr*. (2020) 39:3049–55. doi: 10.1016/j.clnu.2020.01.008
63. Barnard R, Tan J, Roller B, Chiles C, Weaver AA, Boutin RD, et al. Machine learning for automatic Paraspinal muscle area and attenuation measures on Low-dose chest CT scans. *Acad Radiol*. (2019) 26:1686–94. doi: 10.1016/j.acra.2019.06.017

5.4. Third article

Resting energy expenditure estimation by CT body composition analysis.

This article was accepted to review in "Clinical Nutrition", Q1, July 2024.

Clinical Nutrition

Resting energy expenditure estimation by computed tomography body composition analysis.

--Manuscript Draft--

Manuscript Number:	YCLNU-D-24-01804
Article Type:	Full Length Article
Keywords:	resting energy expenditure; computed tomography; indirect calorimetry, body composition
Corresponding Author:	Fiorella Palmas, MD Vall d'Hebron Hospital Universitari SPAIN
First Author:	Fiorella Palmas, MD
Order of Authors:	Fiorella Palmas, MD Andreea Ciudin, PhD Jose Melian Raul Guerra, PhD Alba Zabalegui, MD Guillermo Cárdenas Fernanda Mucarzel Aitor Rodriguez, PhD Nuria Roson, PhD Rosa Burgos, PhD Cristina Hernandez, PhD Rafael Simó, PhD
Abstract:	<p>Summary</p> <p>Background & aims: The assessment of resting energy expenditure (REE) is a challenging task with the current existing methods. The reference method, indirect calorimetry (IC), is not widely available, and other methods show poor correlation with IC. Body composition (BC), in particular muscle mass, plays an important role in REE. In recent years, computed tomography (CT) has emerged as a reliable tool for BC assessment. However, its usefulness for the REE evaluation has not been explored so far. On these bases we explored the possibility to assess the REE based on a CT-scan image using artificial intelligence (AI) models and compare the results with the current methods.</p> <p>Methods: Single-centre observational cross-sectional pilot study were carried out including consecutive patients in-hospital with abdominal CT. All subjects underwent indirect calorimetry and bioimpedance analysis. Their requirements were calculated using different predictive equations. The proposed model is based on a second-order linear regression with three input parameters: weight in kilograms, age in years, and the amount of muscle mass quantified from computed tomography images in square centimetres. The output of this model corresponds to the resting energy expenditure (REE). The model was trained and tested using a cross-validation one-vs-all strategy with 90 subjects with different characteristics.</p> <p>Results: Data from 90 subjects were included in the model. Predictive equations show a low to moderate correlation to IC ($r = 0.48-0.55$, p value <0.001). REE calculated by Bioelectrical Impedance Analysis (BIA) showed better correlation than the predictive equations ($r = 0.636$, p value <0.001). The best correlation was the one obtained through the CT estimation model ($r = 0.647$, p value <0.001). This model was trained using three variables, including age, weight and amount of muscle mass. During the experiments it was observed that replacing any of the aforementioned variables with gender led to poorer results.</p>

Powered by Editorial Manager® and ProduXion Manager® from Aries Systems Corporation

	<p>Conclusions: We demonstrated for the first time that REE can be estimated based on the information extracted from abdominal CT imaging, thus obtaining good correlation with the reference method (IC), which was higher than that obtained with BIA. This finding has the potential to significantly change the paradigm and guidelines for nutritional assessment, and represents a novel and revolutionary concept in the field of precision medicine.</p>
Opposed Reviewers:	

1 **Resting energy expenditure estimation by computed tomography body composition analysis.**

2 Fiorella Palmas^{1,2}, Andreea Ciudin^{1,2,3,4*}, Jose Melian⁵, Raul Guerra⁵, Alba Zabalegui¹, Guillermo
3 Cárdenas¹, Fernanda Mucarzel¹, Aitor Rodríguez⁶, Nuria Roson⁶, Rosa Burgos^{1,3}, Cristina
4 Hernández^{1,2,3,4}, Rafael Simó^{1,2,3,4,*}.

5 ¹Endocrinology and Nutrition Department, Hospital Universitari Vall d'Hebron, Barcelona, Spain.

6 ²Diabetes and Metabolism Research Unit, Vall d'Hebron Institut De Recerca (VHIR), Barcelona. Spain.

7 ³Department of Medicine, Universitat Autònoma De Barcelona, Barcelona, Spain.

8 ⁴Centro De Investigación Biomédica En Red De Diabetes y Enfermedades Metabólicas Asociadas
9 (CIBERDEM), Instituto De Salud Carlos III (ISCIII), Madrid, Spain.

10 ⁵ARTIS Development, Las Palmas, Spain,

11 ⁶Department of Radiology, Institut De Diagnòstic Per La Imatge (IDI), Hospital Universitari Vall
12 d'Hebron, Barcelona, Spain,

13 * Corresponding authors: Fiorella Palmas: fiorellaximena.palmas@vallhebron.cat

14 **Summary**

15 **Background & aims:** The assessment of resting energy expenditure (REE) is a challenging task
16 with the current existing methods. The reference method, indirect calorimetry (IC), is not widely
17 available, and other methods show poor correlation with IC. Body composition (BC), in particular
18 muscle mass, plays an important role in REE. In recent years, computed tomography (CT) has
19 emerged as a reliable tool for BC assessment. However, its usefulness for the REE evaluation has
20 not been explored so far. On these bases we explored the possibility to assess the REE based on
21 a CT-scan image using artificial intelligence (AI) models and compare the results with the current
22 methods.

23 **Methods:** Single-centre observational cross-sectional pilot study were carried out including
24 consecutive patients in-hospital with abdominal CT. All subjects underwent indirect calorimetry
25 and bioimpedance analysis. Their requirements were calculated using different predictive
26 equations. The proposed model is based on a second-order linear regression with three input
27 parameters: weight in kilograms, age in years, and the amount of muscle mass quantified from
28 computed tomography images in square centimetres. The output of this model corresponds to
29 the resting energy expenditure (REE). The model was trained and tested using a cross-validation
30 one-vs-all strategy with 90 subjects with different characteristics.

31 **Results:** Data from 90 subjects were included in the model. Predictive equations show a low to
32 moderate correlation to IC ($r = 0.48-0.55$, p value <0.001). REE calculated by Bioelectrical
33 Impedance Analysis (BIA) showed better correlation than the predictive equations ($r = 0.636$, p
34 value <0.001). The best correlation was the one obtained through the CT estimation model ($r =$
35 0.647 , p value <0.001). This model was trained using three variables, including age, weight and
36 amount of muscle mass. During the experiments it was observed that replacing any of the
37 aforementioned variables with gender led to poorer results.

38 **Conclusions:** We demonstrated for the first time that REE can be estimated based on the
39 information extracted from abdominal CT imaging, thus obtaining good correlation with the
40 reference method (IC), which was higher than that obtained with BIA. This finding has the
41 potential to significantly change the paradigm and guidelines for nutritional assessment, and
42 represents a novel and revolutionary concept in the field of precision medicine.

43 **Funding:** none

44 **Keywords:** resting energy expenditure; computed tomography; indirect calorimetry, body
45 composition

46

47 **Introduction**

48 Body mass in humans is strongly associated with the rate of heat production as defined by
49 resting energy expenditure (REE) (1). Furthermore, the REE is related to the body composition
50 (BC) and both are important determinants of health (2,3). REE usually accounts for more than
51 60% of the total energy expenditure and is directly related to the amount of fat-free mass, which
52 is more metabolically active than fat mass (4,5). Recent guidelines recommend BC (mandatory)
53 and REE (when available) assessment for a proper nutritional and metabolic evaluation and
54 follow up (6–8). REE measurement is useful for preventing or halting under and/or overfeeding
55 in individuals, especially in clinical care, but it is also crucial for setting feasible goals for dietary
56 and exercise interventions (2,3). Currently, the reference method for REE measurement in
57 clinical practice is indirect calorimetry (IC) (9,10). IC calculates REE by measuring the amount of
58 oxygen consumed (VO_2) and carbon dioxide released (VCO_2) by using Weir's equation in a
59 controlled environment (5,11).

60 The more recent ESPEN guidelines recommend the measurement of REE by IC for obtaining an
61 accurate nutritional assessment (9,10,12). However, IC is not widely available due to the price
62 of the device and the need for trained personnel and special conditions for its performance
63 (fasting, resting for more than 5-10 minutes before the test, stable room temperature, stable
64 oxygen in ambient air, etc). When IC is not available, REE can be estimated using surrogates such
65 as mathematical equations or bioimpedance (BIA) (9,10,14). Regarding mathematical equations,
66 they represent an accessible, simple and inexpensive method but with low correlation with
67 reference techniques (IC) (around 60%), even when BC parameters are included in the algorithm
68 (15). BIA has recently emerged as an easily accessible tool for the BC assessment in clinical
69 practice due to its simplicity, portability and low cost. Although this technique does not directly
70 measure REE, some advanced BIA devices include algorithms that estimate the REE using

71 variables such as age, biological sex, and BC, with higher accuracy when compared with the
72 mathematical equations (16).

73 In recent years, computed tomography (CT) has emerged as a useful tool for BC assessment,
74 both on quantity (taking into account muscle area) and on quality (taking into account the tissue
75 radiodensity, measured in Hounsfield units, HU) (17,18). The CT-scan assessment of BC is based
76 on regional analysis of fat and fat-free mass at one slice in the third lumbar vertebrae (19–21).
77 Our group has developed FocusedON-BC software coupled with artificial intelligence (AI), which
78 offers several benefits over traditional methods (22). Firstly, the processing speed is much faster,
79 resulting in significant time savings for healthcare professionals and a reduction in operational
80 costs. Secondly, these systems provide enhanced measurement accuracy due to advanced
81 algorithms that integrate intricately analyses of image features. Moreover, the use of AI
82 minimises inter-observer variability by eliminating the inherent subjectivity of manual
83 evaluations. Despite the evidence of the usefulness of CT scan coupled with an AI-based
84 automatic software for BC assessment, to the best of our knowledge no data regarding the
85 usefulness of the CT-scan for the REE estimation have been reported.

86 On this basis we conducted a pilot study with two main objectives: 1) To evaluate the feasibility
87 of estimating the REE based on the body composition information extracted from a CT-scan
88 image at the L3 lumbar vertebrae using FocusedON-BC software; b) To compare the REE
89 measured using the IC as gold standard with that obtained using predicted equations, BIA and
90 our new methodology based on CT-scan.

91

92 **1. MATERIAL AND METHODS**

93 A single-centre observational cross-sectional pilot study was performed at the Vall d'Hebron
94 University Hospital between January and June 2022. The study was approved by the local Ethics
95 Committee (PR(AG)510/2021) and carried out in accordance with the Declaration of Helsinki.

96 Inclusion criteria: a) Age >18 years.; b) Ability to complete full indirect calorimetry and BIA tests
97 in fasting state; c) Ability to provide a signed informed consent

98 Exclusion criteria: a) Any medical condition that makes unfeasible the performance of CT scan,
99 indirect calorimetry or bioimpedance (e.g.: hemodynamic instability, acute condition,
100 respiratory support; not fasting), b) patients with noninvasive respiratory support.

101 A complete medical history, anthropometric assessment, indirect calorimetry, bioimpedance
102 analysis, abdominal CT-scan was obtained in all cases. The timeframe for the performance of all
103 tests was <72 hours.

104 Body mass index (BMI) was calculated using the following formula: weight (kg)/ height² (m²).

105 *Predictive equations.* The predictive equations chosen to calculate the REE are detailed in Table
106 1, according to current guidelines.

107 Table 1. Predictive equation for REE estimation.

Equation	Factors used for calculation	Adjusted to gender	Formula
Harris- Benedict (1919) (23)	Biological Sex, WT (kg), HT (cm), age (year)	Yes	M: $13.75 \times WT + 5.00 \times HT - 6.75 \times \text{age} + 66.47$ F: $9.56 \times WT + 1.85 \times HT - 0.67 \times \text{age} + 655.09$
Mifflin – St Jeor (1990) (24)	Biological Sex, WT (kg), HT (cm), age (year)	Yes	M: $9.99 \times WT + 6.25 \times HT - 5 \times \text{age} + 5$ F: $9.99 \times WT + 6.25 \times HT - 5 \times \text{age} - 161$
Ireton – Jones (2022) (25)	Biological Sex, WT (kg), age (year), BMI (obesity)	Yes	$629 - (11 \times \text{age}) + (25 \times WT) - (609 \times 1 \text{ if obesity; } \times 0 \text{ if normal BMI})$
25 kcal/kg (ESPEN) (13)	WT (kg)	No	$25 \times WT$
30 kcal/kg (ESPEN) (13)	WT (kg)	NO	$30 \times WT$

108 WT: weight; HT: height; F: female; M male; BMI: body mass index.

109

110 *Indirect calorimetry (IC)*: IC was performed with a Q-NRG device (Cosmed, Roma Italy), by the
111 same trained technician. IC was performed in all cases according to the protocol: resting for at
112 least 5 minutes in the supine position prior to the test and at least 15-20 minutes during the IC,
113 constant ambient temperature and O₂, fasting for 8 hours. The following variables were
114 collected: REE, respiratory quotient (RQ), respiratory oxygen consumption (VO₂) and production
115 of carbon dioxide (VCO₂) per minute.

116 *Bioimpedance analysis (BIA)*: After IC, with the subject still fasting and in resting supine position,
117 a whole-body BIA was performed. For this purpose, we used a tetrapolar Bodystat Quadscan
118 4000 with 50-kHz of frequency. The following variables were collected: phase angle (degrees),
119 total body water (%), fat mass (kg), lean mass (kg), body cell mass (kg), estimated REE (Kcal).

120 *Computed tomography (CT) analysis*: Abdominal computed tomography (CT) images focused on
121 the L3 vertebrae were obtained using a multidetector computed tomography scanner (Aquilion
122 Prime SP, Canon Medical Systems, Japan), with the following technical parameters: 135 kV (tube
123 voltage), 1mm 80 row (detector configuration), tube current modulation, and 0.8 sec/rotation
124 (gantry rotation). The following variables were recorded: skeletal muscle mass area or SMA (cm²
125 and %), skeletal muscle mass index or SMI (cm²/m²), intramuscular adipose tissue area or IMAT
126 (cm² and %), intramuscular adipose tissue index or IIMAT (cm²/m²), area of visceral fat mass
127 (VFA) (cm² and %), subcutaneous fat (SFA) (cm² and %), visceral fat mass index (VFI) (cm²/m²),
128 subcutaneous fat (SFI)(cm²/m²), and mean Hounsfield Units (HU) for each segmented tissue. The
129 CT images centred on the third lumbar vertebra (L3) were analysed using FocusedON-BC
130 software. Tissue density was assessed based on its average Hounsfield Units (HU) value.
131 Standard thresholds were used as follows: -29 to 150 HU for skeletal muscle, -190 to -30 for
132 subcutaneous adipose tissue and -150 to -50 for visceral adipose tissue (20,22).

133

134

135 *REE estimation based on CT-scan image analysed with FocusedON-BC*

136 The proposed method is based on a second-order linear regression with three input parameters:
137 weight in kilograms, age in years, and the amount of muscle mass quantified from computed
138 tomography images in square centimetres from a single computed tomography image centred
139 at L3 vertebrae level. The output of this model corresponds to the resting energy expenditure
140 (REE). In order to validate the viability of the proposed solution, the model was exhaustive
141 trained and tested using a cross-validation one-vs-all strategy using the data corresponding to
142 the 90 subjects recruited for the study, as follows:

143 Firstly, the different variables were collected for each subject and used as input parameters for
144 the described model. The CT-scan image data were collected using FocusedON-BC software. All
145 variables were scaled to a range between 0 and 1 using the minimum and maximum values
146 observed in the dataset for each variable. For this purpose, the equation "scaledValue =
147 (realValue - minValue) / (maxValue - minValue)" was used. Finally, the REE value calculated by
148 IC was used as a reference value both for training the model and for testing its estimation
149 accuracy.

150 It is important to emphasise that this methodology was applied by exhaustively combining all
151 available input variables from the dataset, consistently maintaining a model with three input
152 variables and using a second-order linear regression. The input variables tested included:

- 153 • Demographic variables: weight (kg), height (m), age (years), and sex (0 or 1 for male and
154 female, respectively)
- 155 • CT-scan imaging variables: quantity and mean radiological density of various tissues
156 (skeletal muscle, visceral adipose tissue, subcutaneous adipose tissue, total adipose)
157 quantified using FocusedON software in cm² and Hounsfield units, respectively. All these
158 variables are quantified from a single CT image centred at L3 vertebrae level.

159 The combination that provided the best results of three input variables, as previously described,
160 consists of weight, age, and the amount of muscle mass. It is worth mentioning that using muscle
161 radiodensity instead of muscle mass also provided promising results.

162

163 **2.2 Statistical analysis.**

164 This pioneering study evaluates caloric expenditure using computed tomography (CT) images, a
165 novel approach that is not reflected in the current state of the art. The lack of similar precedents
166 justifies our exploratory approach with a smaller sample size as a pilot study, a common scenario
167 in groundbreaking research where no prior foundation exists for determining optimal sample
168 size.

169 Statistical analysis was carried out using Python 3.11. Continuous variables are presented as
170 mean \pm standard deviation (SD) for normally distributed variables and median \pm interquartile
171 range (IQR) for non-normally distributed variables. Categorical variables are presented using
172 percentages. Statistical significance was accepted at $p < 0.05$. The correlation between BIA,
173 predictive equations and the IC was assessed by linear correlation coefficient (Pearson). Bland-
174 Altman plots were used to estimate agreement of the tested methods (BIA, predictive equations
175 and the proposed method) with respect to the reference one (IC).

176

177 **RESULTS**

178 A total of 90 subjects were included in this study, 56 men and 34 women (62% and 38%,
179 respectively). The mean age was 62.3 ± 15.4 years, and the mean BMI was 24.6 ± 4.7 kg/m².
180 Intentionally, patients with a wide range of BMI (15.4 - 47.9 kg/m²) were included. The results
181 obtained when evaluating the accuracy of the commonly used mathematical equations in
182 comparison to the reference method (IC) are shown in **Table 2**.

183 **Table 2.** Correlation between predictive equations and indirect calorimetry.

Method	Mean (kcal)	MAE	r ²	r	range	p – value
Harris- Benedict (1919)	1488.92 ± 175	230	0.234	0.486	0.311- 0.63	<0.001
Ireton – Jones (1992)	1466.14 ± 335	259	0.075	0.558	0.397-0.686	<0.001
Mifflin – St Jeor (1990)	1576.55 ± 161	231	0.226	0.488	0.312 – 0.631	<0.001
Weight x 25 kcal	1693.64 ± 347	286	-0.254	0.546	0.382-0.677	<0.001
Weight x 30 kcal	2032.37 ± 417	545	-2.628	0.546	0.382-0.677	<0.001
BIA	1555.67 ± 276	216	0.346	0.636	0.494-0.745	<0.001
TC	1502.3 ± 219	192	0.419	0.647	0.508-0.753	<0.001

184 MAE: mean absolute error; BIA: bioimpedance analysis; TC: computed tomography.

185

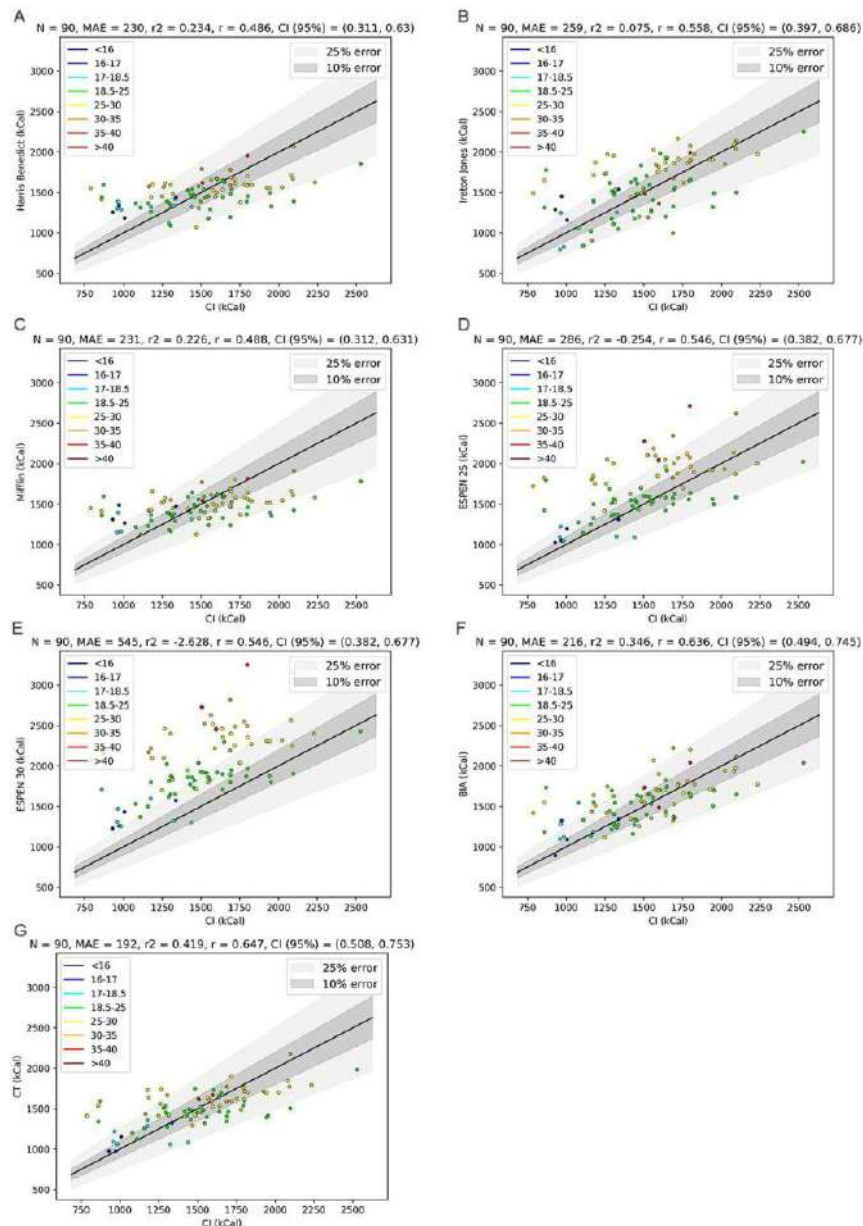
186 Overall, the values of REE calculated by predictive equations showed a low correlation with the
187 reference method, IC, and a high dispersion (**Figure 2 A-E**).

188 Regarding REE assessed by BIA, it presents a higher correlation in comparison with mathematical
189 models (r²=0.636, p value <0.001) and with a similar dispersion (0.494-0.745) (**Figure 2F**).

190 Finally, the values of REE estimated with the proposed model based on the information
191 extracted from CT-scan images at L3 vertebrae using FocusedON-BC software showed the
192 highest correlation with the reference method (IC), r=0.647, p value <0.001, with a lower
193 dispersion (0.508-0.753) (**Figure 2G**).

194

195 **Figure 2.** Correlation between IC (reference method) with predictive equations Harris Benedict
196 (A), Ireton-Jones (B), Mifflin-St Jeor (C), ESPEN 25 (D), ESPEN 30 (E), BIA (F) and CT based
197 estimation (G).



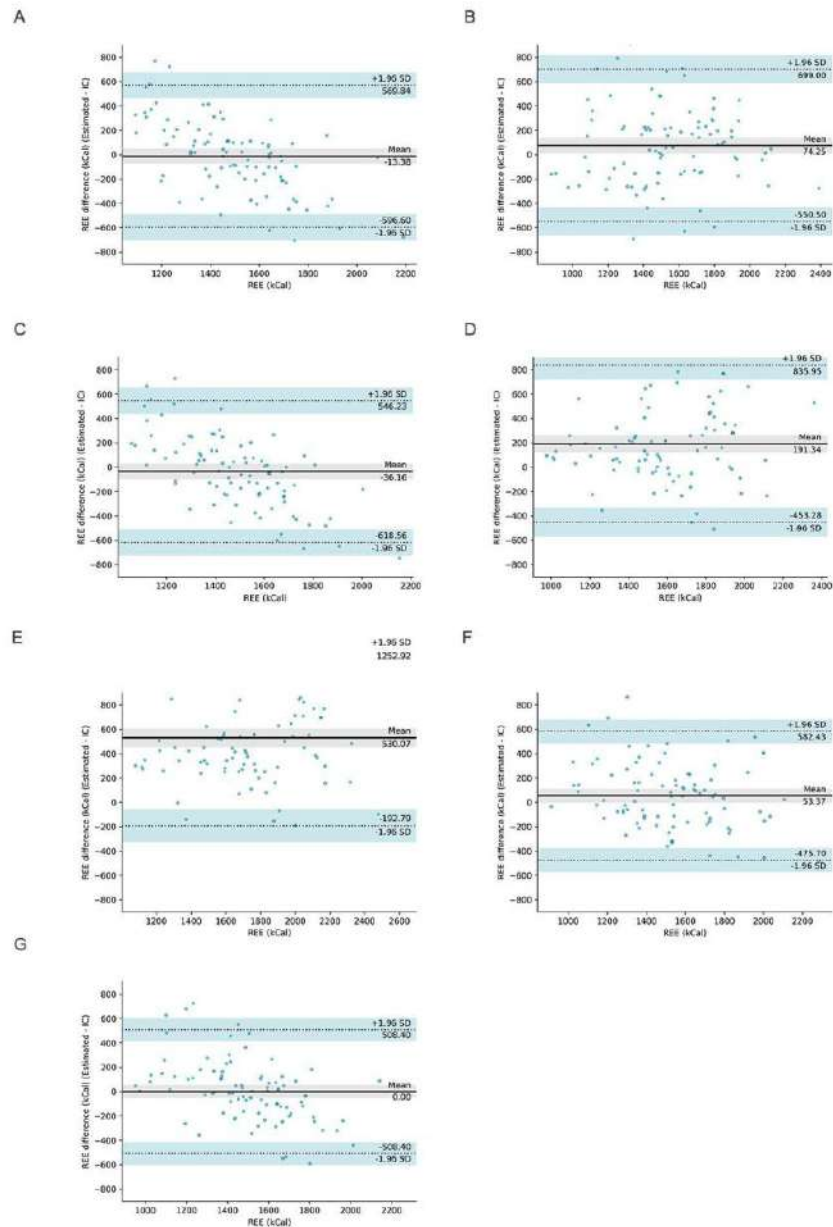
198

199

200 The results of dispersion and agreement between methods have been graphically represented

201 by Bland – Altman plot in **Figure 3**.

202 **Figure 3.** Bland - Altman plots for predictive equations Harris Benedict (A), Ireton-Jones (B),
 203 Mifflin-St Jeor (C), ESPEN 25 (D), ESPEN 30 (E), BIA (F) and CT based estimation (G).



206

207 **DISCUSSION**

208 It has been widely demonstrated that body composition (BC), especially lean tissue, is a
209 fundamental component in REE. BC determination based on abdominal CT-scan images at the
210 L3 level is a high-precision reference technique that provides both quantitative and qualitative
211 information (17,26). Given the high precision of BC determination using CT and its relevance in
212 REE, we proposed the development of a machine learning model for REE estimation. Our results
213 demonstrate for the first-time that REE can be estimated by means of a model based on BC
214 information extracted from abdominal CT-scan images using automatic AI-based software. This
215 finding could open a new era in the nutritional and metabolic assessment by means of AI in daily
216 practice.

217 Currently, the reference technique for measuring REE is IC, which is recommended by
218 most of the clinical guidelines (9,10,12–14,27). Although the devices have improved significantly
219 in recent years, they are still expensive, time-consuming, and trained personnel for its daily
220 clinical use is required. In addition, it must be performed under resting clinical conditions that
221 are not always available in clinical practice. Furthermore, IC has also some limitations, such as a
222 poor accuracy in cases of very low body weight, unstable temperature and involuntary
223 movements (subjects need to stay still for at least 15-20 minutes) (3)

224 Although IC is currently the most accurate technique for measuring REE in clinical
225 practice, the same guidelines that recommend it, suggest to use surrogates, when IC is not
226 available, such predictive equations or empirical calculations. Nevertheless, previous data
227 showed low accuracy of these methods for estimating the REE even when they have been
228 validated in studies with large sample sizes (>1000 subjects) (15). BIA is considered to be a more
229 accurate surrogate of IC than predictive mathematical equations because BC parameters,
230 mainly the fat free mass, is considered. However, BIA is influenced by the presence of acute

231 disease, obesity, and hydration status, besides of the need of special conditions for its
232 performance (introduction of weight and height, skin condition, fasting, body position, etc.)
233 (17,28).

234 It is worth mentioning that the development of machine learning models usually
235 requires a large sample size. As an example, in Achamrah N et al (29) 3.655 subjects have been
236 used just to validate the performance of the Bodystat QuadScan 4000 Manufacturer's equation
237 with respect to dual-energy x-ray absorptiometry (DXA). Our study is meant to be just a proof of
238 concept in which only 90 subjects have been included. This fact strongly limits the performance
239 that can be expected from the developed models based on the proposed methodology.
240 Nevertheless, the results obtained are surprisingly good, even overcoming those provided by
241 the BIA for this cohort. We assume that this may be due to the fact that CT-scan is currently
242 considered the reference technique for body composition assessment, and hence, the muscle
243 mass information extracted from CT-scan images provides very valuable information for
244 estimating the REE. Accordingly, it is expected that increasing the sample size would allow
245 developing and training more complex and robust models that would lead to even more
246 accurate results. As an extra advantage of the proposed methodology, it is also worth
247 mentioning that CT-scan is a method that is widely integrated in clinical practice, which does not
248 require specific preparation, such as fasting, rest, or maintaining the same position for a long
249 period of time. The proposed methodology considerably increases the value of this technique
250 as it allows an "opportunistic" use of the CT-scan images to estimate the REE.

251 Furthermore, CT allows us to study not only the quantity of muscle mass, but also its
252 quality. The muscle tissue radiodensity (HU) is related to the muscle quality and has been
253 previously correlated with fatty infiltration (myosteatosis) and is considered a prognostic
254 variable in severe illness (oncological, surgery) (20,30,31). P). Previous studies from our group
255 have shown that HU allows a more precise estimation of body composition (22). As far as we

256 know, radiodensity has never before been used for the REE calculation. AS previously described,
257 in this study, when we tested the different available CT-scan variables, muscle radiodensity also
258 showed very promising results.

259 It should be noted that BIA and predictive equations include in their algorithm for REE
260 estimation the gender and age as main variables. In the present study, after applying deep
261 learning and developing the most accurate model, the variables accounting for REE in an
262 independent manner were those related to total weight (kg), age, and muscle mass quantity
263 (cm²). Interestingly, gender, a classic variable widely used at present and for more than a
264 century ago (i.e. Harris-Benedict equation) for the estimation of REE, were not valued as
265 significant. This unexpected finding might explain the low correlation of either BIA or predictive
266 equations with the real value of REE, thus suggesting that gender *per se* is not a primary
267 determinant of REE. Our model indicates that the muscle quantity is relevant enough to
268 determinate REE regardless of gender. This finding can have a significant impact and may
269 eventually change the current guidelines and recommendations for REE determination in the
270 setting of nutritional evaluation.

271 It is worth mentioning that the method herein proposed permits us to estimate “at a
272 glance” both BC and REE, thus opening up a new era in the personalised approach of metabolic
273 and nutritional related interventions. In addition, this combined information can favour
274 subjects’ adherence to treatment and follow-up and can contribute to a positive reinforcement.
275 For health care providers, the system will monitor in real time the effects of new emerging
276 pharmacological therapies in different pathologies (i.e. obesity, diabetes, cancer, nutritional
277 pathologies), thus engaging the pharmaceutical industry as a whole.

278 As a limiting factor of our study, the small sample size should be mentioned. However, despite
279 the low sample size and the heterogeneity in age, gender and BMI, the correlation with the
280 reference method (IC) was higher than more elaborated methods such as BIAWe provide first

281 evidence that muscle quantity and quality parameters are the major determinants of REE,
282 regardless of the classically used variables. Another limitation may be that the model is based
283 on the CT-imaging technique, which requires the emission of radiation. However, our study has
284 been carried out in patients who underwent CT for other clinical reasons, given an
285 "opportunistic" use. Furthermore, the level of radiation applied to a single CT slice, is similar to
286 that of a chest X-ray (17,22).

287

288 **Conclusion**

289 In summary, in this pilot study we have demonstrated for the first time that REE can be
290 precisely estimated based on information extracted from CT-scan abdominal imaging using AI-
291 deep learning. Additionally, we have provided evidence that muscle quantity (cm²), age and
292 weight are main variables accounting for the REE. This discovery has the potential significant
293 impact on changing the paradigm and guidelines for nutritional evaluation, and represents a
294 novel and revolutionary concept in the era of precision medicine. Nevertheless, future studies
295 using other cohorts with larger sample size to confirm this proof of concept are needed.

296 **Funding statement:** This research did not receive any specific grant from funding agencies in the
297 public, commercial, or not-for-profit sectors.

298 **Data sharing statement** Not applicable.

299 **Declaration of interests:** FP, AD, JM, RG and RS are researchers who are part of a patent in
300 progress, accepted. The other authors report no conflicts of interest.

301 **Authors Contributions**

302 Conceptualization: FP, AC, RG, JM, RS. Data curation: FP, RG, JM, GC, AZ, FM. Formal analysis:
303 R.G.; J.M. Funding acquisition: RB, RS. Investigation: FP, RG, JM, AZ, GC, FM, AR, NR.
304 Methodology FP, AC, RG, JM, RS. Project administration: FP, AC, RG, JM, RS. Resources: FP, GC,

305 AZ, FM, RB. Software: RG, JM. Supervision: FP, AC, RS, RB, CH. Validation: AC, RS, RB, CH.
 306 Visualisation: FP, AC, RS, RG, NR, AR, RB, RS, CH. Roles/Writing - original draft: FP, AC, RG, RS.
 307 Writing - review & editing: FP, AC, RG, RS, RB, CH.
 308 All authors reviewed the manuscript.
 309 All authors read and approved the final version of the manuscript

310

311

312 REFERENCES

- 313 Heymsfield SB, Thomas DM, Bosy-Westphal A, Müller MJ. The anatomy of resting energy
 314 expenditure: body composition mechanisms. Vol. 73, European Journal of Clinical Nutrition.
 315 Nature Publishing Group; 2019. p. 166–71.
- 316 Delsoglio M, Achamrah N, Berger MM, Pichard C. Indirect calorimetry in clinical practice. Vol.
 317 8, Journal of Clinical Medicine. MDPI; 2019.
- 318 Oshima T, Berger MM, De Waele E, Guttormsen AB, Heidegger CP, Hiesmayr M, et al. Indirect
 319 calorimetry in nutritional therapy. A position paper by the ICALIC study group. Vol. 36, Clinical
 320 Nutrition. Churchill Livingstone; 2017. p. 651–62.
- 321 Heimburger D, Ard J. Handbook of clinical nutrition (Fourth Edition). 2006. 1–645 p.
- 322 Fidilio E, Comas M, Giribés M, Cárdenas G, Vilallonga R, Palma F, et al. Evaluation of Resting
 323 Energy Expenditure in Subjects with Severe Obesity and Its Evolution After Bariatric Surgery.
 324 Obes Surg [Internet]. 2021 Oct 1 [cited 2022 Mar 14];31(10):4347–55.
- 325 Barazzoni R, Jensen GL, Correia MITD, Gonzalez MC, Higashiguchi T, Shi HP, et al. Guidance for
 326 assessment of the muscle mass phenotypic criterion for the Global Leadership Initiative on
 327 Malnutrition (GLIM) diagnosis of malnutrition. Clinical Nutrition. 2022 Jun 1;41(6):1425–33.

328 Fröhbeck G, Busetto L, Dicker D, Yumuk V, Goossens GH, Hebebrand J, et al. The ABCD of
 329 Obesity: An EASO Position Statement on a Diagnostic Term with Clinical and Scientific
 330 Implications. *Obes Facts* [Internet]. 2019 [cited 2022 Nov 12];12:131–6.

331 Donini LM, Busetto L, Bischoff SC, Cederholm T, Ballesteros-Pomar MD, Batsis JA, et al.
 332 Definition and Diagnostic Criteria for Sarcopenic Obesity: ESPEN and EASO Consensus
 333 Statement. *Obes Facts* [Internet]. 2022 May 23 [cited 2022 Oct 17];15(3):321–35.

334 Singer P, Blaser AR, Berger MM, Alhazzani W, Calder PC, Casaer MP, et al. ESPEN guideline on
 335 clinical nutrition in the intensive care unit. *Clinical Nutrition*. 2019 Feb 1;38(1):48–79.

336 Muscaritoli M, Arends J, Bachmann P, Baracos V, Barthelemy N, Bertz H, et al. ESPEN practical
 337 guideline: Clinical Nutrition in cancer. *Clinical Nutrition*. 2021 May 1;40(5):2898–913.

338 Gupta R Das, Ramachandran R, Venkatesan P, Anoop S, Joseph M, Thomas N. Indirect
 339 Calorimetry: From Bench to Bedside. *Indian J Endocrinol Metab* [Internet]. 2017 Jul 1 [cited
 340 2024 Jan 14];21(4):594–9.

341 Bischoff SC, Bernal W, Dasarthy S, Merli M, Plank LD, Schütz T, et al. ESPEN practical
 342 guideline: Clinical nutrition in liver disease. *Clinical Nutrition*. 2020 Dec 1;39(12):3533–62.

343 Thibault R, Abbasoglu O, Ioannou E, Meija L, Ottens-Oussoren K, Pichard C, et al. ESPEN
 344 guideline on hospital nutrition. *Clinical Nutrition*. 2021 Dec 1;40(12):5684–709.

345 Fiaccadori E, Sabatino A, Barazzoni R, Carrero JJ, Cupisti A, De Waele E, et al. ESPEN guideline
 346 on clinical nutrition in hospitalized patients with acute or chronic kidney disease. *Clinical
 347 Nutrition*. 2021 Apr 1;40(4):1644–68.

348 Achamrah N, Jésus P, Grigioni S, Rimbart A, Petit A, Déchelotte P, et al. Validity of predictive
 349 equations for resting energy expenditure developed for obese patients: Impact of body
 350 composition method. *Nutrients*. 2018 Jan 10;10(1).

3651 Barak N, Wall-Alonso E, Cheng A, Sitrin MD. Use of Bioelectrical Impedance Analysis to Predict
3652 Energy Expenditure of Hospitalized Patients Receiving Nutrition Support. Vol. 27, JOURNAL OF
3653 PARENTERAL AND ENTERAL NUTRITION. 2003.

3654 Prado CM, Ford KL, Gonzalez MC, Murnane LC, Gillis C, Wischmeyer PE, et al. Nascent to novel
3655 methods to evaluate malnutrition and frailty in the surgical patient. Vol. 47, Journal of
3656 Parenteral and Enteral Nutrition. John Wiley and Sons Inc; 2023. p. S54–68.

3657 Tolonen A, Pakarinen T, Sassi A, Kytä J, Cancino W, Rinta-Kiikka I, et al. Methodology, clinical
3658 applications, and future directions of body composition analysis using computed tomography
3659 (CT) images: A review. Vol. 145, European Journal of Radiology. Elsevier Ireland Ltd; 2021.

3660 Shen W. Total body skeletal muscle and adipose tissue volumes: estimation from a single
3661 abdominal cross-sectional image. J Appl Physiol [Internet]. 2004;97(6):2333–8.

3662 Aubrey J, Esfandiari N, Baracos VE, Buteau FA, Frenette J, Putman CT, et al. Measurement of
3663 skeletal muscle radiation attenuation and basis of its biological variation. Vol. 210, Acta
3664 Physiologica. 2014. p. 489–97.

3665 Albano D, Messina C, Vitale J, Sconfienza LM. Imaging of sarcopenia: old evidence and new
3666 insights. Eur Radiol. 2020;30(4):2199–208.

3667 Palmas F, Ciudin A, Guerra R, Eiroa D, Espinet C, Roson N, et al. Comparison of computed
3668 tomography and dual-energy X-ray absorptiometry in the evaluation of body composition in
3669 patients with obesity. Front Endocrinol (Lausanne). 2023 Jun 26;14.

3670 Arthur Harris BJ, Benedict FG. Grundzilge der Mengenlehre. Vol. 23, Bull. Amer. Math. Soc. Veit
3671 & Co; 1914.

3672 Mifflin MD, St Jeor ST, Hill LA, Scott BJ, Daugherty SA, Koh YO. A new predictive equation for
3673 resting energy expenditure in healthy individuals. Am J Clin Nutr [Internet]. 1990 [cited 2024
3674 Feb 5];51(2):241–7.

375 Ireton-Jones C, Jones JD. Improved Equations for Predicting Energy Expenditure in Patients:
376 The Ireton-Jones Equations. *Nutrition in Clinical Practice* [Internet]. 2002 Feb 1 [cited 2024 Feb
377 5];17(1):29–31.

378 Lee K, Shin Y, Huh J, Sung YS, Lee IS, Yoon KH, et al. Recent issues on body composition imaging
379 for sarcopenia evaluation. Vol. 20, *Korean Journal of Radiology*. Korean Radiological Society;
380 2019. p. 205–17.

381 Lochs H, Dejong C, Hammarqvist F, Hebuterne X, Leon-Sanz M, Schütz T, et al. ESPEN
382 Guidelines on Enteral Nutrition: Gastroenterology. *Clinical Nutrition*. 2006 Apr;25(2):260–74.

383 Ceniccola GD, Castro MG, Piovacari SMF, Horie LM, Corrêa FG, Barrere APN, et al. Current
384 technologies in body composition assessment: advantages and disadvantages. Vol. 62,
385 *Nutrition*. Elsevier Inc.; 2019. p. 25–31.

386 Achamrah N, Colange G, Delay J, et al. Comparison of body composition assessment by DXA
387 and BIA according to the body mass index: A retrospective study on 3655 measures. *PLoS One*
388 2018;13.

389 Ahn H, Kim DW, Ko Y, Ha J, Shin Y Bin, Lee J, et al. Updated systematic review and meta-
390 analysis on diagnostic issues and the prognostic impact of myosteatosi: A new paradigm
391 beyond sarcopenia. Vol. 70, *Ageing Research Reviews*. Elsevier Ireland Ltd; 2021.

392 Geladari E, Alexopoulos T, Kontogianni MD, Vasilieva L, Mani I, Tenta R, et al. The Presence of
393 Myosteatosi Is Associated with Age, Severity of Liver Disease and Poor Outcome and May
394 Represent a Prodromal Phase of Sarcopenia in Patients with Liver Cirrhosis. *J Clin Med*
395 [Internet]. 2023 May 1 [cited 2023 Aug 5];12(9):3332.

396

5.5. Intellectual property resulted from the studies of this thesis

A training method of a computer-implemented machine learning model for obtaining a resting energy expenditure (REE) parameter of a subject.

Principal claim:

A training method of a computer-implemented machine learning model for obtaining a Resting Energy Expenditure (REE) parameter of a subject, and a system to perform such method, are presented, wherein an REE parameter from an experimental test, and information from a CT scan image of the subject are used to train the computer-implemented machine learning model. A method for estimating a Resting Energy Expenditure (REE) parameter of a subject is also presented, using a computer-implemented machine learning model previously trained by the training method described herein

PCT patent application claiming priority of European application no. EP22383050.6 filed on 31 October 2022.

Patent application code: PCT/EP2023/080242

Authors: Fiorella Palmas, Andreea Ciudin, Rafael Simó, José Melian, Raul Guerra.

Inscription date: October 30, 2023.

Status: accepted, pending completion of process.

Acknowledgement of receipt

We hereby acknowledge receipt of your request for grant of a European patent as follows:

Submission number	300465868	
Application number	EP22383050.6	
File No. to be used for priority declarations	EP22383050	
Date of receipt	31 October 2022	
Your reference	P6144EP00	
Applicant	FUNDACIÓ HOSPITAL UNIVERSITARI VALL D'HEBRON - INSTITUT DE RECERCA	
Country	ES	
Title	A TRAINING METHOD OF A COMPUTER-IMPLEMENTED MACHINE LEARNING MODEL FOR OBTAINING A RESTING ENERGY EXPENDITURE (REE) PARAMETER OF A SUBJECT	
Documents submitted	package-data.xml application-body.xml SPECTRANONEP.pdf\P6144EP00 - REE_Resumen ES.pdf (1 p.) OLF-ARCHIVE.zip\P6144EP00 Preconversion.zip	ep-request.xml ep-request.pdf (5 p.) SPECEPO-1.pdf\P6144EP00 - REE.pdf (32 p.) f1002-1.pdf (2 p.)
Submitted by	CN=Laura Artigas 49835	
Method of submission	Online	
Date and time receipt generated	31 October 2022, 17:45:46 (CET)	
Official Digest of Submission	99:C3:88:2C:D4:9A:98:A9:2F:2A:5D:E1:7B:C5:9E:89:B3:DC:AC:90	

Form 1002 - 1: Public inventor(s)

Designation of inventor

User reference: P6144EP00
Application No:

Public

Inventor	<p>Name: Simó Canonge Rafael</p> <p>Address: 08173 SANT CUGAT DEL VALLÈS Spain</p> <p>The applicant has acquired the right to the European patent: As employer</p>
Inventor	<p>Name: Palmas Candia Fiorella Ximena</p> <p>Address: 08035 BARCELONA Spain</p> <p>The applicant has acquired the right to the European patent: As employer</p>
Inventor	<p>Name: Ciudin Mihai Andreea</p> <p>Address: 08035 BARCELONA Spain</p> <p>The applicant has acquired the right to the European patent: As employer</p>
Inventor	<p>Name: Guerra Hernández Raúl Celestino</p> <p>Address: 35400 ARUCAS Spain</p> <p>The applicant has acquired the right to the European patent: Under agreement: 30 August 2022</p>
Inventor	<p>Name: Melián Álamo José María</p> <p>Address: 35019 LAS PALMAS DE GRAN CANARIA Spain</p> <p>The applicant has acquired the right to the European patent: Under agreement: 30 August 2022</p>

**A training method of a computer-implemented machine learning model for obtaining a
Resting Energy Expenditure (REE) parameter of a subject**

[0001] The present disclosure relates to methods and systems used for the estimation of Resting Energy Expenditure (REE) parameters of a subject.

BACKGROUND

[0002] Recent research has focused on the development of new techniques able to evaluate the human body composition. A first example is the technique known as Magnetic resonance imaging (MRI), which is a type of scan that uses strong magnetic fields and radio waves to produce detailed images of the inside of the body. Another example is Computed tomography, commonly referred to as CT scan, which is able to precisely measure the attenuation of X-ray passing through different types of tissues (i.e., fat, muscle, etc.). However, in contrast to the high amount of technology involved in the acquisition of data when using such techniques, there is a clear lack of tools that allow an efficient and precise analysis of the acquired data. For instance, in most cases, the information within MRI scans or CT scans is manually evaluated by a physician or trained technician performing a visual inspection. Consequently, this leads to a lack of precise quantitative measurements, repetitive and time-consuming tasks, as well as inter-observer dependencies in diagnostics and even possible human errors.

[0003] In order to improve measurements of MRI or CT scans, software tools have emerged aimed at performing quantitative analysis of human body composition, which can be useful for specific purposes in daily clinical practices and/or research activities. These tools mostly provide quantitative information about the volume or area of different tissues and usually require manual selection of the tissues to be quantified, based on the images from MRI or CT scan.

[0004] Different approaches for the estimation of the REE may be based on the use of imaging techniques, such as MRI and CT scans, which allows to obtain an organ and/or tissue volumes. Such methods may include, knowing the average density of each target organ/tissue, estimating the mass of a target organ/tissue, for example in kilograms, as its volume multiplied by its average density. Organ-tissue metabolic rates (OMR), measured in kJ/(kg·day), have been proposed in earlier literature. Each individual organ-tissue mass is then multiplied by its corresponding OMR obtaining the REE for that specific organ-tissue. The calculation of the whole body REE (kJ/day) of a subject is obtained as the sum of the REE for every individual organ/tissue. The mentioned procedure may also be applicable to other imaging methods like dual-energy X-ray absorptiometry (DXA), whose main limitation is that tissue quality or density cannot be estimated. Furthermore, the literature assumes that different organs and tissues are homogeneous in composition. Therefore, subjects with diseases as muscular dystrophy (i.e., lipid replacement of skeletal muscle fibers) or hepatic steatosis (i.e., fatty infiltration of liver) might obtain an erroneous

or low accuracy-REE estimation. Additionally, the state-of-the-art methods to obtain the REE may require mostly whole-body information, which may imply a high quantity of radiation to the subject when CT scans are involved.

[0005] REE estimations in the state of the art based on imaging techniques have a low accuracy and can be affected by factors related to a specific subject.

SUMMARY

[0006] The present disclosure aims at defining a method for an accurate estimation of a REE parameter of a subject based on imaging techniques, particularly characterized in that the REE parameter is obtained based on information extracted from, at least, one image of a computed tomography CT scan of a subject.

[0007] In a first aspect, a training method of a computer-implemented machine learning model for obtaining a Resting Energy Expenditure (REE) parameter of a subject is provided, wherein the method comprises the following steps:

- obtaining one or more ground-truth REE parameters of one or more subjects; the estimation may have been performed using any measurement methodology, for example, by an indirect calorimetry (IC) measurement of a subject or by bioimpedanciometry;
- obtaining the one or more CT scan images of the one or more subjects; the CT scan image(s) may be centered at any level of the subject: in some examples the CT scan image may be centered at leg level, and/or abdomen level, thorax, neck, etc. There are references in the literature of the estimation of body composition in all of them, the most accurate being the abdominal L3 level; each ground-truth REE parameter is associated with each subject and therefore with each CT scan image;
- identifying at least a region of interest, ROI, in each of the obtained CT scan images. This ROI may correspond to one specific tissue (such as muscle, visceral adipose tissue, etc.), to one specific organ (for example, liver, kidney, brain, etc.), or any combination of them, including the whole body of the subject within the CT scan image(s);
- calculating a group of parameters of each ROI; wherein a group comprises one or more parameters of each ROI, and wherein each group is associated with a ground-truth REE parameter; wherein the one or more parameters comprise a radiodensity parameter for at least one of the identified ROIs. The parameter may comprise a quantity expressed in area of the ROI, volume of the ROI, percentage, etc. Each calculated group of parameters of a CT scan image of a particular subject is associated with a ground-truth REE parameter of the particular subject;
- performing a supervised training of the computer-implemented machine learning model,

using a training data set comprising one or more groups of parameters of each ROI and the associated one or more ground-truth REE parameters, and wherein the training further comprises, for each group, setting an output parameter of the model corresponding to the associated ground-truth REE parameter.

[0008] Methods in the state-of-the-art show significant correlation between the quantity of a tissue, such as, for example, muscle mass, measured in a CT scan image of a human body, and the measurement of the total quantity of the same tissue within the whole body, for example, the total amount of body muscle mass. More precisely, it is also possible to draw such correlation in the case of other tissues of the body, such as, for example, visceral adipose tissue (VAT) or subcutaneous adipose tissue (SAT), the correlation being between the quantity of tissue measured in a CT scan image, and the total amount of said tissue within the whole body. Methods in the state-of-the-art may suggest that the value of the Resting Energy Expenditure (REE) measurement i.e., the energy expenditure while a person is at rest, awake, and in an interprandial state, of the same human body may strongly depend on the total amount of fat free mass.

[0009] The methods defined in the present disclosure allow estimating or inferring or calculating REE parameter of a subject departing from a CT scan image of the subject, i.e., the REE corresponds to the same subject from which the CT image and parameters of the ROI come from. The methods defined in the present disclosure allow correlating information obtained from, at least, one image with a Resting Energy Expenditure (REE) parameter in a scalable or reproducible manner.

[0010] The REE parameter can be estimated for all type of subjects, healthy subjects or patients. Among the subjects, different objectives may be pursued, for example, the knowledge of REE parameter may be used for adapting a diet or exercise for a healthy subject or a patient.

[0011] The methods of the present disclosure may be implemented for a baseline evaluation, and for follow-up, to evaluate, for example, evolution in time, including for example physiological aging, to see how body composition and REE change with age or in various stages and circumstances of life, response to treatments, response to diets, response to exercise or response to stress.

[0012] A subject may undergo an indirect calorimetry (IC) test to obtain a ground-truth REE parameter from the subject. Other measurement/estimation techniques may be employed, such as bioimpedanciometry. An IC test (the actual gold-standard method for REE measurements) may calculate heat that living organisms produce by measuring either their production of carbon dioxide and nitrogen waste (frequently ammonia in aquatic organisms, or urea in terrestrial ones), or their consumption of oxygen. This technique provides unique information, is noninvasive, and can be advantageously combined with other experimental methods to investigate numerous aspects of nutrient assimilation, thermogenesis, the energetics of physical exercise, and the pathogenesis of metabolic diseases.

[0013] Generally, in order to perform an IC test, a machine may be used which captures the gases that the subject breathes in and out, in order to measure a parameter corresponding to the subject's REE. Therefore, IC tests are used as reference tests (gold-standard) to measure how much energy the subject expends at rest (in other words, how many calories the subject is burning while resting). Even though IC is an accurate measurement of the subject's REE, it is cumbersome to perform, the machinery used to perform it is expensive, and it needs specially conditioned space and trained personnel for its operation. Therefore, it is rarely performed on the subject in the daily practice setting.

[0014] In parallel, or either before or after the ground-truth REE measurement technique is performed, preferably, for example, within no more than one week, a CT scan may be performed on the subject, and a set of CT scan images may be obtained (comprising at least one image).

[0015] A CT scan image may comprise the following information when obtained:

the area and/or volume corresponding to a region of interest (ROI) can be measured based on the number of pixels of the CT scan image corresponding to that ROI, and the pixel resolution (measured, for example, in cm^2/pixel or cm^3/pixel).

Information about the region of interest (ROI). Generally, each pixel of a digital CT scan image represents the attenuation of the X-rays which pass through the tissue of the body. Therefore, the specific attenuation may be proportional to the density of the tissue; the radiodensity is commonly measured in Hounsfield Unit (HU). Therefore, a parameter related to the radiodensity or density of the ROI can be obtained, such as, for example, the average HU.

[0016] The CT scan image to be used may be located at different positions of the human body, such as, for example, subject's leg, abdomen, thorax, neck, etc. Depending on that location, more or less relevant data may be obtained to estimate the REE.

[0017] For example, at L3 vertebral level, the psoas muscle is very wide, and therefore useful information may be retrieved from a CT scan image performed at this level. Furthermore, at such level which corresponds to an abdomen level, other more prominent tissues are found, such as: visceral adipose tissue (VAT) (excess fat, which tends to accumulate between the intraabdominal organs or inside them), or subcutaneous adipose tissue (fat which accumulates under the skin).

[0018] Even though any other location may be used to perform the scan, L3 vertebral level is a location which statistically correlates best the amounts of fat and muscles tissues and its features within the body as a whole.

[0019] Other parts of the body or other abdominal vertebral levels, such as L5 or L7, may not correlate the muscle and fat tissues as exactly as in L3, and thus other parts may not be as representative of the body as a whole (regarding fat and muscle) but would still be useful to perform an REE estimation. Regardless of the chosen part of the body, the training procedure of the present disclosure may not vary.

[0020] Once one or more CT scan images are obtained, at least a region of interest, ROI, is identified and at least one parameter of the ROI is calculated, for example, an area, or a volume or a density. The ROI may correspond to a subject's area or volume that may include, at least, one tissue (i.e., muscle, visceral adipose tissue, subcutaneous adipose tissue, etc.), one organ (i.e., liver, kidney, brain, heart, etc.) or any combination of them, including an entire subject's body within the image. Derived information, such as size (i.e., cm^2 , cm^3 , etc.), radiodensity (in Hounsfield Unit, HU) or any other metric can be obtained from that ROI. In the present disclosure "entire subject's body within the image" may be understood as a region of a CT scan image representing or showing at least a part of a subject's body. For example, entire subject's body within the image may comprise a slice of a body abdomen resulting from a transversal cut and representing the whole/entire perimeter of the abdomen, with the tissues and organs included. For example, entire subject's body within the image may comprise a slice of a leg resulting from a transversal cut and representing the whole/entire perimeter of the leg, with the tissues and bones included. For example, entire subject's body within the image may comprise a slice of a part of a body resulting from a transversal cut and representing a whole/entire at least a region of the part of the body, not necessarily the whole or entire perimeter.

[0021] In some examples, the ROI may represent a specific tissue or organ in the image. Identifying a ROI may comprise performing a segmentation of the one or more obtained images. At least one predetermined type of tissue or organ, or any combination of them, including the entire subject's body within the image may be identified. More precisely, in segmentation, different tissues or organs can be identified on the image, such as, for example, muscle, subcutaneous adipose tissue, visceral adipose tissue or intramuscular adipose tissue. Such segmentation may be performed by a computing system, by identifying different types of tissues within the CT scan image or may be performed by receiving data related to such areas of the CT scan image, from, for example, a Graphic User Interface (GUI), wherein a physician or a trained technician has visually identified and marked parts of the CT scan image and has inputted such identified parts into a computing system by inputting means, for example a mouse, a keyboard, or a touchpad.

[0022] After a ROI is identified, at least one ROI parameter may be calculated related to an amount of the identified ROI, from the segmented image, wherein an amount may comprise an area or a volume.

[0023] An example of a ROI parameter may be a premeasured quantity, for example, an area or volume in cm^2 or cm^3 . In such example, the pixels of the CT scan image occupied by a ROI may be counted, and a conversion from pixels to, for example, cm^2 may be performed, using the pixel resolution provided within metadata which may be integrated in the CT scan image.

[0024] Alternatively, a parameter related to the percentage of a ROI with respect to the total subject's body within the image may also be calculated. This percentage represents a relative measure of a specific ROI within the subject, thus giving a more representative measurement of

the amount of ROI within a person's body. For example, two subjects may have a similar amount of muscle, but one of them may be fatter than the other. Thus, in the thinner subject, the amount of muscle may be the same as in the fatter subject, but the relative amount of muscle may be higher, thus resulting in different energy expenditure. Therefore, using a percentage may lead to a more accurate estimation of REE. Furthermore, different measurements (i.e., parameters) may be used for different identified ROIs, in order to use a combination which may enhance the accuracy of REE estimations. Different groups combining different types of ROIs segmented from a CT scan can be obtained and subsequently used as a training data set, to infer a more accurate REE parameter of the subject. More precisely, the resulting REE estimation may consider different scenarios, wherein different types of tissues have different energy expenditures, and the same type of tissue may have a different energy expenditure depending on the ratios of tissue in each body and the type of body itself.

[0025] Finally, the supervised training of a machine learning model is performed, using a training data set which comprises one or more groups of the calculated parameters corresponding to one or more subjects. More precisely, the supervised training may be performed using a training data set wherein the data is organized at least in pairs. The pairs may comprise a group that includes at least one calculated parameter of the ROI of a CT scan image of a subject, and an output parameter corresponding to the ground-truth REE parameter measured on the same subject, for example by means of an IC test or bioimpedanciometry. The received training data set may be processed through the machine learning model. The machine learning model may implement supervised learning logic, wherein the model is given the training data set to ingest and told a result to be interpreted from the data -supervised-. The result is the ground-truth REE parameter measured on the subject for each respective obtained CT scan image. The model is trained to arrive at the result based on the ingested data and the accuracy of the trained model is dependent in part on the diversity of the received training data set being ingested. A trained model results from the supervised training. The trained model may result when a deviation or error or validation error between the output of the model and a reference/real/ground-truth REE parameter is lower than, for example, 5% or lower than a 10%. The deviation may be tested during a validation of the model.

[0026] The training data set may further include, in some examples, numerical variables or values such as anthropometric information of subjects, height, weight, age, information from the CT image, areas or volumes of different ROIs measured, for example, in cm^2 , cm^3 and/or in % and averages of Hounsfield units, among others. The training data set may also include categorical variables such as a subject's gender, demographic information, race, clinical information, etc. Such variables may be obtained by the disclosed methods by receiving them from an external source or by calculating them. When a system implements the methods disclosed herein, the system may comprise reception means, such as an interface, for receiving the input variables and

CT scan image, or calculating means such as a processor, for calculating one or more of the variables used for training the model. When calculating the variables, the method disclosed herein may calculate one or more of them from the CT scan image.

[0027] By using the previously described method, a machine learning model may be trained in a way in which, when provided with processed data extracted from a CT scan image of a subject, the machine learning model provides a REE parameter which may be more accurate than an REE parameter provided by other REE estimation methods.

[0028] In some examples, the steps of obtaining one or more ground-truth REE parameters of one or more subjects; obtaining the one or more CT scan images of the one or more subjects; identifying at least a ROI; and calculating one or more parameters of each ROI may be performed by a first entity or processor. The parameters may then be sent by means of a wired or wireless connection to a second entity or second server which may be configured to perform the step of performing a supervised training of the computer-implemented machine learning model, using a training data set comprising the calculated one or more parameters of each ROI and associated ground-truth REE parameters, and wherein the training further comprises for each of the one or more parameters of each ROI, setting an output parameter of the model corresponding to the associated ground-truth REE parameter.

[0029] Generally, a CT scan is performed more regularly and is much easier to perform than a method for obtaining an REE parameter experimentally, such as an IC test or bioimpedancemetry, which is physically demanding on the subject, involving cumbersome and error-sensitive equipment. Therefore, by performing the above-described method, once the model is trained, the model may be stored in non-volatile memory or non-transitory computer readable media to be used for estimating a further REE parameter.

[0030] Methods for obtaining an REE parameter using a trained model as described herein avoids experimental measurement methods for determining REE parameters of new subjects. More precisely, by using a machine learning model trained by the above-described method steps, a REE parameter may be obtained by inputting information extracted from one or more CT scan images to a system where the trained machine learning model runs and obtaining, from the model, the REE parameter. The methods of the present disclosure avoid obtaining an REE parameter experimentally (i.e., by IC tests or by bioimpedanciometry), while obtaining an REE parameter with a similar accuracy to the REE estimation method used to provide the training data set.

[0031] While literature describes methods for estimating a REE parameter departing from CT images, the method proposed herein provides a more accurate correlation between CT scan images and real or ground-truth REE measurements. Furthermore, the methods described herein may be more efficient and less computationally demanding, since the REE parameter can be inferred using information obtained from even one single CT scan image.

[0032] In examples, the computer-implemented machine learning model may be a regression

model since the expected result is an estimated numerical value (corresponding to the ground-truth REE of the subject). Different types of machine learning models may be used. The computer-implemented machine learning model may be one of a neural network, or a model comprising assembled decision trees, or a neural network comprising at least one fully connected layer, or a combination of one or more neural networks and one or more decision trees used to execute regression.

[0033] For example, the machine learning model may be an artificial neural network ANN. ANNs have a very high performance when the datasets to be used both for training and, subsequently, for regression, are composed of homogeneous data. It may be understood that the data in a dataset are homogeneous when they are made up only of elements of the same type, such as, for example, numerical data, whether discrete or continuous. These datasets may include only numerical variables, containing information of the subjects, such as: anthropometric information (height, weight), demographic information (age), information from the CT scan (quantity of different ROIs in, for example, cm^2 , cm^3 and/or % and radiodensity values). ANNs are very efficient at modelling non-linear relationships between multiple variables. They are also very useful for finding relationships between variables that are difficult to predict in a first instance. During the training process of the ANN, weights of the ANN are calculated which assign greater or lesser importance to each of the existing relationships between the different input parameters inputted in the network. The number of trainable parameters of the network, i.e., weights and bias, directly depends on the number of layers and the number of neurons per layer and the type of layers used.

[0034] One of the criteria by which ANNs can be classified is based on the degree of connection between their neurons, a classification that divides networks into partially or fully connected. Fully connected networks are those whose layers are all of the fully connected type. All the neurons in a fully-connected ANN in a layer are connected to all the outputs of the neurons of a previous layer. Among all the possible architectures of NNs, those including fully-connected layers (also known as densely-connected) may be very suitable to perform regression. As an example, the fact that the model used may comprise at least one fully connected layer allows

- during the training process, each of the at least one fully connected layer automatically finds all the existing relationships between the outputs of the neurons of a previous layer;
- during a neural network design stage, the fully connected layer can be used to modify the dimensions of the network, i.e., it is possible to vary the number of neurons between successive layers. This is very useful when the fully connected layer is used as the output layer of the neural network as it allows adjusting the number of estimations to be performed. During tests for testing the methods and systems of the present disclosure, this fact has allowed to go from N variables in the input layer of the network to a single output corresponding to the estimation of the basal energy expenditure (REE).

[0035] The machine learning model may be also, for example, based on “decision trees”. This kind of machine learning models is especially useful when the set of input parameters is heterogeneous. Heterogeneous sets of input parameters may contain any combination of different types of parameters, such as numerical variables (i.e., area/volume, radiodensity, height, weight, age, etc.) and categorical ones (i.e., gender, race, clinical information, etc.). Decision trees are machine learning models that aim to build a model that can predict the value of a target variable. These may be represented with a tree structure, that uses branches to illustrate the output of each decision. Each node represents a test on a specific variable and each branch represents the result of that test. These models use simple decision rules that infer the expected outcome, known as leaves, from the characteristics of the input data.

[0036] However, the use of a single decision tree tends to produce overfitting on the training data. The use of such a model to infer a result with real data can therefore produce a high error. Ensembled decision trees models may be used to profit from the benefits of decision trees when working with heterogeneous data, while reducing overfitting. In this way, the predictions of a multitude of decision trees may be combined to generalize the machine learning model and make it robust. This allows the variance of the results of the individual decision trees to be reduced. Therefore, a category of machine learning models which may work for the methods and systems of the present disclosure may be based on ensemble decision trees, i.e., learning algorithms that contain at least two decision trees. There are currently at least two families of learning models based on ensemble decision trees:

- Averaging methods. Among others, there are Bagging and Random Forest methods. These methods are constructed with several independent trees and provide a result that is the average value of the predictions of each decision tree separately. This results in the reduction of the variance of the predictions of each independent decision tree.

- Boosting methods. Algorithms such as AdaBoost, Gradient Boosting Decision Tree and Light GBM, among others, belong to this category. With this methodology, decision trees are incorporated sequentially, so that a decision tree tries to reduce the error produced by its predecessors. In this way, the combination of several weak models produces a robust, efficient, and accurate one.

[0037] For using any machine learning model for regression, such as those previously described, to estimate the REE parameter, a supervised training strategy may previously be performed to train the model.

[0038] As an example, a cross-validation may be employed when training the machine learning model for regression to prevent overfitting or underfitting. As an example, a stratified k-fold cross

validation strategy may be followed. This strategy consists in separating the data set in k subsets arranged in such a way that each subset is a good representation of the entire data set. Then, $k-1$ subsets are grouped as the training set, and the other subset is the testing set. In this way, the training is executed using $k-1$ subsets (training set), and the model is validated using the remaining subset (testing set). This is repeated k times, leaving out a different subset each time (as testing set). Finally, the average validation error is obtained as the average of the validation error obtained in each of the k iterations for the testing set. Similarly, the average training error is obtained by averaging the error in the training set in the k iterations. By doing so, overfitting may be identified when the validation error is considerably higher than the training error. On the contrary, underfitting is identified when both the training error and the validation error are high. If the machine learning model consists in an ANN, additional techniques may be also used to prevent overfitting. For example, dropout regularization may be used. If the machine learning model is based on decision trees, additional techniques may be also used to prevent overfitting. For example, pruning strategies, such as bottom-up pruning or top-down pruning may be used.

[0039] As another example, to carry out a good selection of the hyperparameters involved in the machine learning model for regression, hyperparameters tuning may be executed during the training. This may also reduce the overfitting. As an example, the hyperparameter tuning may be executed based on a grid search strategy, where all the possible combinations of the hyperparameters are exhaustively tested and the combination that provides the best results is preserved. As another example, the hyperparameter tuning may be also executed based on a randomized search or a Bayesian optimization to reduce the number of combinations of hyperparameters to be tested and to reduce the overall training time.

[0040] A supervised training strategy to train the model may also be based on the following. In examples, the training data set may comprise data from different subjects with different ages, types of bodies, different ROIs and different parameters associated to these ROIs, or even health problems. Using such training data sets with information from different subjects, the REE parameter is estimated based on all the input parameters. Including different types of subjects in the training data set may result in a more accurate regression model for estimating the REE for any kind of subject.

[0041] Preferably, in an example, in order to obtain a more precise estimation, both the CT scan image and the obtaining of the ground-truth REE parameter using experimental test (i.e., indirect Calorimetry (IC) or bioimpedancemetry) may be performed within a relatively short period of time between them (for example, within one week). Within such timeframe, the characteristics of the subject, such as, for example, its body composition, its clinical condition, etc. may not vary significantly, and the resulting REE parameter of the subject may be more accurate.

[0042] In examples, a parameter referring to the quantity of, at least, a specific ROI may be calculated in different ways. One of them may be to count the number of pixels in a CT image

corresponding to that specific ROI and multiply it by the pixel resolution (for example in cm^2/pixel or cm^3/pixel), thus obtaining the area (in cm^2) or the volume (in cm^3) corresponding to that ROI. Other way may be to divide the number of pixels corresponding to that ROI by the number of pixels corresponding to other ROI, thus obtaining a relative measurement that can be represented, for example, in percentage (%).

[0043] In another example, a parameter referring to the radiodensity of, at least, a specific ROI may be calculated in different ways. One way may be to compute the average value of the radiodensity of that specific ROI. This may be done by averaging the radiodensity value of all the pixels included in that specific ROI, measured, for example, in Hounsfield Units (HU). The radiodensity, in HU, corresponding to each image pixel may be included in the CT scan metadata, or at least, computed based on the CT scan metadata.

[0044] According to a further example, parameters over the plurality of CT scan images may be combined for a single subject. For example, two CT images captured at different vertebral levels may be used. For example, at least one ROI may be identified in each CT scan image corresponding, for example, to a specific tissue such as muscle tissue or adipose tissue. Furthermore, a parameter may be obtained for the target ROI as the average value of that parameter obtained for that target ROI in both images. While this kind of strategy may increase the estimation accuracy of the REE parameter, it also increases the computational cost.

[0045] In case of using software tools, including semiautomatic labeling of scans, when performing the segmentation or ROI identification, the overall training method may be streamlined and it may further allow the machine learning model to keep improving its performance in future analysis of new CT scans (i.e., when inferring the REE parameter with information from new scan images).

[0046] Additionally, other subject data can also be added as input parameters of the machine learning model, to increase the model accuracy. Such data may comprise, for example, demographic data, anthropometric data. Furthermore, REE measurements may also change according to the subject clinical state. Accordingly, clinical information regarding the subject state may also be added to increase the model accuracy.

[0047] According to an example of the present disclosure, a method for estimating a Resting Energy Expenditure (REE) parameter of a subject is also provided, comprising the steps of:

- obtaining at least one computed tomography CT scan image of the subject;
- identifying at least a region of interest, ROI, of the CT scan image;
- calculating at least one parameter of each ROI;
- inferring or estimating the REE parameter using a supervised machine learning model trained using the training method of a computer-implemented machine learning model previously described, wherein the inferring comprises inputting a data set comprising the at least one calculated ROI parameter, to obtain an REE parameter as the output of the model.

[0048] In some examples the steps of obtaining at least one computed tomography CT scan image of the subject; identifying at least a region of interest, ROI, of the CT scan image; and calculating at least one parameter of each ROI are performed by a first entity and the inferring or estimating the REE parameter is performed by a second entity. An entity may be understood as a processor, or processing means or computer.

[0049] In another aspect, a computer program product is disclosed. The computer program product may comprise program instructions for causing a computing system to perform a supervised training of the computer-implemented machine learning model, using a training data set comprising one or more groups of parameters of respective ROI of CT scan images and associated one or more ground-truth REE parameters, and wherein the training further comprises, for each group, setting an output parameter of the model corresponding to the associated ground-truth REE parameter.

[0050] The computer program may further comprise program instructions for causing the computing system to

- obtain one or more ground-truth REE parameters of one or more subjects;
- obtain the one or more CT scan images of the one or more subjects;
- identify at least a region of interest, ROI, in the obtained CT scan images; and
- calculating a group of one or more parameters of each ROI.

[0051] The computer program product may be embodied on a storage medium (for example, a CD-ROM, a DVD, a USB drive, on a computer memory or on a read-only memory) or carried on a carrier signal (for example, on an electrical or optical carrier signal).

[0052] The computer program may be in the form of source code, object code, a code intermediate source and object code such as in partially compiled form, or in any other form suitable for use in the implementation of the processes. The carrier may be any entity or device capable of carrying the computer program.

[0053] For example, the carrier may comprise a storage medium, such as a ROM, for example a CD ROM or a semiconductor ROM, or a magnetic recording medium, for example a hard disk. Further, the carrier may be a transmissible carrier such as an electrical or optical signal, which may be conveyed via electrical or optical cable or by radio or other means.

[0054] When the computer program is embodied in a signal that may be conveyed directly by a cable or other device or means, the carrier may be constituted by such cable or other device or means.

[0055] Alternatively, the carrier may be an integrated circuit in which the computer program is

embedded, the integrated circuit being adapted for performing, or for use in the performance of, the relevant methods.

BRIEF DESCRIPTION OF THE DRAWINGS

[0056] Non-limiting examples of the present disclosure will be described in the following, with reference to the appended drawings, in which:

[0057] Figures 1 and 2 depict two different examples of a computer-implemented neural network for obtaining a Resting Energy Expenditure (REE) parameter of a subject, according to the present disclosure.

[0058] Figure 3 depicts an example of a CT scan image used by a method according to the present disclosure.

[0059] Figure 4 depicts a flow chart of an example of the training method of any of the neural networks depicted in figures 1 and 2, according to the present disclosure.

[0060] Figure 5 depicts a solution according to the present disclosure.

[0061] Figure 6 depicts a system for providing an estimated REE parameter of a subject.

[0062] Figure 7 depicts a system for providing an estimated REE parameter of a subject

DETAILED DESCRIPTION OF EXAMPLES

[0063] Figure 1 depicts a neural network which may be trained by one of the training methods according to the present disclosure. Figure 1 depicts a machine learning model embodied in a fully connected neural network 100. In this specific embodiment, the machine learning model is a neural network comprising only fully connected layers 101 and 102 resulting in a fully connected neural network 100. In this case, the neural network comprises only the input and output layer and does not include any hidden layer.

[0064] Figure 2 depicts a machine learning model embodied in a fully connected neural network 200. In this specific embodiment, the machine learning model is a neural network comprising only fully connected layers 201, 202, 203 and 204 resulting in a fully connected neural network 200. In this case, the neural network comprises two hidden layers 202 and 203.

[0065] In the present example, as seen in figure 2, the number of neurons in the input layer 201 and output layer 204 of neural network 200 corresponds to the number of input and output parameters, respectively. In this case, the number of input parameters is eleven: Weight, Height and Age of the subject, area of subject's body within the image (in cm²), radiodensity of subject's body within the image (in HU), area of Muscle (in % related to subject's body within the image), radiodensity of Muscle (in HU), area of VAT (in % related to subject's body within the image), radiodensity of VAT (in HU), area of SAT (in % related to subject's body within the image), and radiodensity of SAT (in HU). As seen, the methods of the present disclosure include that the one or more parameters of each ROI comprise a percentage of an identified ROI, relative to a tissue or an organ or to any combination of thereof, with regards to a different ROI relative to other tissues, other organs, or any combination of thereof, including the entire subject's body within the obtained CT scan image

[0066] As seen, in a neural network comprising at least one fully connected layer, each neuron in a fully connected layer is connected to all neurons in the previous layer. In this way the resulting neural network may consider multiple relationships between the input parameters to achieve an output value. The methods and systems according to the present disclosure may use different and varied physical features of the subjects to construct a training data set; many different relationships may therefore be established between the input parameters of the neural network. For example, a body with a high amount of muscle may commonly mean that the subject is fit, but if a further input parameter related to the radiodensity of the muscle tissue shows a low radiodensity value it may suggest that the patient is not as fit, and it may indicate a lower REE. As another example, a body with a high amount of muscle may commonly mean that the subject is fit, but if another input parameter indicating a high amount of visceral adipose tissue, it may suggest that the subject is not so healthy, which may affect his REE. Therefore, hidden relationships between input parameters may be considered when using a neural network comprising at least one fully connected layer, and its training may lead to more accurate REE parameters in further inferences for new subjects.

[0067] In the examples of figure 1 and figure 2, the CT scan image may be obtained at L3 vertebral level of a subject, in order to obtain the maximum correlation of an area or volume of tissues found in the CT scan image in L3, and the amount of the same tissues in the whole body of the subject.

[0068] In another example, if the amount of data available for training is considerably large (in the order of thousands of samples), the complexity of the model may be increased, and other

models may be used, including other types of neural networks, or decision trees, any combination thereof, etc.

[0069] As an example, if the amount of data available for training is considerably large (in the order of thousands of samples), an ANN with a larger number of input parameters and a larger number of trainable parameters than the examples of figures 1 and figure 2 may be used. By increasing the input parameters and trainable parameters (the total amount of weights and biases of the ANN as a whole), a more accurate estimation of a REE parameter may be obtained.

[0070] Figure 3 depicts an example of a CT scan image 304 of vertebral level L3 used by a method of the present disclosure. In this figure, the entire subject's body within the obtained CT scan image may be the region referenced as 300. The image is represented as segmented, wherein different tissues are differentiated as follows: muscle 301, visceral adipose tissue 302, subcutaneous adipose tissue 303.

[0071] Figure 4 depicts a flow chart of an example of the training method of any of the neural networks depicted in figure 1 or figure 2, for obtaining a Resting Energy Expenditure (REE) parameter of a subject according to the present disclosure. In the present example, the method is performed by a computing device which comprises a fully connected untrained neural network.

[0072] More precisely, in step 401 of figure 4, the method starts by the computing device receiving a ground-truth REE parameter obtained from an indirect calorimetry measurement or by bioimpedanciometry of a subject.

[0073] In step 402, the computing device receives an axial computed tomography CT scan image of the same subject. The image may be centered at L3, or L5 or L7 vertebral level or at a leg level or at thorax level or at neck level, or any other level. The CT scan image is embedded in a digital file, comprising the scan image itself and a set of metadata. In this example, the metadata comprises the value of tissue radiodensity measured in Hounsfield Units (HU) of each pixel within the CT scan image, the resolution in $\text{cm}^2/\text{pixels}$ of the scan image (all of them embedded within the CT scan image), and an extra packet of data, inputted by the user of the computing device through a User Interface, which is related to the weight, height and age of the subject.

[0074] In step 403, further data corresponding to the subject is retrieved. Such data may be obtained from the CT scan image metadata or may be inputted externally from an interface. More precisely, the data relating to weight, height and age of the subject may be retrieved from the CT scan image metadata.

[0075] In step 404, the received CT scan image is segmented by a segmenting module of the computing device. The segmentation is performed by identifying a plurality of ROIs corresponding to predetermined types of tissues within the CT scan image. More precisely, the segmenting module identifies the part of the CT scan corresponding to the body of the subject, and other objects or parts depicted in the CT scan image which do not correspond to the body of the subject are discarded (i.e., area corresponding to the bed where the subject was lying when the CT scan is performed, or other objects or parts of the CT scan which may have accidentally showed up in the image, and are not part of the subject's body). Also, the segmenting module further identifies, within the identified part of the CT scan image corresponding to the body of the subject, the parts corresponding to Muscle, VAT and SAT tissues.

[0076] In step 405, a parameter corresponding to the area of each ROI (Region of Interest) is obtained. First, the area of the ROI corresponding to the body of the subject is calculated, using the resolution of the CT scan, in cm^2/pixel . Furthermore, a parameter corresponding to the area of the other ROIs (Muscle, VAT and SAT tissues) is also obtained, by calculating the real area corresponding to these ROIs, using the resolution of the CT scan, in cm^2/pixel .

[0077] The real areas of each identified ROI (either the total subject body, Muscle, VAT or SAT areas) are calculated by counting the number of pixels corresponding to the ROI for which the area is to be calculated, and multiplying said number of pixels by the pixel size in cm^2 . The pixel size in cm^2 is obtained from the CT scan image metadata, for example, using a Pixel Spacing Attribute which may be included in the metadata. The pixel spacing attribute provides the physical distance in the patient between the center of each pixel, specified by a numeric pair (adjacent row spacing and adjacent column spacing, for example, in mm).

[0078] In step 406, a parameter corresponding to each of the areas of the ROIs corresponding to Muscle, VAT and SAT tissues is further calculated, in percentage respective to the ROI that corresponds to the entire body of the subject within the image. More precisely, each parameter is calculated by counting the number of pixels corresponding to the target ROI for which the area in percentage is to be calculated and dividing said number of pixels by the number of pixels corresponding to the ROI that corresponds to the entire body of the subject within the image. The value obtained is then multiplied by 100. This type of parameter may be a more objective metric than the area in cm^2 because it is a proportional value.

[0079] In step 407, a parameter corresponding to the average value of tissue radiodensity measured in Hounsfield Units (HU) is calculated for each ROI (body of the subject, Muscle, VAT

and SAT), using the CT scan image metadata. More precisely, for each identified ROI, the computing device retrieves the values of tissue radiodensity of all the pixels corresponding to that ROI and calculates the average radiodensity of the specific ROI by calculating the arithmetic mean.

[0080] When assembling the training data sets to perform the training of neural network 200 according to the example of the present disclosure, it may be more computationally efficient that all input parameters are within the same numerical range in order to accelerate the algorithm convergence speed.

[0081] Therefore, since each input parameter of the neural network represents the quantification of a different feature of the subject, in step 408, each parameter is scaled using reasonable ranges (for example, it may be established that the weight of an adult human body may be between 45kg and 120kg). More precisely, a scaling is performed for each parameter, in order to scale all parameters so they take values inside or close to a desired numeric range, for example, 0 and 1. In the present example, all the parameters are scaled using the following reasonable values for each parameter:

Weight: 45 to 120 kg

Height: 1.4 to 2 m

Age: 0 to 100 years

Region of interest (ROI) (area): 250 to 1250 cm².

ROI (density): -100 to 100 HU

Muscle (%): 0 to 100

Muscle (density): -30 to 150 HU

visceral adipose tissue (VAT) (%): 0 to 100

VAT (density): -150 to -50 HU

subcutaneous adipose tissue (SAT) (%): 0 to 100

SAT (density): -190 to -30 HU

Intramuscular adipose tissue (IMAT) (%): 0 to 100

IMAT (density): -190 to -30 HU.

[0082] In examples of the present disclosure, the scaling of each parameter may be carried out using the following equation:

[0083]
$$\text{scaled parameter} = (\text{unscaled parameter} - \text{minimum_reasonable_value}) / (\text{maximum_reasonable_value} - \text{minimum_reasonable_value})$$

[0084] Following this procedure, if the parameter value was included within the reasonable values range, its scaled value will be between 0 and 1 (both included). If the parameter value was higher than the maximum reasonable value, its scaled value will be higher than 1. If the parameter value was lower than the minimum reasonable value, its scaled value will be lower than 0.

[0085] Then, in step 409, a training data set is assembled, by coupling the scaled parameters based on the calculated parameters area in cm^2 of each ROI (body of the subject, Muscle, VAT and SAT), average radiodensity (in HU) of each ROI (body of the subject, Muscle, VAT and SAT), area the ROIs corresponding to Muscle, VAT and SAT tissues measured as a percentage (%) with respect to the area corresponding to the ROI that corresponds to the body of the subject within the image, and the retrieved parameters (weight, height and age of the subject), with the corresponding output parameter: the REE parameter received in step 401.

[0086] Then, in step 410, a supervised training is performed on the neural network, using the assembled training data set.

[0087] In step 411, once the neural network has been trained with a first training data set corresponding to a first subject, if the user wishes to keep training the neural network, the method may restart in step 401, wherein new IC test data or bioimpedanciometry test and a new CT scan image is used, corresponding to a new subject. Thus, the training method may be performed by the computing device in an iterative manner, using a plurality of training data sets from different subjects.

[0088] In examples, a data processing system is provided. The system comprises a processor configured to perform a supervised training of a computer-implemented machine learning model using a training data set comprising one or more groups of parameters of respective ROI of CT scan images. A group of parameters comprises one or more parameters of each ROI. The one or more parameters comprise a radiodensity parameter for at least one of the ROIs. Each group is associated with a ground-truth REE parameter. The ground-truth REE parameter associated with each group corresponds to a corresponding subject from which the group of parameters of each image comes from. The supervised training further comprises, for each group of parameters, setting an output parameter of the model corresponding to the associated ground-truth REE parameter.

[0089] In some examples, the data processing system further comprises a first interface to obtain the one or more ground-truth REE parameters of one or more subjects, a second interface to

obtain the one or more computed tomography, CT, scan images of the one or more subjects, and the processor is further configured to:

- obtain the one or more CT scan images from the second interface;
- identify at least a region of interest, ROI, in each obtained CT scan image; and
- calculate at least one group of parameters of each ROI, wherein one or more of the parameters of at least one group comprises a radiodensity parameter for at least one of the ROIs.

[0090] In some examples, the processor is further configured, once a trained model results from the supervised training, to either:

- receive new one or more groups of parameters of a new ROI of a new CT scan image and to infer a new REE parameter using the trained model; or
- receive a new CT image obtained by the second interface; to identify a new region of interest, ROI, in the new obtained CT scan image; to calculate new one or more groups of parameters of the ROI, wherein the new one or more groups of parameters comprises at least a radiodensity parameter for at least one of the ROIs; and to infer a new REE parameter using the trained model.

[0091] In some examples the first interface and /or the second interface may comprise, for example, one or more cables or antennas and supporting hardware and/or software for enabling communications with a wired or wireless communication network. Additionally, or alternatively, the interface may include the circuitry for interacting with the antenna(s) to cause transmission of signals via the antenna(s) or to handle receipt of signals received via the antenna(s). In some environments, the communication interface may alternatively or also support wired communication.

[0092] The data processing system may include a user interface, the user interface may be in communication with processing circuitry and a memory device to receive an indication of a user input and/or to provide an output to a user. The user interface may include, for example, a display and one or more speakers for providing visual and audible output to a user. Other examples of the user interface include a keyboard, a mouse, a joystick, a microphone and/or other input/output mechanisms.

[0093] In examples, a solution according to the present disclosure and shown in figure 5 comprises a system 500 for providing a new estimated REE parameter 508 of a subject, the system comprising:

- an interface 501 to receive one or more computed tomography CT scan images 505; for illustration purposes, the image 505 is represented in figure 5 without non representative white contour around the region of the entire subject's body within the image;
- a second interface 502 to receive at least one ground-truth REE parameter for each corresponding CT scan image; the second interface 502 is represented as a different interface of the interface 501 but a unique interface may be used for the purposes of receiving at least one computed tomography CT scan image and at least one REE parameter for each corresponding CT scan image;
- a processor 503 in communication with the interfaces 501, 502; and
- non-transitory computer readable media 504 in communication with the processor that stores instruction code, which when executed by the processor, causes the processor to:
 - identify a ROI of each one or more computed tomography CT scan image;
 - calculate at least one parameter of each ROI;
 - train a model 507 to estimate a REE parameter, using a supervised learning methodology, based on a training data set that comprises the at least one ground-truth REE parameter and the at least one parameter of each ROI, wherein the model receives as input the at least one ROI parameter and is told to infer or estimate the ground-truth REE parameter from the training data set.

[0094] In examples, once a trained model results from the supervised training, the model may be stored in non-volatile computer readable media.

[0095] In examples, the non-transitory computer readable media 504 further stores instruction code, which when executed by the processor 503, further causes the processor to:

- receive a new CT scan image of a new subject;
- process the new CT scan image to estimate a new REE parameter; and
- provide the new estimated REE parameter 508 via an output interface (not shown).

[0096] In examples, a solution according to the present disclosure comprises, as represented in figure 6, a system 600 for providing an estimated REE parameter 608 of a subject, the system comprising:

- one or more interfaces 601, 602 to receive one or more computed tomography CT scan images 605;
- an output interface 606 to provide the estimated REE parameter 608;
- a processor 603 in communication with the one or more interfaces 601, 602; and
- non-transitory computer readable media 604 in communication with the processor 603 that stores

- a trained model 607 which has been trained using a supervised learning methodology as described in the present disclosure, based on a training data set that comprises at least one ground-truth REE parameter and at least one parameter of a ROI of one or more CT scan images;
- instruction code, which when executed by the processor 603, causes the processor to:
 - identify at least a ROI of a received CT scan images 605;
 - calculate at least one parameter of the ROI;
 - input the at least one parameter of the ROI to the trained model 607, obtaining an estimated REE parameter therefrom; and
 - provide the estimated REE parameter 608 via the output interface 606.

[0097] In examples a solution according to the present disclosure comprises a method for providing a REE parameter of a subject, the method comprising:

- receiving a computed tomography CT scan image;
- identifying a ROI of the computed tomography CT scan image;
- calculate at least one parameter of the ROI;
- estimate the REE parameter using a model trained to estimate a REE parameter of a subject from at least one parameter of a ROI of at least one CT scan image; and
- providing the REE parameter of the subject.

[0098] In examples the above defined method for providing a REE parameter of a subject further includes training the model to estimate a new REE parameter, using a supervised learning methodology, based on a training data set that comprises the at least one training ROI parameter and the corresponding training REE parameter and, wherein the model receives as input the at least one training ROI parameter and is told to infer or estimate the training REE parameter from the training data set as output.

[0099] In some examples, a solution according to the present disclosure comprises, as represented in figure 7, a system 700 for providing an estimated REE parameter 702 of a subject, the system comprising:

- at least one interface 701 to receive one or more calculated parameters of a ROI of a CT scan image of a subject;
- an output interface 703 to provide the estimated REE parameter 702;
- a processor 704 in communication with the interface 701; and
- non-transitory computer readable media 705 in communication with the processor 704 that stores
- a trained model 706 which has been trained using a supervised learning methodology as described in the present disclosure, based on a training data set that comprises at least one

ground-truth REE parameter and at least one parameter of a ROI of one or more CT scan images;

- instruction code, which when executed by the processor 704, causes the processor to:
 - input the one or more calculated parameters of a ROI to the trained model 706, obtaining an estimated REE parameter 702 therefrom; and
 - provide the estimated REE parameter 702 at the output interface 703.

[0100] Although only a number of examples have been disclosed herein, other alternatives, modifications, uses and/or equivalents thereof are possible. Furthermore, all possible combinations of the described examples are also covered. Thus, the scope of the present disclosure should not be limited by particular examples but should be determined only by a fair reading of the claims that follow. If reference signs related to drawings are placed in parentheses in a claim, they are solely for attempting to increase the intelligibility of the claim and shall not be construed as limiting the scope of the claim.

[0101] Further, although the examples described with reference to the drawings comprise computing apparatus/systems and processes performed in computing apparatus/systems, the invention also extends to computer programs, particularly computer programs on or in a carrier, adapted for putting the system into practice.

CLAIMS

1. A training method of a computer-implemented machine learning model for obtaining a Resting Energy Expenditure, REE, parameter of a subject from one or more computed tomography, CT, scan images of a subject, the method comprising the steps of:

- obtaining one or more ground-truth REE parameters of one or more subjects;
- obtaining the one or more CT scan images of the one or more subjects;
- identifying at least a region of interest, ROI, in each of the obtained CT scan images;
- calculating a group of parameters of each ROI; wherein a group comprises one or more parameters of each ROI, the one or more parameters comprising a radiodensity parameter for at least one of the identified ROIs; and wherein each group is associated with a ground-truth REE parameter; and
- performing a supervised training of the computer-implemented machine learning, ML, model, using a training data set comprising one or more groups of parameters of each ROI and the associated one or more ground-truth REE parameters, and wherein the supervised training further comprises, for each group, setting an output parameter of the ML model corresponding to the associated ground-truth REE parameter.

2. A training method according to claim 1 wherein

- identifying at least a region of interest, ROI, comprises segmenting each of the obtained CT scan images, identifying thereby at least one predetermined type of tissue, organ, or any combination of them within the obtained image;
- and wherein calculating one or more parameters of each ROI comprises calculating at least one parameter related to an amount of the at least one identified ROI or related to a radiodensity of the ROI, from the segmented CT scan image.

3. A training method according to claim 1 or 2 wherein the computer-implemented machine learning model is a regression model; or wherein the computer-implemented machine learning model is one of a neural network, or a model comprising assembled decision trees, or a neural network comprising at least one fully connected layer, or a combination of one or more neural networks and one or more decision trees.

4. A training method according to any of claims 1 to 3 wherein the one or more parameters of each ROI are obtained by calculating an area or volume of an identified tissue, organ, or any combination of them from the CT scan image and a resolution of the CT scan image.

5. A training method according to any of claims 1 to 4 wherein the one or more parameters of

each ROI comprise a percentage of an identified ROI, relative to a tissue or an organ or to any combination of thereof, with regards to a different ROI relative to other tissues, other organs, or any combination of thereof, including an entire subject's body within the obtained CT scan image.

6. A training method according to any of claims 1 to 5, wherein the one or more parameters further comprise an amount of a Muscle tissue, and/or of a visceral adipose tissue, VAT, and/or of a subcutaneous adipose tissue, SAT, and/or of an entire subject's body within the CT scan image.

7. A training method according to any of claims 1 to 6, wherein the training data set further comprises at least one of demographic data, and/or anthropometric data and/or clinical data of the subject.

8. A training method according to any of claims 1 to 7 wherein the steps of

- obtaining the one or more CT scan images of the one or more subjects;
 - identifying at least a region of interest, ROI, in each of the obtained CT scan images; and
 - calculating a group of parameters of each ROI
- are performed by a first entity; and
- the method further comprises receiving one or more parameters of each ROI by a second entity before performing a supervised training of the computer-implemented machine learning model by the second entity.

9. A method for inferring a Resting Energy Expenditure (REE) parameter of a subject, comprising inferring the Resting Energy Expenditure (REE) parameter using a computer-implemented machine learning model trained using the method of any of claims 1 to 8, wherein the inferring comprises inputting a calculated group of parameters into the machine learning model, and obtaining an REE parameter as the output of the model.

10. The method for inferring a REE parameter of claim 9 further comprising, before inferring the REE parameter:

- obtaining at least one CT scan image of the subject;
- identifying at least a ROI in the CT scan image; and
- calculating a group of parameters of each ROI, wherein the group of parameters comprise a radiodensity parameter for at least one of the ROIs.

11. A data processing system, the system comprising a processor configured to perform a supervised training of a computer-implemented machine learning model, using a training data set comprising one or more groups of parameters of respective ROI of CT scan images; wherein a

group comprises one or more parameters of each ROI, wherein the one or more parameters comprise a radiodensity parameter for at least one of the ROIs, wherein each group is associated with a ground-truth REE parameter, and wherein the supervised training further comprises, for each group, setting an output parameter of the model corresponding to the associated ground-truth REE parameter.

12. The data processing system of claim 11 further comprising:

- a first interface to obtain the one or more ground-truth REE parameters of one or more subjects;
- a second interface to obtain the one or more computed tomography, CT, scan images of the one or more subjects;
- and wherein the processor is further configured to:
 - obtain the one or more CT scan images from the second interface;
 - identify at least a region of interest, ROI, in each obtained CT scan image; and
 - calculate at least one group of parameters of each ROI, wherein one or more of the parameters of at least one group comprises a radiodensity parameter for at least one of the ROIs.

13. The data processing system of claim 11 or 12 wherein the processor is further configured, once a trained model results from the supervised training, to either:

- receive new one or more groups of parameters of a new ROI of a new CT scan image and to infer a new REE parameter using the trained model; or
- receive a new CT image obtained by the second interface; to identify a new region of interest, ROI, in the new obtained CT scan image; to calculate new one or more groups of parameters of the ROI, wherein the new one or more groups of parameters comprises at least a radiodensity parameter for at least one of the ROIs; and to infer a new REE parameter using the trained model.

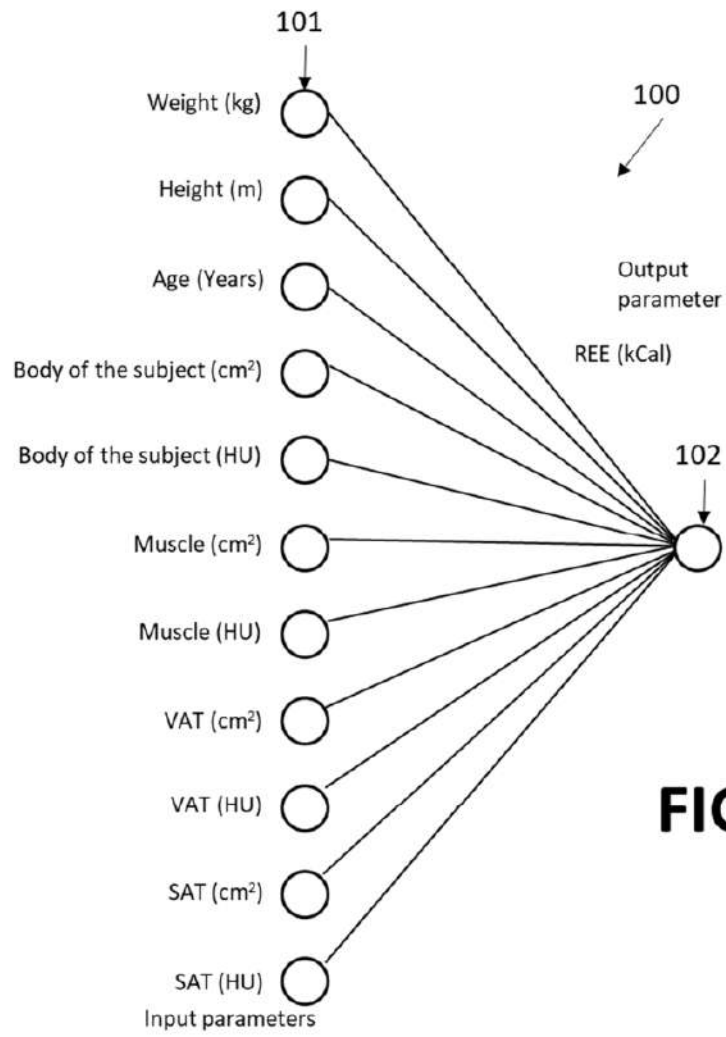
14. A computer program product comprising program instructions for causing a computing system to perform a method according to any one of claims 1 to 8.

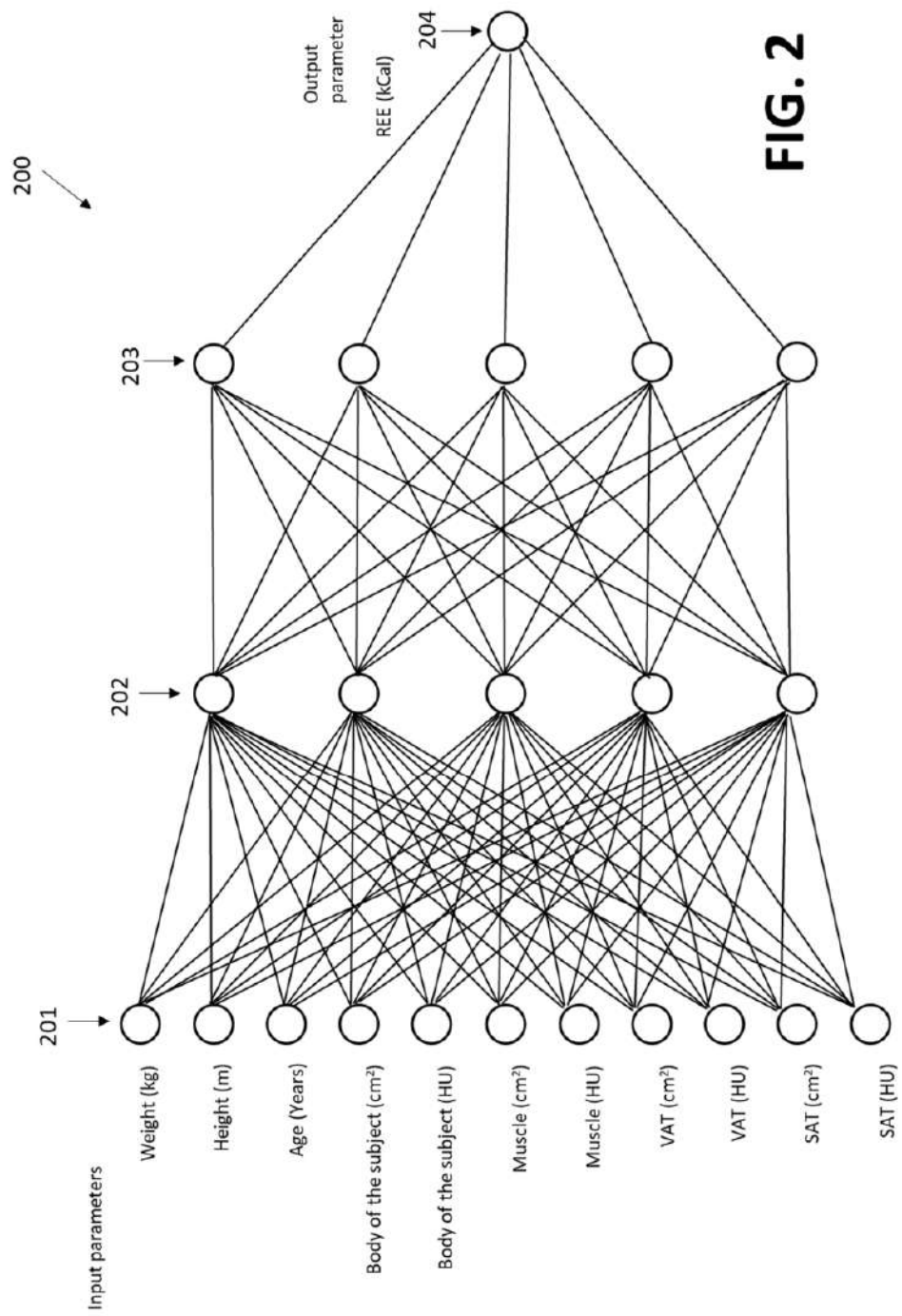
15. A computer program product comprising program instructions for causing a computing system to perform a method according to claim 9.

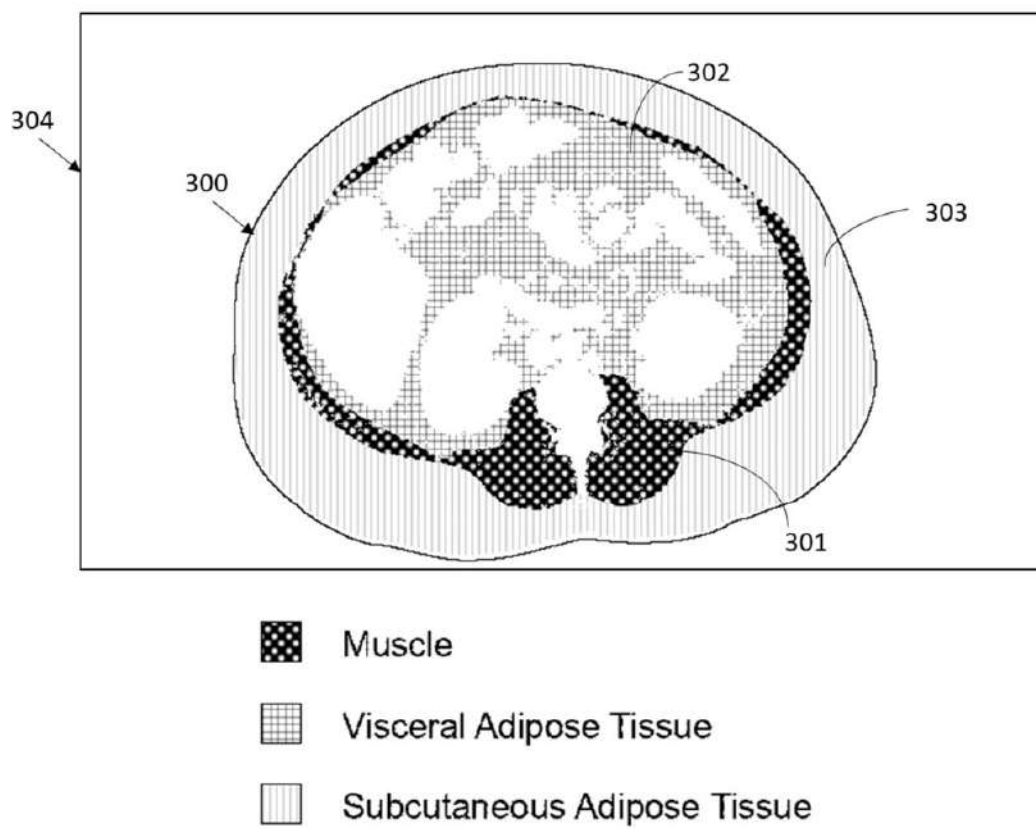
ABSTRACT

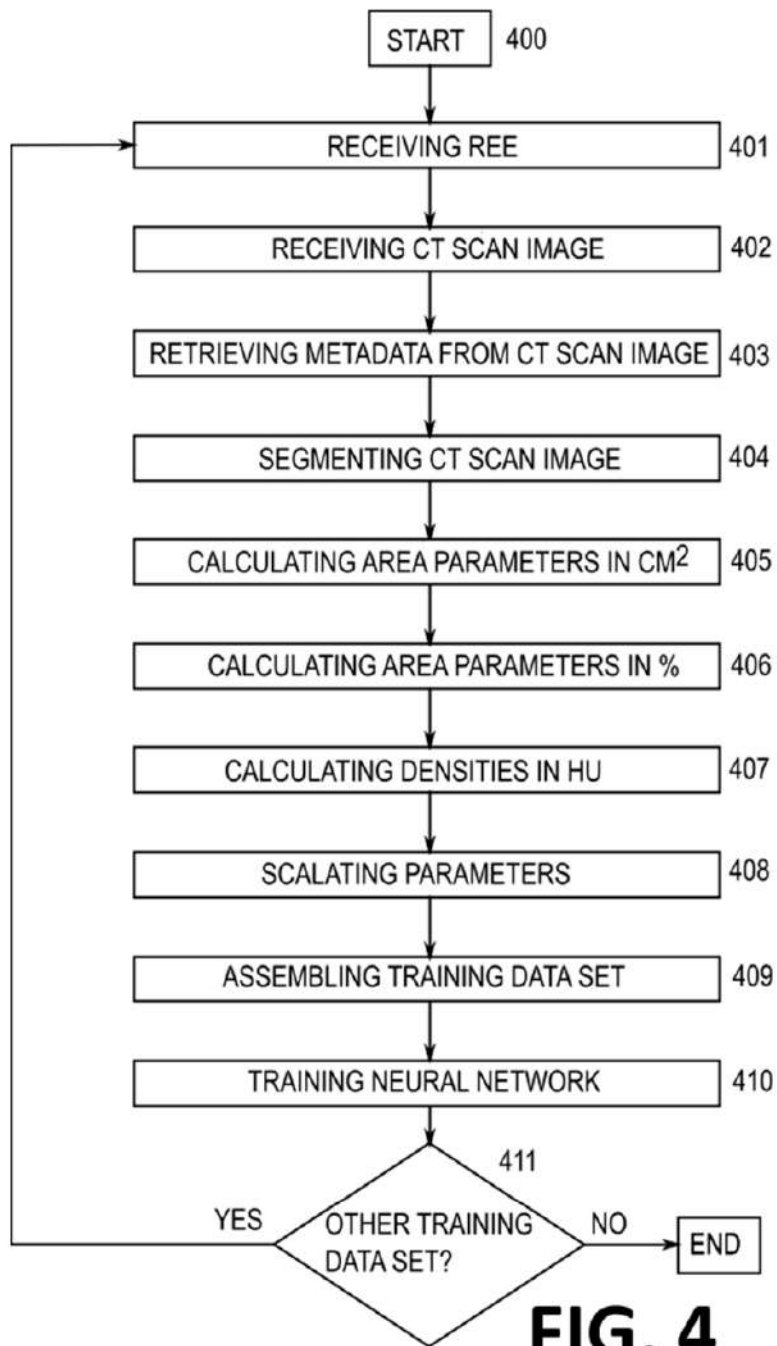
A training method of a computer-implemented machine learning model for obtaining a Resting Energy Expenditure (REE) parameter of a subject, and a system to perform such method, are presented, wherein an REE parameter from an experimental test, and information from a CT scan image of the subject are used to train the computer-implemented machine learning model. A method for estimating a Resting Energy Expenditure (REE) parameter of a subject is also presented, using a computer-implemented machine learning model previously trained by the training method described herein.

FIGURES





**FIG. 3**



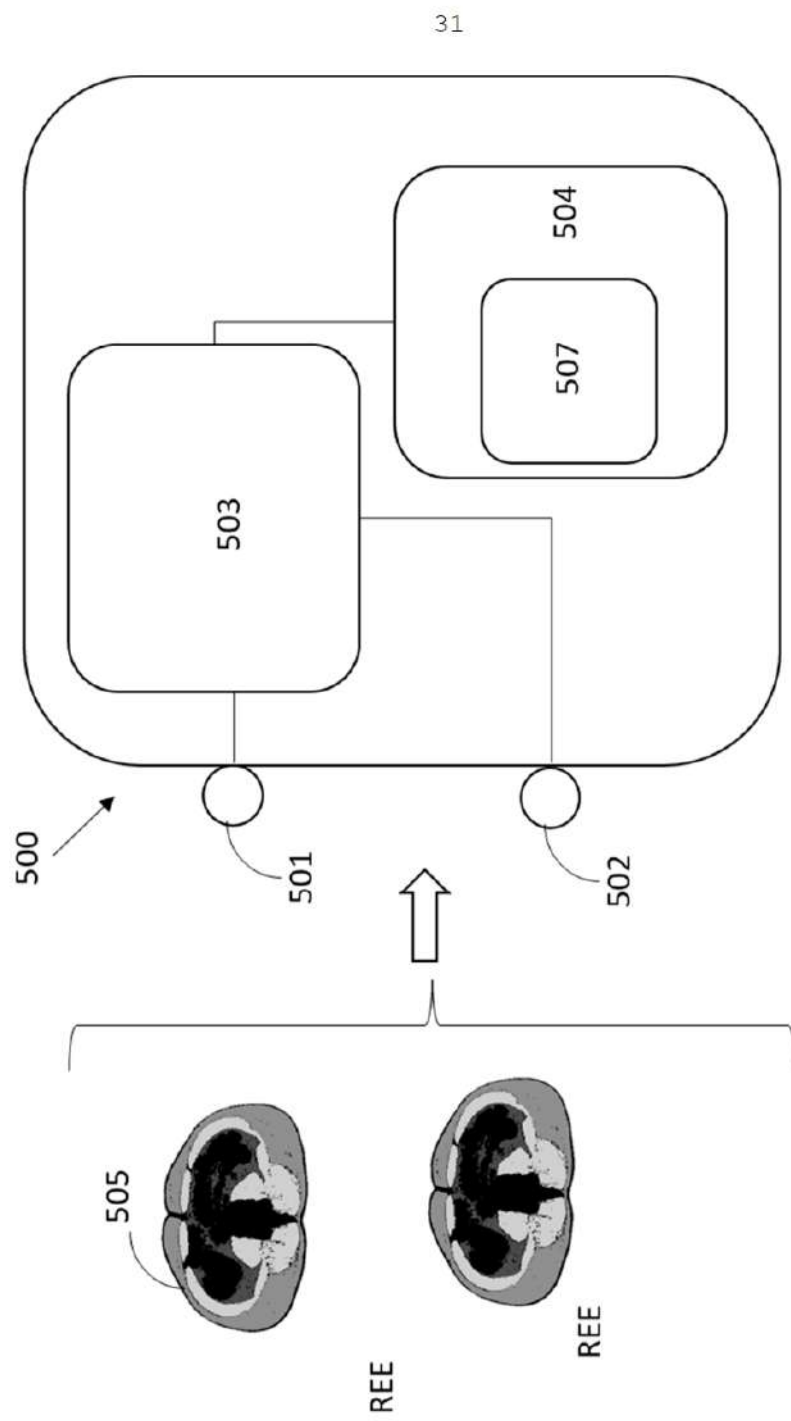


FIG. 5

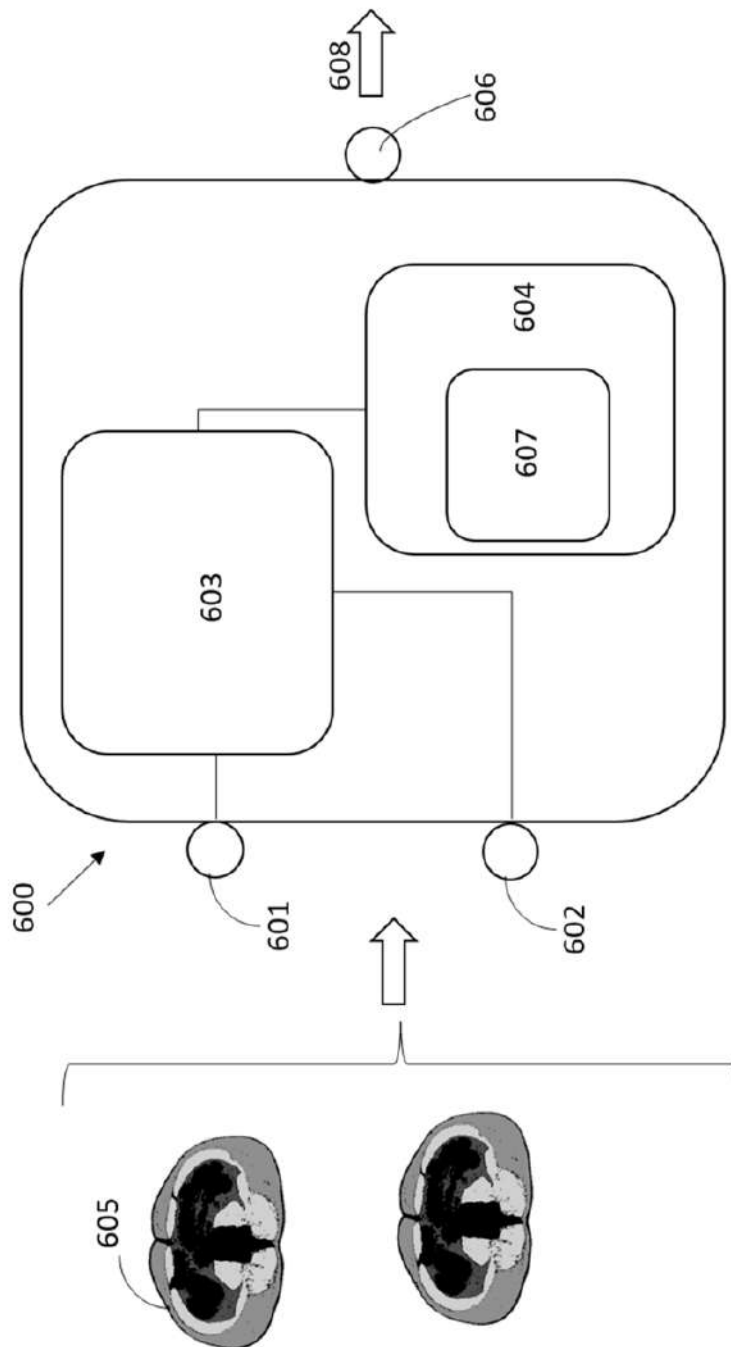
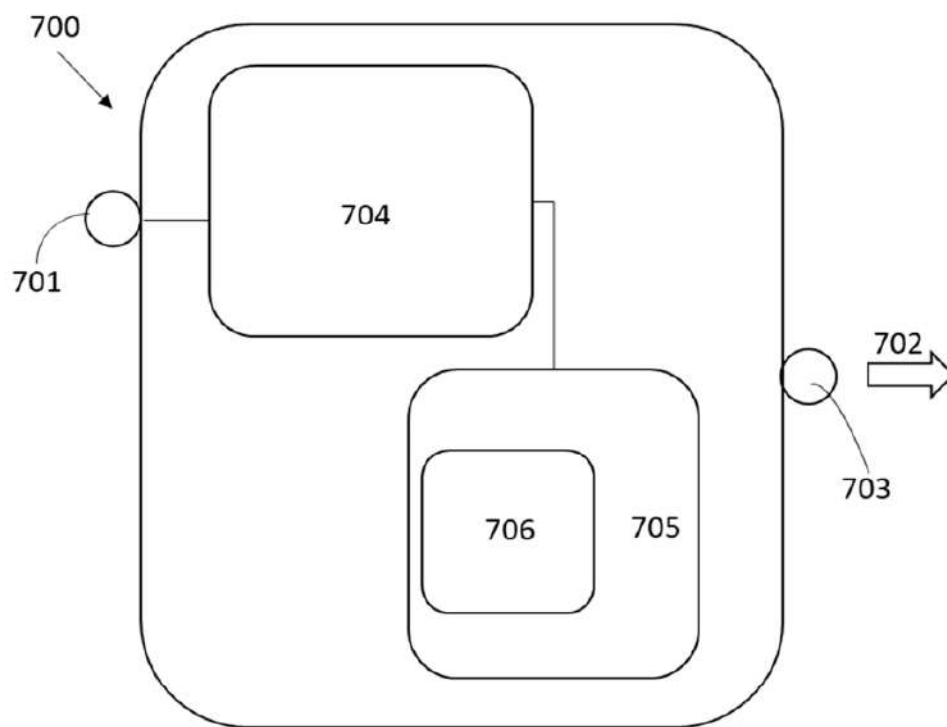


FIG. 6

**FIG. 7**

6. OVERALL SUMMARY OF RESULTS

This thesis justifies its findings in three articles, two of them already published and one accepted pending publication. The main results are summarized below:

6.1. Study 1: “Comparison of computed tomography and dual-energy X-ray absorptiometry in the evaluation of body composition in patients with obesity.”

A total of 70 patients were included in this study. Of them, 59% were women, with a mean age of 47.37 ± 12.8 years. From the clinical point of view, the data set is divided into two groups of patients, patients living with severe obesity and patients without obesity. The control group consisted of 24 patients with a mean BMI of 26.27 ± 4.86 kg/m², and the case group consisted of 46 subjects with a mean BMI of 43.56 ± 4.69 . 16 slices of the abdominal CT at the L3 level were analyzed and compared with the results obtained from a single slice. The correlation and agreement obtained with each model when using only 1 CT slice is very close to the one obtained when using 16 slices. This suggests that a single slice may be representative enough.

We applied the classical model (model 1 or Mourtzakis model) to compare CT and DXA. We also developed and applied a second model using the same variables as in the classical model. Both models presented similar correlations and that these were not higher than 0.76 for FFM. We developed a new model using other variables such as radiodensity per HU and quantification by percentage. FocusedON Model presents a better agreement with respect to DXA, in both tissues, FFM ($r=0.916$, p value <0.001), and FM ($r=0.926$, p value <0.001).

Nevertheless, to better assess agreement Bland-Adman plots have been calculated and clearly shows that FocusedON Model is the one presenting the best agreement with DXA.

Finally, to illustrate it error grids have been generated and the estimates carried out by each of the tested models. The error has been measured as the difference between the estimated value and the reference value provided by DXA. It can be observed that FocusedON Model presents lower errors than the other two models.

6.2. Study 2: “Body composition assessment with ultrasound muscle measurement: optimization through the use of semi-automated tools in colorectal cancer”.

A total of 174 patients were included in this study. Of them, 60% were male, with a mean age of 68.91 ± 11.52 years. All participants had colorectal neoplasia, with the colon and sigmoid colon being the most commonly affected sites. Notably, 65% of the recruited patients presented with stage II-III disease at the time of diagnosis, although an overwhelming 95% maintained a good baseline functional status ($\text{ECOG} \leq 1$). According to the GLIM criteria, 21% of the patients met the criteria for malnutrition, although the average BMI was above the normal range (BMI 26 kg/m²). Sarcopenia was screened screening using the SARC-F questionnaire, which showed a 9% risk of sarcopenia within in the sample.

In a first evaluation of the ultrasound, the level of correlation with the CT was determined. We observed a good correlation, especially with the area ($r=0.67$, IC (0.57, 0.74), p value <0.05) and the Y axis ($r=0.66$, IC (0.56, 0.74), p value <0.05). Where it is worth highlighting a remarkable correlation between both CT and US findings, in particular related to patients without overflow.

It should be noted, since it is not a common practice in muscle ultrasound, that the averages of the main variables obtained by ultrasound improve when we normalize this measurement by the square of the height (m²). In example, muscle area improves its AUC from 0.62 to 0.64. and Y axis from 0.59 to 0.61. Similarly, when the patient's whit overflow was removed from the sample, muscle area improves its AUC from 0.64 to 0.71). In addition, automatic variables also improve their prognosis capabilities when normalized by patient's height.

On the other hand, the use the software tool, which allows carrying the analysis in a more automatic and user independent way, also increases the performance of the different metrics. For instance, muscle Y axis improves from 0.56 to 0.68, and even to 0.72 when using the y-eigenvector. Similarly, muscle area improves from 0.71 (after normalized by height and remove overflow) to 0.73 using semiautomatic tool.

Although this trend can be clearly seen in the results, the difference between the manual and automatic metrics is not statistically significant (p-value >0.05).

6.3. Study 3: “Resting energy expenditure estimation by CT body composition analysis”.

A total of 90 patients were included in this study. Of them, 62% were men, with a mean age of 62.3 ± 15.4 years, and the mean BMI was 24.6 ± 4.7 kg/m². Intentionally, patients with a wide range of BMI (15.4-47.9 kg/m²) were included.

Resting energy requirements were calculated using some of the commonly used mathematical equations in comparison to the reference method (IC). In general, equations showed a low correlation with the reference method (0.486 to 0.558), and a high dispersion. The equation with the best results was the Ireton-Jones equation (1992) with an $r = 0.558$ (IC 0.397-0.686, p value <0.001).

After applying deep learning and developing the most accurate model, the variables accounting for REE in an independent manner were those related to total weight (kg), age, and muscle mass quantity (cm²). Interestingly, gender, were not valued as significant for REE model.

Regarding REE assessed by BIA, the CT model, presents a higher correlation in comparison with mathematical models ($r=0.636$, p value <0.001) and with a similar dispersion (0.494-0.745).

7. OVERALL SUMMARY OF THE DISCUSSION

In this thesis we have been able to demonstrate the validity and potential of assessing the body composition (BC) and surprisingly the resting energy expenditure (REE) by means of the analysis of an abdominal CT-scan image through segmentation performed with semi-automatic software trained with AI developed by our group- FocusedON. In addition, we have developed software for BC assessment through US image analysis.

The main objective of the thesis has been to demonstrate that abdominal CT is a useful technique in the field of BC assessment, with different and innovative clinical applications. For this purpose, we actively collaborated in the development of a semi-automatic software with AI called FocusedOn-BC, which has been used for the segmentation of images in all studies and whose development is specified in the “Clarifications regarding the methodology” section.

Knowledge of BC and the amount and distribution of muscle and adipose tissue is especially relevant in patients with severe obesity, given its importance in understanding the impact on metabolic and cardiovascular complications of the patient. However, this is a particularly difficult population to analyse given the body characteristics and the current limitations of BC techniques. Until now, DXA has been used as a reference technique for the study of BC in general and especially in patients with obesity. We know that one of the limitations of DXA is that the greater the thickness of the patient, the lower its ability to discriminate tissues, especially lean or muscle tissue. Additionally, DXA is a technique that emits little radiation as one of its advantages in comparison with CT, but it loses precision in patients with obesity (38, 82)(1). CT is a technique that is related to a slightly higher dose of radiation and could be considered as a disadvantage. However, technically CT is a method that provides high-quality and precise quantitative and qualitative information on BC. Until the present thesis there was no data regarding the usefulness of CT for BC assessment in patients with severe obesity. In order to validate CT in patients with severe obesity, we conducted the first study, where we compared the results obtained by CT with those of DXA, considered currently the reference method. We observed that CT had a good correlation with DXA for the measurement of FFM, using the classic models ($r=0.75$, p value <0.05). In addition,

it was possible to demonstrate for the first time that the use of a single slice presented similar results to those obtained by the average of 16 slices, reducing the time dedicated to the analysis by CT. It is also important to highlight the development of a new model that optimises the results obtained from CT measured by kilograms. DXA expresses its results in kg, so classically the comparison of BC results by CT vs DXA has been done in kg, therefore, the CT results (cm²) had to be converted to kg. The equation developed by Mourtzakis et al. (118) is the most used in routine practice. We observed that this equation had been developed with a small population sample of cancer patients with normal BMI or overweight. We tested the model proposed by Mourtzakis (118), defined as Model 1, and an adjusted version defined as Model 2 (see Methodology). Both models underestimate the FM for the subjects with obesity and overestimate it in the subjects with normal BMI.

Based on these findings we developed a new model that could be applied with better results in different phenotypes and a wider range of BMI. Two innovative concepts were included for this model. On the one hand, we use the percentage (%) of tissue instead of cm² to measure the area of each body tissue, thus obtaining a better proportionality of the distribution of the tissues. On the other hand, the CT image also provides information on the tissue radiodensity, expressed by the Hounsfield Units (HU) and allows to evaluate the tissue quality (119). Finally, in this study we have created a new model that considers, for the first time, both the percentages of adipose and muscle tissue and their average HU, instead of just each tissue area in cm² as in the models used so far in the literature. This new model (FocusedON- Model) has provided results that are more accurate and the data was confirmed by three different statistical analysis methods. The correlation between FocusedON- Model and DXA was the strongest. It also showed better agreement with DXA based on Bland-Atman plots, also without under or overestimating the FM and FFM in any of the two groups. This new model has demonstrated to be superior in accuracy to those presented in previous studies, which only take into account the quantity of tissue measured in cm². **These findings underlie the importance of revisiting the traditional equations and models where they only used CT measurements expressed in cm².** We have shown in our study that these models are not optimal for the assessment of PwO, so the present cut-off levels should be reevaluated. Our study highlights the

relevance of the CT as a reliable technique for BC assessment, pointing out the relevance and need to include qualitative information (UH) besides quantitative for the evaluation of BC in PwO.

After carrying out the previous study, we were able to conclude that CT is an excellent technique for the study of BC and that further studies are necessary to better understand its clinical applications and the development of cut-off points and normative data bases in our population. One main limitation that can be found for the CT as widely used technique for BC assessment is its low accessibility, especially in primary care and outside specialised clinics, as well as the radiation dose. For this reason, we designed the second study of the thesis, with the aim of finding a more accessible muscle assessment technique, such as ultrasound, which could serve as an alternative when CT is not available. Ultrasound (US) is a simple, reproducible, cost-effective and non-invasive technique that can be performed with portable devices. Furthermore, several guidelines already mention the US for the assessment of BC. (20, 38, 47). Some authors consider the US as the “stethoscope of body composition,”. For the purpose of our study, we included patients with colorectal cancer as they require CT scans as part of their follow-up, staging and overall assessment (123). This positioning allows CT to be used as an “opportunistic” technique to analyse BC with a high degree of precision, thus providing a valuable validation platform for emerging techniques, such as US. We therefore performed this study in patients with a recent diagnosis of colon cancer, in whom we performed rectus femoris muscle ultrasound coinciding with the CT scan in a short period of time. We observed a good correlation between the results of the CT and the ultrasound ($r = 0.67$, CI 0.57–0.74, $p < 0.001$).

One of the limitations of the US as a technique for BC assessment is that it is observer-dependent. Operator manipulation is especially important at two key moments, the performance of the examination (taking the image) and the taking of measurements. Measurement is a manual process, in which the different metrics (area, X axis, Y axis) are measured by means of the ultrasound device (105). This moment of image manipulation can increase the differences between operators, reducing the effectiveness of the technique. As a solution to this high manipulation, we propose the development of a semi-automatic marking tool. In this study, a semi-

automatic tool called “Bat” is developed that provides the metrics of the Y axis, X axis, adipose tissue and grayscale automatically through manual marking of the muscle area. Reducing the observer’s manipulation to only the marking of the muscle area.

Another contribution generated by the use of software is that regardless of the probe's orientation, the principal axes of the muscle's image will consistently adjust. By focusing on the intrinsic geometric properties of the muscle tissue, measurements become more reflective of the actual dimensions of the muscle and less dependent on the probe positioning. Consequently, this approach leads to more accurate and objective assessments of muscle size, shape, and potentially its quality status. This technique greatly reduces the reliance on the operator skill or consistency in probe placement. Different observers can perform the scan, and the main axes will remain consistent for the same anatomical structure, ensuring more objective and reproducible measurements.

Reduction in muscle mass (MM) is strongly associated with a prognosis in terms of postoperative complications, prolonged hospital stays, discharge outcomes, treatment response and mortality (18). Consistent with this premise, our study results confirm that lower MM, as measured by the US, is associated with longer hospital stays and decreased likelihood of discharge home, essentially indicating a more difficult prognosis for the patient. Given the accessibility of US as a technique, serious consideration should be given to its more frequent incorporation into protocols for prevention and clinical optimization in patients with colorectal cancer. Furthermore, the results obtained can play a key role in tailoring multimodal treatments in cases where low muscle mass is evident or its deterioration is observed over time.

RF area (cm²) emerged as the variable with the strongest correlation with CT, although results were also noted for the Y axis (see Table 2). This may be related to the fact that the favourable performance of the axis due to its vertical measurement, which is not affected by possible image displacement from the screen. In this sense, we observed that a significant percentage of the images (62%) acquired according to our protocol in the lower third of the leg showed an area that extended beyond the edges of the screen. This overflow situation, where the area

extends beyond the edges of the screen, introduces a potential source of imprecision in area measurements compared to situations where the area is fully displayed. We therefore, stratified the sample into two groups, with and without overflow. We re-run the clinical correlation in the group without overflow, and observed an improvement in the ROC curves, indicating a lower rate of false positives and false negatives. An increase in the correlation with clinical complications, discharge destination and hospital stay were also observed. However, it is recognised that these results may be influenced by the fact that many patients without overflow generally have worst muscle mass.

A limitation of our tool is its partial automation, which requires a manual measurement by a researcher. However, it has been shown that a reduction in manual measurement leads to significantly better results. It is necessary to carry out studies with a larger sample size to fully automate the tool. In addition, it would have been interesting to measure the RF area a few centimetres closer to the patella to see if this would provide an improvement that we should definitely include in our protocols when eliminating the overflow.

In the first study we were able to familiarise ourselves with the importance of qualitative assessment in BC, through the use of the HU of the TC.

One of the challenges in the clinical practice of nutritional treatment is to know the energy needs as accurately as possible, in order to carry out the most effective treatment and with the lowest rate of associated complications, both due to over or under nutrition. Indirect calorimetry (IC) is the reference method today. Despite the important technological improvements that it has had in recent years, it is still an expensive technique due to the expense of the device, the consumables and the time required by a trained operator. However, there are no alternative methods to IC that are simple, accessible and precise at the same time. There are methods such as direct calorimetry or double water labelling, but they are technically very expensive methods that are not applied in clinical practice. As a simple alternative, although less precise, estimates using predictive equations or empirical contributions are usually used according to recommendations of international guidelines such as ESPEN (134-138). These equations have insufficient precision and also little ability to adapt to changes in the physical or pathological conditions

of the patient. One of the possible explanations is that these equations do not usually include body composition parameters, but rather more generic variables such as weight or BMI. Bioimpedance is capable of providing estimates of energy requirements, through predictive equations that include BC parameters estimated by the BIA itself. These equations have been validated and developed over the years with multiple studies, with sample sizes greater than 1000 patients. It is worth mentioning that the development of machine learning models usually requires a large sample size. As an example, in Achamrah N et al (139) 3.655 subjects have been used just to validate the performance of the Bodystat QuadScan 4000 Manufacturer's equation with respect to dual-energy x-ray absorptiometry (DXA).

In the third study we hypothesise that if energy requirements are closely related to BC and the state of muscle mass, a technique as precise as CT should be able to provide a good estimation of resting energy expenditure. Thus, we proposed the development of a machine learning model for REE estimation through the use of clinical variables and the measurement of body composition through CT and analysed data from 90 subjects that underwent abdominal CT, BIA and IC. We observed a low correlation and a high dispersion of the comparison of the different predictive equations, that are currently included in the clinical guidelines, and IC. The model developed using AI with CT showed the best estimation of REE when compared with the reference technique IC. Our study was designed as a proof of concept in which only 90 subjects have been included. This fact strongly limits the performance that can be expected from the developed models based on AI and the proposed methodology. Despite this limitation, the results obtained are surprisingly good, even overcoming those provided by the BIA for this cohort. We assume that this is due to the fact that CT-scan analysis includes specific and precise data on muscle quantity and quality, information which is very relevant for estimating the REE.

In addition, due to the sample size, the model could not contain more than three variables, which limits its power and adaptability. After applying deep learning and developing the most accurate model, the variables accounting for REE in an independent manner were those related to total weight (kg), age, and muscle mass quantity (cm²). Interestingly, gender, a classic variable widely used at present and

for more than a century ago (i.e. Harris-Benedict equation) for the estimation of REE, were not valued as significant. This unexpected finding might explain the low correlation of either BIA or predictive equations with the real value of REE, thus suggesting that gender per se is not a primary determinant of REE. **This finding can have a significant impact and may eventually change the current guidelines and recommendations for REE determination in the setting of nutritional evaluation. For sure, this study has the potential to impose a revision of the current mathematical equations, proposed for the REE estimation, that all include gender as a variable and not muscle quality and/or quantity.** As previously described, in the first study, when we tested the different available CT-scan variables, muscle radiodensity also showed very promising results. We observed a high influence of the HU in the following models, but data needs to be validated in a model with more variables and higher sample size. As far as we know, radiodensity (HU) has never before been used for the REE calculation. We believe that the introduction of a variable that so faithfully reflects the metabolic state and muscle quality will significantly improve the prediction capacity of the model. In the future we aim to validate and refine these results.

It is expected that increasing the sample size would allow developing and training more complex and robust models that would lead to even more accurate results. As an extra advantage of the proposed methodology, it is also worth mentioning that CT-scan is a method that is widely integrated in clinical practice, which does not require specific preparation, such as fasting, rest, or maintaining the same position for a long period of time. The proposed methodology considerably increases the value of this technique as it allows an "opportunistic" use of the CT-scan images to estimate the REE.

Our results demonstrate for the first-time that REE can be estimated by means of a model based on BC information extracted from abdominal CT-scan images using automatic AI-based software. It is worth mentioning that the method herein proposed, based on the AI model, permits to estimate "at a glance" both BC and REE, thus opening up a new era in the personalised approach of metabolic and nutritional assessment and follow-up after interventions. In addition, this combined information can favour subjects' adherence to treatment and follow-

up and can contribute to a positive reinforcement. For health care providers, the system will monitor in real time the effects of new emerging pharmacological therapies in different pathologies (i.e. obesity, diabetes, cancer, nutritional pathologies), thus engaging the pharmaceutical industry as a whole.

7.1. Clinical relevance

At a time when technology and artificial intelligence are demonstrating their broad clinical applications and value in optimising more personalised management, our goal has been to continue contributing to this field with improvements for the personalization and optimization of BC techniques and nutritional and metabolic treatment.

We demonstrated the validity of using CT as a BC assessment technique in patients with severe obesity. One of the advantages obtained from the use of CT for the BC assessment in obesity is the ability to phenotype different types of obesity, based on the distribution of adipose tissue (subcutaneous and visceral); muscle quantity (sarcopenic or non-sarcopenic); muscle quality (myosteatosis or normal).

In addition, we also demonstrate in this thesis that measuring the area in cm² is not the optimal way to quantify tissues using CT in patients with obesity, as was proposed by previous models, and we showed superiority of metrics when using proportions. **This represents an important finding and has the potential of changing the current methods and guidelines.**

Additionally, we showed for the first time that the estimation of REE by means of CT-scan has a strong correlation with the current reference method and we submitted the finding for intellectual property. This result also has the potential of changing the current guidelines and will allow a personalised approach “at a glance” as well as a reliable, easy and reproducible tool for follow-up. Many clinical situations and pathologies will benefit from both the assessment of BC and REE through CT “at a glance”, such as patients with obesity and metabolic diseases, cancer, inflammatory bowel diseases, patients with abdominal surgery, critical patients, etc. In general, all of them require CT to be performed at relevant times of their pathology, which will serve to identify sarcopenia or alterations in body composition and a correct adjustment of their nutritional treatment that would not be sufficient with the usual tools. In addition, it provides us with energy requirements, which are a fundamental aspect of the nutritional treatment plan and its success.

Furthermore, apart from the fact that sarcopenia is associated with a worse prognosis and greater complications related to oncological treatment and surgery, it has been shown that lower muscle density is also associated with a high risk, regardless of the amount of muscle. The information obtained from the CT scan analysis with FocusedON during the BC assessment provides information regarding the muscle quality by the inclusion of the HU in the model. This sensible and refined information allows one to adjust the therapeutic risk and choose the best preparation prior to the indicated therapy, such as either as prehabilitation prior to chemotherapy or pre-surgical prehabilitation, for instance. **This finding, and the utility of the HU for the muscle quality assessment also has the potential of changing the current guidelines.**

On the other hand, muscle ultrasound is a technique that is shown to be a good alternative to CT-scan, since it is an accessible technique, without radiation and of low cost, providing good quality images. However, it is a technique that requires trained personnel for obtaining the proper image, and its results are operator-dependent and needs several manual measurements. The software developed by our group together with Artis Development showed to help reduce the examination time by being able to obtain the information for the BC assessment from just one measurement, also adding qualitative muscle information. This means great advantages in the applicability of this technique, such as a reduction in the examination time, results that are less manipulated by the operator, variables corrected by image analysis using AI, and qualitative information. These improvements could help to increase the number of personnel who can perform it more easily and with better results, helping, for example, primary care personnel who require accessible techniques that cost little operator time.

8. FUTURE PERSPECTIVE

One of our objectives is the development of:

1. **Normative data base in healthy Spanish population.**
2. **Development of cut-off in different chronic pathologies.**

2.1. We have already started the validation in cancer:

- Unicentric colon cancer study, 2021-2024. Morphofunctional study and 12-month follow-up in patients diagnosed with colon cancer undergoing surgery. Pending completion of follow-up, 204 patients are recruited with visits every 3-6 months.
- Development of cut-off points in patients with colon cancer. Closed recruitment, sample size of 580 patients. Led by our centre, together with the Regional Hospital of Malaga and the Virgen de la Victoria Hospital in Malaga. First publication on May 21, 2024 in the journal *Nutrients*.
- Study in patients with gastric cancer. Preliminary results presented at the 36th National Congress of the Spanish Society of Parenteral and Enteral Nutrition (SENPE), in Madrid, October 2021. Awarded as the best oral communication of the congress. Closing date of the study July/2024.

2.2. Obesity and MASLD: We are currently continuing to expand the sample size of the third article, on which the patent is based, in patients admitted with multiple types of pathologies or phenotypes, including obesity. And add CT scan hepatic infiltration, to decide on the optimal treatment for the improvement, not only of obesity, but also of associated metabolic complications. The project does not currently have funding but is pending the resolution of the public-private call ISCIII requested by VHIR in collaboration with Artis Development: SCPP2300C010524XV0.

3. Validation and improvement of the REE assessment by CT-scan.

3.1. One of the most innovative aspects contributed by the thesis is the patent (PCT/EP2023/080242), currently submitted and of which 100% of its claims have been accepted. Pending completion of the European process.

3.2. A proof of concept has been published, and we continue to recruit patients with the characteristics of the third study to expand the sample size and improve the estimation models.

4. Implementation of FocusedON at large scale. obtention of the CE marking.

4.1. Utilisation in multicentric, pharma sponsored clinical trials with new drugs for obesity and MASLD. Preliminary results on body composition and energy expenditure were presented at the ECO 2024 congress, Venice 11-15.05.2024, and there is already interest from the pharmaceutical industry (Boehringer Ingelheim) to evaluate the incorporation of the FocusedOn software in the company's clinical trials to assess body composition. In this regard, the first contacts have been established and meetings have been scheduled.

4.2. The internationalisation of the project and the tool and the capacity to bring together clinical centres from most of the European member countries of EASO. In this regard, contact has already been established and the preliminary idea of the protocol for the multicentre clinical trial has been designed with several EASO-COMs centres: Hasharon Hospital- Rabin Medical Centre, Israel (Prof Dror Diker), Centre for the study and the integrated treatment of obesity-bariatric unit department of medicine-DIMED-Clinica Medica 3, University of Padova (Prof Roberto Vettor) and University of Health Sciences Istanbul (Prof Volkan Yumuk- president of EASO). In addition, we have contacts with the European Coalition of People with Obesity (ECPO) and citizen participation will be counted on for the internationalisation of the project and the clinical trial.

5. Development of the use of CT for BC and REE assessment at other levels, different from L3 vertebrae, such as thoracic or cervical CT.

5.1 Study of assessment of BC at the cervical level in patients with head and neck neoplasia receiving radiotherapy at our centre.

5.2. Collaboration study with the Radiotherapy service of the Negrin Hospital in Las Palmas de Gran Canaria, for the validation of BC at the cervical level.

5.3 Project VALONC (Valoración Morfofuncional en paciente con cáncer de pulmón). Study formed by 10 national hospitals led by Dr. García Almeida, where our group coordinates the BC analysis section by image (FocusedOn-BC), where BC will be studied at the cervical, thoracic and abdominal levels. A FIS ISCIII project has been requested, pending the resolution.

6. Validation of “Bat” software for US muscle assessment.

Another important point of innovation has been the creation of the semi-automatic software “Bat” for marking muscle ultrasound images in the rectus femoris.

- We are currently waiting to complete the “Single-centre colon cancer study”, 2021-2024. Morphofunctional study and 12-month follow-up in patients diagnosed with colon cancer undergoing colon surgery. These patients have undergone a complete morphofunctional assessment including muscle and abdominal ultrasound every 3 months and marking with the “Bat” software. Pending completion of follow-up, 204 patients were recruited. It will allow training and validation of the “Bat” software.
- VALONC study, multicenter (15 national centres) in patients with lung cancer. The “Bat” software will be used for marking ultrasounds. A FIS ISCIII project was requested in March 2024 and has been awarded.

9. GLOBAL CONCLUSIONS

1. The analysis of a single slice CT-scan image with the FocusedON software showed accurate BC assessment when compared with the reference technique DXA in patients with obesity.
2. Variables such as muscle quantity measured in percentage and qualitative assessment (HU) showed greater relevance for BC estimation than ones being widely used at present in the clinical practice (as cm^2), for any BMI.
3. There is a high correlation between abdominal CT muscle measurement as a reference technique, compared to ultrasound in the rectus femoris, so we can consider ultrasound as an alternative technique when CT is not feasible.
4. The new developed software for US images analysis- Bat- allows a precise, reproducible and objective analysis, based on one measurement, optimising therefore the procedure
5. CT-scan is a useful tool for the estimation of REE with a high correlation with the current gold standard method: indirect calorimetry.
6. The gender, a classical variable used so far by all the algorithms for the REE estimation, was ruled out by the AI, indicating that current methods and guidelines need to be revisited.

10. BIBLIOGRAPHY

1. Holmes CJ, Racette SB. The utility of body composition assessment in nutrition and clinical practice: an overview of current methodology. Vol. 13, *Nutrients*. MDPI; 2021.
2. Wang ZM, Pierson RN, Heymsfield SB. The five-level model: a new approach to organizing body-composition research. *Am J Clin Nutr* [Internet]. 1992 Jul 1 [cited 2023 Apr 9];56(1):19–28. Available from: <https://academic.oup.com/ajcn/article/56/1/19/4715618>
3. Kuriyan R. Body composition techniques. Vol. 148, *Indian Journal of Medical Research*. Wolters Kluwer Medknow Publications; 2018. p. 648–58.
4. Heymsfield SB, Wang ZM, Baumgartner RN, Ross R. Human body composition: Advances in models and methods. *Annu Rev Nutr*. 1997;17:527–58.
5. Janssen I, Heymsfield SB, Wang ZM, Ross R. Skeletal muscle mass and distribution in 468 men and women aged 18–88 yr. *J Appl Physiol* [Internet]. 2000 [cited 2022 Nov 28];89(1):81–8. Available from: <https://journals.physiology.org/doi/10.1152/jappl.2000.89.1.81>
6. Bauer J, Morley JE, Schols AMWJ, Ferrucci L, Cruz-Jentoft AJ, Dent E, et al. Sarcopenia: A Time for Action. An SCWD Position Paper. *J Cachexia Sarcopenia Muscle* [Internet]. 2019 Oct 1 [cited 2022 Nov 12];10(5):956–61. Available from: <https://onlinelibrary.wiley.com/doi/full/10.1002/jcsm.12483>
7. Merz KE, Thurmond DC. Role of skeletal muscle in insulin resistance and glucose uptake. *Compr Physiol*. 2020 Jul 1;10(3):785–809.
8. Landi F, Camprubi-Robles M, Bear DE, Cederholm T, Malafarina V, Welch AA, et al. Muscle loss: The new malnutrition challenge in clinical practice. *Clinical Nutrition* [Internet]. 2019 Oct 1 [cited 2022 Nov 12];38(5):2113–20. Available from: <http://www.clinicalnutritionjournal.com/article/S0261561418325548/fulltext>
9. Bell KE, Paris MT, Avrutin E, Mourtzakis M. Altered features of body composition in older adults with type 2 diabetes and prediabetes compared with matched controls. *J Cachexia Sarcopenia Muscle*. 2022 Apr 1;13(2):1087–99.
10. Liu AW, Song SO, Hayashi T, Sato KK, Kahn SE, Leonetti DL, et al. Change in CT-measured abdominal subcutaneous and visceral but not thigh fat areas predict future insulin sensitivity. *Diabetes Res Clin Pract*. 2019 Aug 1;154:17–26.
11. Bauer JM, Cruz AJ, Roger J, John AF, Reginster JY. Is There Enough Evidence for Osteosarcopenic Obesity as a Distinct Entity ? A Critical Literature Review. *Calcif Tissue Int* [Internet]. 2019;(0123456789). Available from: <https://doi.org/10.1007/s00223-019-00561-w>
12. Hunter GR, Singh H, Carter SJ, Bryan DR, Fisher G. Sarcopenia and Its Implications for Metabolic Health. Vol. 2019, *Journal of Obesity*. Hindawi Limited; 2019.

13. Lee K, Shin Y, Huh J, Sung YS, Lee IS, Yoon KH, et al. Recent issues on body composition imaging for sarcopenia evaluation. Vol. 20, Korean Journal of Radiology. Korean Radiological Society; 2019. p. 205–17.
14. Janssen I. Evolution of sarcopenia research. <https://doi.org/10.1139/H10-067> [Internet]. 2010 [cited 2022 Nov 28];35(5):707–12. Available from: <https://cdnsiencepub.com/doi/10.1139/H10-067>
15. Cruz-Jentoft AJ, Baeyens JP, Bauer JM, Boirie Y, Cederholm T, Landi F, et al. Sarcopenia: European consensus on definition and diagnosis. Age Ageing. 2010 Apr 13;39(4):412–23.
16. Gold SL, Raman M, Sands BE, Ungaro R, Sabino J. Review article: Putting some muscle into sarcopenia—the pathogenesis, assessment and clinical impact of muscle loss in patients with inflammatory bowel disease. Aliment Pharmacol Ther. 2023 Jun 1;57(11):1216–30.
17. Paris M, Mourtzakis M. Assessment of skeletal muscle mass in critically ill patients: considerations for the utility of computed tomography imaging and ultrasonography. Curr Opin Clin Nutr Metab Care. 2016 Mar 1;19(2):125–30.
18. Xia L, Zhao R, Wan Q, Wu Y, Zhou Y, Wang Y, et al. Sarcopenia and adverse health-related outcomes: An umbrella review of meta-analyses of observational studies. 2020;
19. Salinas-Miranda E, Deniffel D, Dong X, Healy GM, Khalvati F, O’Kane GM, et al. Prognostic value of early changes in CT-measured body composition in patients receiving chemotherapy for unresectable pancreatic cancer. European Radiology 2021 31:11 [Internet]. 2021 May 2 [cited 2022 Oct 13];31(11):8662–70. Available from: <https://link.springer.com/article/10.1007/s00330-021-07899-6>
20. Cruz-Jentoft AJ, Bahat G, Bauer J, Boirie Y, Bruyère O, Cederholm T, et al. Sarcopenia: Revised European consensus on definition and diagnosis. Age Ageing. 2019;48(1):16–31.
21. Lee JW, Ban MJ, Park JH, Lee SM. Visceral adipose tissue volume and CT-attenuation as prognostic factors in patients with head and neck cancer. Head Neck. 2019;41(6):1605–14.
22. Petersen MC, Shulman GI. Mechanisms of Insulin Action and Insulin Resistance. Physiol Rev [Internet]. 2018;98:2133–223. Available from: www.prv.org
23. Ahn H, Kim DW, Ko Y, Ha J, Shin Y Bin, Lee J, et al. Updated systematic review and meta-analysis on diagnostic issues and the prognostic impact of myosteatosi s: A new paradigm beyond sarcopenia. Vol. 70, Ageing Research Reviews. Elsevier Ireland Ltd; 2021.
24. Frühbeck G, Busetto L, Dicker D, Yumuk V, Goossens GH, Hebebrand J, et al. The ABCD of Obesity: An EASO Position Statement on a Diagnostic Term with Clinical and Scientific Implications. Obes Facts [Internet]. 2019 [cited 2022 Nov 12];12:131–6. Available from: www.karger.com/ofa

25. Mechanick JL, Hurley DL, Garvey WT. Adiposity-based chronic disease as a new diagnostic term: The American association of clinical endocrinologists and American college of endocrinology position statement. *Endocrine Practice* [Internet]. 2017 Mar 1 [cited 2022 Nov 12];23(3):372–8. Available from: <http://www.endocrinepractice.org/article/S1530891X20358341/fulltext>
26. Ballesteros Pomar MD, Vilarrasa García N, Rubio Herrera MÁ, Barahona MJ, Bueno M, Caixàs A, et al. Abordaje clínico integral SEEN de la obesidad en la edad adulta: resumen ejecutivo. *Endocrinol Diabetes Nutr* [Internet]. 2021 Feb 1 [cited 2022 Nov 12];68(2):130–6. Available from: <https://www.elsevier.es/es-revista-endocrinologia-diabetes-nutricion-13-articulo-abordaje-clinico-integral-seen-obesidad-S2530016420301622>
27. Vilalta A, Gutiérrez JA, Chaves SZ, Hernández M, Urbina S, Hompesch M. Adipose tissue measurement in clinical research for obesity, type 2 diabetes and NAFLD/NASH. Vol. 5, *Endocrinology, Diabetes and Metabolism*. John Wiley and Sons Inc; 2022.
28. Chen WZ, Shen Z Le, Zhang FM, Zhang XZ, Chen WH, Yan XL, et al. Prognostic value of myosteatorsis and sarcopenia for elderly patients with colorectal cancer: A large-scale double-center study. *Surgery (United States)* [Internet]. 2022 Oct 1 [cited 2023 Nov 12];172(4):1185–93. Available from: <http://www.surgjournal.com/article/S0039606022004160/fulltext>
29. Covassin N, Sert-Kuniyoshi FH, Singh P, Romero-Corral A, Davison DE, Lopez-Jimenez F, et al. Experimental Weight Gain Increases Ambulatory Blood Pressure in Healthy Subjects: Implications of Visceral Fat Accumulation HHS Public Access Author manuscript. *Mayo Clin Proc*. 2018;93(5):618–26.
30. Vasamsetti SB, Natarajan N, Sadaf S, Florentin J, Dutta P. Regulation of cardiovascular health and disease by visceral adipose tissue-derived metabolic hormones. *J Physiol* [Internet]. 2023 Jun 1 [cited 2023 Sep 20];601(11):2099–120. Available from: <https://onlinelibrary.wiley.com/doi/full/10.1113/JP282728>
31. Kanaya AM, Harris T, Goodpaster BH, Tykavsky F, Cummings SR. Adipocytokines Attenuate the Association Between Visceral Adiposity and Diabetes in Older Adults. *Diabetes Care* [Internet]. 2004 Jun 1 [cited 2022 Nov 12];27(6):1375–80. Available from: <https://diabetesjournals.org/care/article/27/6/1375/22813/Adipocytokines-Attenuate-the-Association-Between>

32. Simpson G, Manu N, Magee C, Wilson J, Moug S, Vimalachandran D. Measuring sarcopenia on pre-operative CT in older adults undergoing emergency laparotomy: a comparison of three different calculations. *Int J Colorectal Dis* [Internet]. 2020;35(6):1095–102. Available from: <https://doi.org/10.1007/s00384-020-03570-6>
33. Brandt E, Tengberg LT, Bay-Nielsen M. Sarcopenia predicts 90-day mortality in elderly patients undergoing emergency abdominal surgery. *Abdominal Radiology* [Internet]. 2019;44(3):1155–60. Available from: <https://doi.org/10.1007/s00261-018-1870-z>
34. Petersen A, Bressen K, Albrecht J, Thieß HM, Vahldiek J, Hamm B, et al. The role of visceral adiposity in the severity of COVID-19: Highlights from a unicenter cross-sectional pilot study in Germany. 2020 [cited 2022 Nov 12]; Available from: <https://doi.org/10.1016/j.metabol.2020.154317>
35. Yang S, Guo B, Ao L, Yang C, Zhang L, Zhou J, et al. Obesity and activity patterns before and during COVID -19 lockdown among youths in China. *Clin Obes*. 2020 Dec;10(6).
36. Khadra D, Itani L, Tannir H, Kreidieh D, Masri D El, Ghoch M El. Association between sarcopenic obesity and higher risk of type 2 diabetes in adults: A systematic review and meta-analysis. *World J Diabetes*. 2019 May 15;10(5):311–23.
37. Polyzos SA, Margioris AN. Sarcopenic obesity. Vol. 17, *Hormones*. Springer; 2018. p. 321–31.
38. Cappellari GG, Guillet C, Poggiogalle E, Pomar MDB, Batsis JA, Boirie Y, et al. Sarcopenic obesity research perspectives outlined by the sarcopenic obesity global leadership initiative (SOGLI) – Proceedings from the SOGLI consortium meeting in Rome November 2022. *Clinical Nutrition* [Internet]. 2023 May 1 [cited 2023 May 23];42(5):687–99. Available from: <http://www.clinicalnutritionjournal.com/article/S0261561423000547/fulltext>
39. Dodds RM, Syddall HE, Cooper R, Benzeval M, Deary IJ, Dennison EM, et al. Grip strength across the life course: normative data from twelve British studies. *PLoS One* [Internet]. 2014 Dec 4 [cited 2024 Jun 13];9(12). Available from: <https://pubmed.ncbi.nlm.nih.gov/25474696/>
40. Gallagher D, Heymsfield SB, Heo M, Jebb SA, Murgatroyd PR, Sakamoto Y. Healthy percentage body fat ranges: an approach for developing guidelines based on body mass index. *Am J Clin Nutr* [Internet]. 2000 [cited 2024 Jun 13];72(3):694–701. Available from: <https://pubmed.ncbi.nlm.nih.gov/10966886/>
41. Janssen I, Heymsfield SB, Ross R. Low relative skeletal muscle mass (sarcopenia) in older persons is associated with functional impairment and physical disability. *J Am Geriatr Soc* [Internet]. 2002 [cited 2024 Jun 13];50(5):889–96. Available from: <https://pubmed.ncbi.nlm.nih.gov/12028177/>

42. Piccoli A, Brunani A, Savia G, Pillon L, Favaro E, Berselli ME, et al. Discriminating between body fat and fluid changes in the obese adult using bioimpedance vector analysis. *Int J Obes*. 1998;22(2):97–104.
43. Armstrong LE. Assessing Hydration Status: The Elusive Gold Standard. <https://doi.org/10.1080/07315724200710719661> [Internet]. 2013 Oct 1 [cited 2022 Nov 13];26:575S-584S. Available from: <https://www.tandfonline.com/doi/abs/10.1080/07315724.2007.10719661>
44. Chamney PW, Wabel P, Moissl UM, Müller MJ, Bosy-Westphal A, Korth O, et al. A whole-body model to distinguish excess fluid from the hydration of major body tissues 1-3 [Internet]. 2007. Available from: <https://academic.oup.com/ajcn/article/85/1/80/4649204>
45. da Silva AT, Hauschild DB, de Almeida Oliveira LD, de Fragas Hinnig P, Franco Moreno YM, Wazlawik E. Association of hyperhydration evaluated by bioelectrical impedance analysis and mortality in patients with different medical conditions: Systematic review and meta-analyses. *Clin Nutr ESPEN* [Internet]. 2018 Dec 1 [cited 2022 Nov 13];28:12–20. Available from: <http://clinicalnutritionespen.com/article/S2405457718304522/fulltext>
46. Lohman TG, 1940-, Roche AF, 1921-, Martorell R, 1947-. Anthropometric standardization reference manual. Health Care (Don Mills) [Internet]. 1988 [cited 2023 Apr 12];59(2):31–6. Available from: <https://agris.fao.org/agris-search/search.do?recordID=US201300683431>
47. Cederholm T, Jensen GL, Correia MITD, Gonzalez MC, Fukushima R, Higashiguchi T, et al. GLIM criteria for the diagnosis of malnutrition – A consensus report from the global clinical nutrition community. *Clinical Nutrition*. 2019 Feb 1;38(1):1–9.
48. Jahoda G. Quetelet and the emergence of the behavioral sciences. *Springerplus*. 2015 Dec 8;4(1).
49. Physical status : the use of and interpretation of anthropometry , report of a WHO expert committee [Internet]. [cited 2022 Nov 28]. Available from: <https://apps.who.int/iris/handle/10665/37003>
50. Okorodudu DO, Jumeau MF, Montori VM, Romero-Corral A, Somers VK, Erwin PJ, et al. Diagnostic performance of body mass index to identify obesity as defined by body adiposity: A systematic review and meta-analysis. Vol. 34, *International Journal of Obesity*. 2010. p. 791–9.
51. Borga M, West J, Bell JD, Harvey NC, Romu T, Heymsfield SB, et al. Advanced body composition assessment: From body mass index to body composition profiling. Vol. 66, *Journal of Investigative Medicine*. BMJ Publishing Group; 2018. p. 887–95.

52. Thomas EL, Frost G, Taylor-Robinson SD, Bell JD. Excess body fat in obese and normal-weight subjects. 2000 [cited 2022 Nov 12]; Available from: <https://doi.org/10.1017/S0954422412000054>
53. Prentice AM, Jebb SA. Beyond body mass index. 2001.
54. Xia JY, Lloyd-Jones DM, Khan SS. Association of body mass index with mortality in cardiovascular disease: New insights into the obesity paradox from multiple perspectives. Vol. 29, Trends in Cardiovascular Medicine. Elsevier Inc.; 2019. p. 220–5.
55. Lavie CJ, Alpert MA, Arena R, Mehra MR, Milani R V., Ventura HO. Impact of obesity and the obesity paradox on prevalence and prognosis in heart failure. Vol. 1, JACC: Heart Failure. 2013. p. 93–102.
56. Geneva. Waist Circumference and Waist-Hip Ratio: Report of a WHO Expert Consultation. [cited 2022 Oct 24]; Available from: www.who.int
57. Schneider HJ, Klotzsch J, Silber S, Stalla GK, Wittchen HU. Measuring abdominal obesity: Effects of height on distribution of cardiometabolic risk factors risk using waist circumference and waist-to-height ratio. Vol. 34, Diabetes Care. 2011.
58. Tuttle MS, Montoye AHK, Kaminsky LA. THE BENEFITS OF BODY MASS INDEX AND WAIST CIRCUMFERENCE IN THE ASSESSMENT OF HEALTH RISK Learning Objectives [Internet]. 2016. Available from: www.acsm-healthfitness.org
59. Gonzalez MC, Mehrnezhad A, Razaviarab N, Barbosa-Silva TG, Heymsfield SB. Calf circumference: Cutoff values from the NHANES 1999-2006. American Journal of Clinical Nutrition. 2021 Jun 1;113(6):1679–87.
60. Prado CM, Ford KL, Gonzalez MC, Murnane LC, Gillis C, Wischmeyer PE, et al. Nascent to novel methods to evaluate malnutrition and frailty in the surgical patient. Vol. 47, Journal of Parenteral and Enteral Nutrition. John Wiley and Sons Inc; 2023. p. S54–68.
61. Elmadfa I, Meyer AL. Developing Suitable Methods of Nutritional Status Assessment: A Continuous Challenge 1-3. Adv Nutr [Internet]. 2014 [cited 2022 Nov 14];5:590–8. Available from: <https://academic.oup.com/advances/article/5/5/590S/4565778>
62. Pozzi A Del. Comparison of Body Composition Prediction Equations with Air Displacement Plethysmography in Overweight and Obese Caucasian Males [Internet]. 2019. Available from: <http://www.intjexersci.com>
63. Si S, Tewara MA, Ji X, Wang Y, Liu Y, Dai X, et al. Body surface area, height, and body fat percentage as more sensitive risk factors of cancer and cardiovascular disease. Cancer Med. 2020 Jun 1;9(12):4433–46.

64. Jayedi A, Soltani S, Motlagh SZT, Emadi A, Shahinfar H, Moosavi H, et al. Anthropometric and adiposity indicators and risk of type 2 diabetes: systematic review and dose-response meta-analysis of cohort studies. *The BMJ*. 2022;376(1).
65. Sánchez Marta Sánchez Àngels Betriu Ferran Rius Gerard Torres E, Purroy Reinald Pamplona Marta Ortega Carolina López-Cano Marta Hernández Marta Bueno Elvira Fernández Javier Salvador F, Lecube A, project collaborators I. Are Obesity Indices Useful for Detecting Subclinical Atheromatosis in a Middle-Aged Population? 2020 [cited 2023 Aug 5]; Available from: www.karger.com/ofa
66. Gómez-Ambrosi J, Silva C, Catalán V, Rodríguez A, Galofré JC, Escalada J, et al. Clinical Usefulness of a New Equation for Estimating Body Fat. 2012 [cited 2023 Apr 10]; Available from: <http://care.diabetesjournals.org/lookup/suppl/doi:10>
67. Martín V, Dávila-Batista V, Castilla J, Godoy P, Delgado-Rodríguez M, Soldevila N, et al. Comparison of body mass index (BMI) with the CUN-BAE body adiposity estimator in the prediction of hypertension and type 2 diabetes. *BMC Public Health*. 2016 Jan 27;16(1).
68. Deurenberg P, Andreoli A, Borg P, Kukkonen-Harjula K, De Lorenzo A, Van Marken Lichtenbelt WD, et al. The validity of predicted body fat percentage from body mass index and from impedance in samples of five European populations. *European Journal of Clinical Nutrition* 2001 55:11 [Internet]. 2001 Oct 25 [cited 2022 Nov 13];55(11):973–9. Available from: <https://www.nature.com/articles/1601254>
69. Deurenberg P, Weststrate JA, Seidell JC. Body mass index as a measure of body fatness: age- and sex-specific prediction formulas. *British Journal of Nutrition*. 1991 Mar;65(2):105–14.
70. Shannon CA, Brown JR, Pozzi AT Del. Comparison of Body Composition Prediction Equations with Air Displacement Plethysmography in Overweight and Obese Caucasian Males [Internet]. Vol. 12, *International Journal of Exercise Science*. 2019. Available from: <http://www.intjexersci.com>
71. Valdez R. A simple model-based index of abdominal adiposity. *J Clin Epidemiol* [Internet]. 1991 Jan 1 [cited 2023 Apr 17];44(9):955–6. Available from: <http://www.jclinepi.com/article/0895435691900591/fulltext>
72. Bonora E, Micciolo R, Ghiatas AA, Lancaster JL, Alyassin A, Muggeo M, et al. Is it possible to derive a reliable estimate of human visceral and subcutaneous abdominal adipose tissue from simple anthropometric measurements? *Metabolism* [Internet]. 1995 Dec 1 [cited 2022 Nov 12];44(12):1617–25. Available from: <http://www.metabolismjournal.com/article/0026049595900845/fulltext>
73. Bergman RN, Stefanovski D, Buchanan TA, Sumner AE, Reynolds JC, Sebring NG, et al. A better index of body adiposity. *Obesity*. 2011 May;19(5):1083–9.

74. Thomas DM, Bredlau C, Bosy-Westphal A, Mueller M, Shen W, Gallagher D, et al. Relationships between body roundness with body fat and visceral adipose tissue emerging from a new geometrical model. *Obesity*. 2013 Nov;21(11):2264–71.
75. Krakauer NY, Krakauer JC. A new body shape index predicts mortality hazard independently of body mass index. *PLoS One*. 2012 Jul 18;7(7).
76. Hume R. Prediction of lean body mass from height and weight. *J clin Path*. 1966;19:389.
77. Carnevale V, Piscitelli PA, Minonne R, Castriotta V, Cipriani C, Guglielmi G, et al. Estimate of body composition by Hume's equation: validation with DXA. *Endocrine*. 2015 May 1;49(1):65–9.
78. Albano D, Messina C, Vitale J, Sconfienza LM. Imaging of sarcopenia: old evidence and new insights. *Eur Radiol*. 2020;30(4):2199–208.
79. Carmelo Messina, Domenico Albano, Salvatore Gitto, Laura Tofanelli, Alberto Bazzocchi, Fabio Massimo Ulivieri, et al. Body composition with DXA: from basics to new tools DXA: technical aspects. [cited 2022 Nov 14]; Available from: <http://dx.doi.org/10.21037/qims.2020.03.02>
80. Lee SY, Gallagher D. Assessment methods in human body composition. *Curr Opin Clin Nutr Metab Care* [Internet]. 2008 Sep [cited 2022 Nov 13];11(5):566–72. Available from: https://www.researchgate.net/publication/23154393_Lee_SY_Gallagher_D_Assessment_methods_in_human_body_composition_Curr_Opin_Clin_Nutr_Metab_Care_11_566-572
81. Kaul S, Rothney MP, Peters DM, Wacker WK, Davis CE, Shapiro MD, et al. Dual-energy X-ray absorptiometry for quantification of visceral fat. *Obesity*. 2012;20(6):1313–8.
82. Prado CMM, Heymsfield SB. Lean tissue imaging: A new era for nutritional assessment and intervention. *Journal of Parenteral and Enteral Nutrition*. 2014 Nov 11;38(8):940–53.
83. Ceniccola GD, Castro MG, Piovacari SMF, Horie LM, Corrêa FG, Barrere APN, et al. Current technologies in body composition assessment: advantages and disadvantages. Vol. 62, *Nutrition*. Elsevier Inc.; 2019. p. 25–31.
84. Buffa R, Saragat B, Cabras S, Rinaldi AC, Marini E. Accuracy of Specific BIVA for the Assessment of Body Composition in the United States Population. [cited 2023 Aug 5]; Available from: <http://veprints.unica.it/809/>
85. Walter-Kroker A, Kroker A, Mattiucci-Guehlke M, Glaab T. A practical guide to bioelectrical impedance analysis using the example of chronic obstructive pulmonary disease. 2011 [cited 2023 Aug 5]; Available from: <http://www.nutritionj.com/content/10/1/35>

86. Foster KR, Lukaski HC. Whole-body impedance--what does it measure? *Am J Clin Nutr* [Internet]. 1996 Sep 1 [cited 2022 Nov 13];64(3):388S-396S. Available from: <https://academic.oup.com/ajcn/article/64/3/388S/4651608>
87. Marra M, Sammarco R, De Lorenzo A, Iellamo F, Siervo M, Pietrobelli A, et al. Assessment of body composition in health and disease using bioelectrical impedance analysis (bia) and dual energy x-ray absorptiometry (dxa): A critical overview. Vol. 2019, *Contrast Media and Molecular Imaging*. Hindawi Limited; 2019.
88. Piccoli A, Nigrelli S, Caberlotto A, Bottazzo S, Rossi B, Pillon L, et al. Bivariate normal values of the bioelectrical impedance vector in adult and elderly populations. *Am J Clin Nutr* [Internet]. 1995 Feb 1 [cited 2022 Nov 13];61(2):269–70. Available from: <https://academic.oup.com/ajcn/article/61/2/269/4651254>
89. Kyle UG, Bosaeus I, De Lorenzo AD, Deurenberg P, Elia M, Gómez JM, et al. Bioelectrical impedance analysis—part I: review of principles and methods. *Clinical Nutrition* [Internet]. 2004 Oct 1 [cited 2022 Nov 12];23(5):1226–43. Available from: <http://www.clinicalnutritionjournal.com/article/S0261561404000937/fulltext>
90. Thanapholsart J, Khan E, Lee GA. A Current Review of the Uses of Bioelectrical Impedance Analysis and Bioelectrical Impedance Vector Analysis in Acute and Chronic Heart Failure Patients: An Under-valued Resource? *Biological Research for Nursing*. SAGE Publications Inc.; 2022.
91. De Palo T, Messina G, Edefonti A, Perfumo F, Pisanello L, Peruzzi L, et al. Normal values of the bioelectrical impedance vector in childhood and puberty. *Nutrition*. 2000 Jun 1;16(6):417–24.
92. Piccoli A, Rossi B, Pillon L, Bucciante G. A new method for monitoring body fluid variation by bioimpedance analysis: The RXc graph. *Kidney Int*. 1994;46(2):534–9.
93. Piccoli A, Codognotto M, Cianci V, Vettore G, Zaninotto M, Plebani M, et al. Differentiation of Cardiac and Noncardiac Dyspnea Using Bioelectrical Impedance Vector Analysis (BIVA). *J Card Fail*. 2012 Mar 1;18(3):226–32.
94. Piccoli A. Bioelectric impedance vector distribution in peritoneal dialysis patients with different hydration status. *Kidney Int*. 2004;65:1050–63.
95. Mattiello R, Amaral MA, Mundstock E, Ziegelmann PK. Reference values for the phase angle of the electrical bioimpedance: Systematic review and meta-analysis involving more than 250,000 subjects. *Clinical Nutrition* [Internet]. 2020 May 1 [cited 2023 Aug 5];39(5):1411–7. Available from: <http://www.clinicalnutritionjournal.com/article/S0261561419302869/fulltext>

96. Fernández-Jiménez R, Dalla-Rovere L, García-Olivares M, Abuín-Fernández J, Sánchez-Torralvo FJ, Doulatram-Gamgaram VK, et al. Phase Angle and Handgrip Strength as a Predictor of Disease-Related Malnutrition in Admitted Patients: 12-Month Mortality. *Nutrients* [Internet]. 2022 May 1 [cited 2022 Oct 27];14(9):1851. Available from: /pmc/articles/PMC9105999/
97. Tsaousi G, Panagidi M, Papakostas P, Grosomanidis V, Stavrou G, Kotzampassi K. Phase Angle and Handgrip Strength as Complements to Body Composition Analysis for Refining Prognostic Accuracy in Cardiac Surgical Patients. *J Cardiothorac Vasc Anesth*. 2021 Aug 1;35(8):2424–31.
98. Panagidi M, Papazoglou AS, Moysidis D V., Vlachopoulou E, Papadakis M, Kouidi E, et al. Prognostic value of combined preoperative phase angle and handgrip strength in cardiac surgery. *J Cardiothorac Surg*. 2022 Dec 1;17(1).
99. Colin-Ramirez E, González-Ortiz A, Nacional de Pediatría I, Camila Orsso M, Reyes-Torres C, Zhao Q. Phase angle derived from bioelectrical impedance analysis as a marker for predicting sarcopenia.
100. Perkisas S, Bastijns S, Sanchez-Rodriguez D, Piotrowicz K, De Cock AM. Application of ultrasound for muscle assessment in sarcopenia: 2020 SARCUS update: reply to the letter to the editor: SARCUS working group on behalf of the Sarcopenia Special Interest Group of the European Geriatric Medicine Society. Vol. 12, *European Geriatric Medicine*. Springer Science and Business Media Deutschland GmbH; 2021. p. 427–8.
101. Berger J, Bunout D, Barrera G, de la Maza MP, Henriquez S, Leiva L, et al. Rectus femoris (RF) ultrasound for the assessment of muscle mass in older people. *Arch Gerontol Geriatr*. 2015 Jul 1;61(1):33–8.
102. Perkisas S, Baudry S, Bauer J, Beckwée D, De Cock AM, Hobbelen H, et al. Application of ultrasound for muscle assessment in sarcopenia: towards standardized measurements. *Eur Geriatr Med* [Internet]. 2018 Dec 1 [cited 2022 Nov 14];9(6):739–57. Available from: <https://research.rug.nl/en/publications/application-of-ultrasound-for-muscle-assessment-in-sarcopenia-tow>
103. Cuatrecasas G, de Cabo F, Coves MJ, Patrascioiu I, Aguilar G, March S, et al. Ultrasound measures of abdominal fat layers correlate with metabolic syndrome features in patients with obesity. *Obes Sci Pract*. 2020 Dec 1;6(6):660–7.
104. Pillen S, Van Dijk JP, Weijers G, Raijmann W, De Korte CL, Zwarts MJ. Quantitative gray-scale analysis in skeletal muscle ultrasound: A comparison study of two ultrasound devices. *Muscle Nerve*. 2009 Jun;39(6):781–6.
105. García-Almeida JM, García-García C, Vegas-Aguilar IM, Ballesteros Pomar MD, Cornejo-Pareja IM, Fernández Medina B, et al. Nutritional ultrasound®: Conceptualisation, technical considerations and standardisation. *Endocrinología, Diabetes y Nutrición*. Sociedad Española de Endocrinología y Nutrición; 2022.

106. Beaudart C, McCloskey E, Bruyère O, Cesari M, Rolland Y, Rizzoli R, et al. Sarcopenia in daily practice: assessment and management. *BMC Geriatr*. 2016;16(1):1–10.
107. Tolonen A, Pakarinen T, Sassi A, Kyttä J, Cancino W, Rinta-Kiikka I, et al. Methodology, clinical applications, and future directions of body composition analysis using computed tomography (CT) images: A review. Vol. 145, *European Journal of Radiology*. Elsevier Ireland Ltd; 2021.
108. Mitsiopoulos N, Baumgartner RN, Heymsfield SB, Lyons W, Gallagher D, Ross R. Cadaver validation of skeletal muscle measurement by magnetic resonance imaging and computerized tomography. *J Appl Physiol*. 1998;85(1):115–22.
109. Shen W. Total body skeletal muscle and adipose tissue volumes: estimation from a single abdominal cross-sectional image. *J Appl Physiol* [Internet]. 2004;97(6):2333–8. Available from: <http://jap.physiology.org/cgi/doi/10.1152/japplphysiol.00744.2004>
110. Zwart AT, van der Hoorn A, van Ooijen PMA, Steenbakkens RJHM, de Bock GH, Halmos GB. CT-measured skeletal muscle mass used to assess frailty in patients with head and neck cancer. *J Cachexia Sarcopenia Muscle*. 2019 Oct 1;10(5):1060–9.
111. Vangelov B, Bauer J, Kotevski D, Smee RI. The use of alternate vertebral levels to L3 in computed tomography scans for skeletal muscle mass evaluation and sarcopenia assessment in patients with cancer: A systematic review. Vol. 127, *British Journal of Nutrition*. Cambridge University Press; 2022. p. 722–35.
112. Bril SI, Chargini N, Wendrich AW, Wegner I, Bol GH, Smid EJ, et al. Validation of skeletal muscle mass assessment at the level of the third cervical vertebra in patients with head and neck cancer. *Oral Oncol*. 2021 Dec 1;123.
113. Arribas L, Sabaté-Llobera A, Domingo MC, Taberna M, Sospedra M, Martin L, et al. Assessing dynamic change in muscle during treatment of patients with cancer: Precision testing standards. *Clinical Nutrition*. 2022 May 1;41(5):1059–65.
114. Schiaffino S, Albano D, Cozzi A, Messina C, Arioli R, Bnà C, et al. CT-derived Chest Muscle Metrics for Outcome Prediction in Patients with COVID-19. *Radiology* [Internet]. 2021 Aug 1 [cited 2022 Nov 13];300(2):E328–36. Available from: [/pmc/articles/PMC7971428/](https://pubmed.ncbi.nlm.nih.gov/3471428/)
115. Kim JW, Yoon JS, Kim EJ, Hong HL, Kwon HH, Jung CY, et al. Prognostic Implication of Baseline Sarcopenia for Length of Hospital Stay and Survival in Patients with Coronavirus Disease 2019. *J Gerontol A Biol Sci Med Sci* [Internet]. 2021 Aug 1 [cited 2022 Nov 13];76(8):E110–6. Available from: [/pmc/articles/PMC8083663/?report=abstract](https://pubmed.ncbi.nlm.nih.gov/3471428/)

116. Ma D, Chow V, Popuri K, Beg MF. Comprehensive Validation of Automated Whole Body Skeletal Muscle, Adipose Tissue, and Bone Segmentation from 3D CT images for Body Composition Analysis: Towards Extended Body Composition. 2021 Jun 1; Available from: <http://arxiv.org/abs/2106.00652>
117. Van Der Werf A, Langius JAE, De Van Der Schueren MAE, Nurmohamed SA, Van Der Pant KAMI, Blauwhoff-Buskermolen S, et al. Percentiles for skeletal muscle index, area and radiation attenuation based on computed tomography imaging in a healthy Caucasian population. *Eur J Clin Nutr*. 2018 Feb 1;72(2):288–96.
118. Mourtzakis M, Prado CMM, Lieffers JR, Reiman T, McCargar LJ, Baracos VE. A practical and precise approach to quantification of body composition in cancer patients using computed tomography images acquired during routine care. *Applied Physiology, Nutrition and Metabolism*. 2008 Oct;33(5):997–1006.
119. Aubrey J, Esfandiari N, Baracos VE, Buteau FA, Frenette J, Putman CT, et al. Measurement of skeletal muscle radiation attenuation and basis of its biological variation. Vol. 210, *Acta Physiologica*. 2014. p. 489–97.
120. Rollins KE, Javanmard-Emamghissi H, Awwad A, Macdonald IA, Fearon KCH, Lobo DN. Body composition measurement using computed tomography: Does the phase of the scan matter? *Nutrition*. 2017 Sep 1;41:37–44.
121. Molwitz I, Recklies F, Stark M, Horvatits T, Salamon J, Huber S, et al. Muscle quality determined by computed tomography predicts short-term and long-term survival after liver transplantation. *Sci Rep [Internet]*. 2023 Dec 1 [cited 2023 Aug 5];13(1). Available from: [/pmc/articles/PMC10172199/](https://pmc/articles/PMC10172199/)
122. Geladari E, Alexopoulos T, Kontogianni MD, Vasilieva L, Mani I, Tenta R, et al. The Presence of Myosteatorsis Is Associated with Age, Severity of Liver Disease and Poor Outcome and May Represent a Prodromal Phase of Sarcopenia in Patients with Liver Cirrhosis. *J Clin Med [Internet]*. 2023 May 1 [cited 2023 Aug 5];12(9):3332. Available from: [/pmc/articles/PMC10179726/](https://pmc/articles/PMC10179726/)
123. van Vugt JLA, Levolger S, Gharbharan A, Koek M, Niessen WJ, Burger JWA, et al. A comparative study of software programmes for cross-sectional skeletal muscle and adipose tissue measurements on abdominal computed tomography scans of rectal cancer patients. *J Cachexia Sarcopenia Muscle*. 2017 Apr 1;8(2):285–97.
124. Amini B, Boyle SP, Boutin RD, Lenchik L. Approaches to Assessment of Muscle Mass and Myosteatorsis on Computed Tomography (CT): A Systematic Review. Available from: <https://academic.oup.com/biomedgerontology/advance-article-abstract/doi/10.1093/gerona/glz034/5308117>
125. Aleixo GFP, Shachar SS, Nyrop KA, Muss HB, Malpica L, Williams GR. Myosteatorsis and prognosis in cancer: Systematic review and meta-analysis. Vol. 145, *Critical Reviews in Oncology/Hematology*. Elsevier Ireland Ltd; 2020.

126. Fosbøl MO, Zerah B. Contemporary methods of body composition measurement. *Clin Physiol Funct Imaging* [Internet]. 2015 Mar 1 [cited 2022 Nov 13];35(2):81–97. Available from: <https://onlinelibrary.wiley.com/doi/full/10.1111/cpf.12152>
127. Ross R, Janssen I. Computed Tomography and Magnetic Resonance Imaging. *Human Body Composition* [Internet]. 2005 [cited 2022 Nov 13]; Available from: <https://www.humankineticslibrary.com/encyclopedia-chapter?docid=b-9781492596950&tocid=b-9781492596950-chapter7>
128. Nayak KS, Cui SX, Tasdelen B, Yagiz E, Weston S, Zhong X, et al. Body composition profiling at 0.55T: Feasibility and precision. *Magn Reson Med*. 2023 Sep 1;
129. Haugen AH, Chan LN, Li F. Indirect calorimetry: A practical guide for clinicians. Vol. 22, *Nutrition in Clinical Practice*. 2007. p. 377–88.
130. Gupta R Das, Ramachandran R, Venkatesan P, Anoop S, Joseph M, Thomas N. Indirect Calorimetry: From Bench to Bedside. *Indian J Endocrinol Metab* [Internet]. 2017 Jul 1 [cited 2024 Jan 14];21(4):594–9. Available from: <https://pubmed.ncbi.nlm.nih.gov/28670546/>
131. Achamrah N, Delsoglio M, De Waele E, Berger MM, Pichard C. Indirect calorimetry: The 6 main issues. Vol. 40, *Clinical Nutrition*. Churchill Livingstone; 2021. p. 4–14.
132. Hopkins M, Finlayson G, Duarte C, Whybrow S, Ritz P, Horgan GW, et al. Modelling the associations between fat-free mass, resting metabolic rate and energy intake in the context of total energy balance. *Int J Obes*. 2016 Feb 1;40(2):312–8.
133. Oshima T, Berger MM, De Waele E, Guttormsen AB, Heidegger CP, Hiesmayr M, et al. Indirect calorimetry in nutritional therapy. A position paper by the ICALIC study group. Vol. 36, *Clinical Nutrition*. Churchill Livingstone; 2017. p. 651–62.
134. Muscaritoli M, Arends J, Bachmann P, Baracos V, Barthelemy N, Bertz H, et al. ESPEN practical guideline: Clinical Nutrition in cancer. *Clinical Nutrition*. 2021 May 1;40(5):2898–913.
135. Singer P, Blaser AR, Berger MM, Alhazzani W, Calder PC, Casaer MP, et al. ESPEN guideline on clinical nutrition in the intensive care unit. *Clinical Nutrition*. 2019 Feb 1;38(1):48–79.
136. Arvanitakis M, Ockenga J, Bezmarevic M, Gianotti L, Krznarić Ž, Lobo DN, et al. ESPEN guideline on clinical nutrition in acute and chronic pancreatitis. *Clinical Nutrition*. 2020 Mar 1;39(3):612–31.
137. Fiaccadori E, Sabatino A, Barazzoni R, Carrero JJ, Cupisti A, De Waele E, et al. ESPEN guideline on clinical nutrition in hospitalized patients with acute or chronic kidney disease. *Clinical Nutrition*. 2021 Apr 1;40(4):1644–68.

138. Barazzoni R, Bischoff SC, Breda J, Wickramasinghe K, Krznaric Z, Nitzan D, et al. ESPEN expert statements and practical guidance for nutritional management of individuals with SARS-CoV-2 infection. Vol. 39, *Clinical Nutrition*. Churchill Livingstone; 2020. p. 1631–8.
139. Achamrah N, Jésus P, Grigioni S, Rimbert A, Petit A, Déchelotte P, et al. Validity of predictive equations for resting energy expenditure developed for obese patients: Impact of body composition method. *Nutrients*. 2018 Jan 10;10(1).
140. Arthur Harris BJ, Benedict FG. *Grundzilge der Mengenlehre*. Vol. 23, *Bull. Amer. Math. Soc.* Veit & Co; 1914.
141. Mifflin MD, St Jeor ST, Hill LA, Scott BJ, Daugherty SA, Koh YO. A new predictive equation for resting energy expenditure in healthy individuals. *Am J Clin Nutr* [Internet]. 1990 [cited 2024 Feb 5];51(2):241–7. Available from: <https://pubmed.ncbi.nlm.nih.gov/2305711/>
142. Ireton-Jones C, Jones JD. Improved Equations for Predicting Energy Expenditure in Patients: The Ireton-Jones Equations. *Nutrition in Clinical Practice* [Internet]. 2002 Feb 1 [cited 2024 Feb 5];17(1):29–31. Available from: <https://onlinelibrary.wiley.com/doi/full/10.1177/011542650201700129>
143. Thibault R, Abbasoglu O, Ioannou E, Meija L, Ottens-Oussoren K, Pichard C, et al. ESPEN guideline on hospital nutrition. *Clinical Nutrition*. 2021 Dec 1;40(12):5684–709.
144. Pironi L, Cuerda C, Bekker Jeppesen P, Joly F, Jonkers C, Krznari Z, et al. ESPEN Guideline ESPEN guideline on chronic intestinal failure in adults e Update 2023. 2023 [cited 2024 Jun 26]; Available from: <https://doi.org/10.1016/j.clnu.2023.07.019>
145. Wunderle C, Gomes F, Schuetz P, Stumpf F, Austin P, Ballesteros-Pomar MD, et al. ESPEN Guideline ESPEN guideline on nutritional support for polymorbid medical inpatients. 2023 [cited 2024 Jun 26]; Available from: <https://doi.org/10.1016/j.clnu.2023.06.023>
146. Bischoff SC, Bager P, Escher J, Forbes A, ebuterne XH, Lodberg Hvas C, et al. ESPEN guideline on Clinical Nutrition in inflammatory bowel disease. [cited 2024 Jun 26]; Available from: <https://doi.org/10.1016/j.clnu.2022.12.004>
147. Bischoff SC, Barazzoni R, Busetto L, Campmans-Kuijpers M, Cardinale V, Chermesh I, et al. European guideline on obesity care in patients with gastrointestinal and liver diseases – Joint ESPEN/UEG guideline. *Clinical Nutrition*. 2022 Oct 1;41(10):2364–405.
148. Bischoff SC, Bernal W, Dasarathy S, Merli M, Plank LD, Schütz T, et al. ESPEN practical guideline: Clinical nutrition in liver disease. *Clinical Nutrition*. 2020 Dec 1;39(12):3533–62.

149. Burgos R, Bret I, Cereda E, Desport JC, Dziewas R, Genton L, et al. ESPEN guideline clinical nutrition in neurology. 2018 [cited 2024 Jun 26]; Available from: <https://doi.org/10.1016/j.clnu.2017.09.003>
150. Weimann A, Braga M, Carli F, Higashiguchi T, Hübner M, Klek S, et al. ESPEN guideline: Clinical nutrition in surgery. 2017 [cited 2024 Jun 26]; Available from: <http://dx.doi.org/10.1016/j.clnu.2017.02.013>
151. Arends J, Bachmann P, Baracos V, Barthelemy N, Bertz H, Bozzetti F, et al. ESPEN Guideline ESPEN guidelines on nutrition in cancer patients *. 2016 [cited 2024 Jun 26]; Available from: <http://dx.doi.org/10.1016/j.clnu.2016.07.015>
152. Barak N, Wall-Alonso E, Cheng A, Sitrin MD. Use of Bioelectrical Impedance Analysis to Predict Energy Expenditure of Hospitalized Patients Receiving Nutrition Support. Vol. 27, JOURNAL OF PARENTERAL AND ENTERAL NUTRITION. 2003.
153. Fidilio E, Comas M, Giribés M, Cárdenas G, Vilallonga R, Palma F, et al. Evaluation of Resting Energy Expenditure in Subjects with Severe Obesity and Its Evolution After Bariatric Surgery. *Obes Surg* [Internet]. 2021 Oct 1 [cited 2022 Mar 14];31(10):4347–55. Available from: <https://pubmed.ncbi.nlm.nih.gov/34345955/>
154. Compher C, Frankenfield D, Keim N, Roth-Yousey L. Best Practice Methods to Apply to Measurement of Resting Metabolic Rate in Adults: A Systematic Review. *J Am Diet Assoc*. 2006 Jun;106(6):881–903.
155. Fullmer S, Benson-Davies S, Earthman CP, Frankenfield DC, Gradwell E, Lee PSP, et al. Evidence analysis library review of best practices for performing indirect calorimetry in healthy and non-critically ill individuals. *J Acad Nutr Diet* [Internet]. 2015 Sep 1 [cited 2024 Jun 26];115(9):1417-1446.e2. Available from: <https://pubmed.ncbi.nlm.nih.gov/26038298/>
156. Delsoglio M, Achamrah N, Berger MM, Pichard C. Indirect calorimetry in clinical practice. Vol. 8, *Journal of Clinical Medicine*. MDPI; 2019.